

# Special Observing Period (SOP) Data for the Year of Polar Prediction site Model Intercomparison Project (YOPPsiteMIP)

Zen Mariani<sup>1</sup>, Sara M. Morris<sup>2,11</sup>, Taneil Uttal<sup>2</sup>, Elena Akish<sup>3,2</sup>, Robert Crawford<sup>1</sup>, Laura Huang<sup>1</sup>, Jonathan Day<sup>4</sup>, Johanna Tjernström<sup>12</sup>, Øystein Godøy<sup>12</sup>, Lara Ferrighi<sup>12</sup>, Leslie M. Hartten<sup>3,2</sup>, Jareth Holt<sup>6</sup>, Christopher J. Cox<sup>2</sup>, Ewan O'Connor<sup>9</sup>, Roberta Pirazzini<sup>9</sup>, Marion Maturilli<sup>13</sup>, Giri Prakash<sup>10</sup>, James Mather<sup>8</sup>, Kimberly Strong<sup>5</sup>, Pierre Fogal<sup>5</sup>, Vasily Kustov<sup>7,14</sup>, Gunilla Svensson<sup>6</sup>, Michael Gallagher<sup>3,2</sup>, Brian Vase<sup>11</sup>

<sup>1</sup>Meteorological Research Division, Environment and Climate Change Canada, Toronto, Canada

<sup>2</sup>NOAA Physical Sciences Laboratory, Boulder, CO, USA

<sup>3</sup>Cooperative Institute for Research in Environmental Science, University of Colorado, Boulder, Colorado, USA

<sup>4</sup>European Centre for Medium-Range Weather Forecasts, Reading, UK

<sup>5</sup>Department of Physics, University of Toronto, Toronto, Canada

<sup>6</sup>Department of Meteorology, Stockholm University, Sweden

<sup>7</sup>Arctic and Antarctic Research Institute, Air-sea interaction department, St. Petersburg, Russia

<sup>8</sup>Pacific Northwest National Laboratory, Richland, WA, USA

<sup>9</sup>Finnish Meteorological Institute, Finland

<sup>10</sup>Environmental Sciences Division, Oak Ridge National Laboratory, Oak Ridge, TN, USA

<sup>11</sup>NOAA Global Monitoring Laboratory, Boulder, CO, USA

<sup>12</sup>Norwegian Meteorological Institute, Norway

<sup>13</sup>Alfred Wegener Institute, Helmholtz Centre for Polar and Marine Research, Potsdam, Germany

<sup>14</sup>Freelance entrepreneur, Belgrade, Serbia

*Correspondence to:* Zen Mariani ([zen.mariani@ec.gc.ca](mailto:zen.mariani@ec.gc.ca)) and Sara Morris ([Sara.Morris@noaa.gov](mailto:Sara.Morris@noaa.gov))

**Abstract.** The rapid changes occurring in the polar regions require an improved understanding of the processes that are driving ~~the~~these changes. At the same time, increased human activities, such as marine navigation, resource exploitation, aviation, commercial fishing, and tourism, require reliable and relevant ~~weather~~ information. One of the primary goals of the World Meteorological Organization's Year of Polar Prediction (YOPP) Project is to improve the accuracy of numerical weather prediction (NWP) at high latitudes. During YOPP, two Canadian ~~observatories~~supersites were commissioned and equipped with new ground-based instruments for enhanced meteorological and system process observations ~~that are considered to be "supersites" for addressing YOPP objectives, while other. Additional~~ pre-existing supersites in Canada, the United States, Norway, Finland, and Russia ~~also~~ provided data from ongoing long-term observing programs. ~~Data from these seven supersites were amalgamated and are being used to evaluate NWP systems from several international forecast centers and to perform meteorological process studies with the aim~~These supersites collected a ~~wealth of~~ improving NWP performance in the Polar Regions~~observations that are well-suited to address YOPP objectives~~. In order to increase data useability and station interoperability, novel Merged Observatory Data Files (MODFs) ~~have been~~were created for ~~these~~the seven~~international~~ supersites over two Special Observing Periods (February to March 2018 and July to September 2018).

39 All observations collected at the ~~seven~~ supersites were compiled into this ~~new~~ standardized NetCDF MODF format,  
40 simplifying the process of conducting pan-Arctic NWP verification and process evaluation studies. This paper describes the  
41 seven Arctic YOPP supersites, their instrumentation, data collection and processing methods, ~~and~~ the novel MODF format  
42 and output files, which together, and examples of the observations contained therein. MODFs comprise the observational  
43 contribution to the ~~associated~~ model intercomparison effort, termed YOPP supersite Model Intercomparison Project  
44 (YOPPsiteMIP). All YOPPsiteMIP MODFs are publicly accessible via the YOPP Data Portal (Whitehorse:  
45 <https://doi.org/10.21343/a33e-j150>, Iqaluit: <https://doi.org/10.21343/yrnf-ck57>, Sodankylä: [https://doi.org/10.21343/m16p-](https://doi.org/10.21343/m16p-pq17)  
46 [pq17](https://doi.org/10.21343/a2dx-nq55), Utqiagvik: <https://doi.org/10.21343/a2dx-nq55>, Tiksi: <https://doi.org/10.21343/5bwn-w881>, Ny-Ålesund:  
47 <https://doi.org/10.21343/y89m-6393>, Eureka: <https://doi.org/10.21343/r85j-tc61>), hosted by MET Norway, with  
48 corresponding output from NWP models.

## 49 **1 Introduction**

50 In the Arctic there is a recognized lack of process-level information supplementing meteorological observations to characterize  
51 the atmosphere and the cryosphere for operational forecasting (Cassano et al., 2011; Illingworth et al., 2015; Lawrence et al.,  
52 2019). As the climate continues to change, information on weather and climate is becoming more critical in ensuring the health  
53 and safety of local communities. Unfortunately, climate models do a poor job of capturing key features of Arctic climate, such  
54 as the Arctic amplification factor, likely as a result of inaccurate representation of key physical processes, as shown by  
55 Rantanen et al. (2022). Similarly, the accuracy of weather forecasts in the Polar Regions is also lower than in mid-latitudes  
56 (Jung et al., 2016) partly due to the scattered and limited availability of observing networks (Lawrence et al., 2019). Advances  
57 in Polar weather forecast prediction are expected to improve weather forecasts and climate predictions elsewhere (Jung et al.,  
58 20142016 and Day et al., 2019), but understanding the causes of poor model performance in the Arctic is limited by the  
59 availability of observatory data. Data from observatories, where sometimes hundreds of parameters are measured, are needed  
60 for detailed investigations into the cause of model error, such as boundary-layer processes and turbulent exchanges (e.g., Day  
61 et al., 20232024).

62  
63 To address the need to improve Numerical Weather Prediction (NWP) performance in the Polar Regions, the World  
64 Meteorological Organization (WMO) launched the international Polar Prediction Project with its flagship activity, the Year of  
65 Polar Prediction (YOPP). During YOPP's core phase, from mid-2017 to mid-2019, several intensive observing periods were  
66 conducted with close coordination between the international network of polar observatories and weather forecast centers. The  
67 aim was to produce highly-concentrated sets of observed and modelled data for supporting forecast evaluation and process  
68 studies (Koltzow et al., 2019; Goessling et al., 2016; Jung et al., 2016).

70 One of the flagship activities of YOPP was the YOPP supersite Model Intercomparison Project (YOPPsiteMIP), an initiative  
71 to assess the performance of NWP systems at the process level by comparing with observatory data (Day et al., [20232024](#)).  
72 To achieve this, a dataset of weather forecasts was produced by various NWP centers for supersite locations. In the Arctic  
73 dataset covers two Special Observing Periods (SOPs), SOP1 (February 1 – March 31, 2018) and SOP2 (July 1 – September  
74 30, 2018). During this period the number of routine observations (e.g. radiosonde launches, buoy deployments, etc.) were  
75 enhanced in the Arctic (doubled in the case of radiosondes), field campaigns were conducted, and enhanced observations from  
76 the designated YOPP “supersite” observatories were taken. [In general, the suite of several additional instruments that enable  
77 an enhanced measurement program, including remote sensing, radiation, and other meteorological sensors, is what  
78 distinguishes a ‘supersite’ from a typical weather site.](#) This paper documents the efforts to compile the supersite ([hereafter  
79 referred to as “sites”](#)) data collected during this period as part of the YOPPsiteMIP. These [supersitesites](#) (Figure 1) are  
80 distributed over a diverse range of geographical locations capturing some of the diversity in the terrestrial high-latitude climate  
81 zones.

82  
83 Prior to YOPP, data collection, processing, geophysical variable reporting cadences, and file output type and format were not  
84 standardized across the [supersitesites](#), which are operated by different international agencies and consortiums. This lack of  
85 interoperability made performing multi-site comparisons, evaluations, and process studies difficult and time consuming,  
86 deterring potential users of [supersitethe](#) data (Wohner et al., 2022). In order to address this problem, the concept of standardized  
87 Merged Observatory Data Files (MODFs) was developed as part of the YOPPsiteMIP (Uttal et al., [20232024](#)). This concept  
88 is based on combining measurements from multiple international research observatories’ instruments into a single NetCDF  
89 file that complies with established data management standards. Prior to MODFs, there generally existed no standardized  
90 procedures for coordinated data management at these research sites such as those that have been developed for operational  
91 datasets. Thus, the data from these sites’ separate instruments were scattered between separate files with different authors,  
92 formats, metadata, post-processing techniques, physical archive locations, and requirements for usage. As such, they could not  
93 be amalgamated to provide a pan-Arctic observational dataset.

94  
95 MODF files bring together observations from different earth system components in a standardized NetCDF file format to  
96 enable utilization of research-grade, process-level observations for model evaluation and parameterization development. At  
97 the same time, MODFs are compatible with and mirror Merged Model Data Files (MMDFs) that are produced by each NWP  
98 centre participating in YOPP (Day et al., [20232024](#)). Each geophysical variable observed at a site is matched to its  
99 corresponding NWP model geophysical variable using [identical a standardized](#) data format, cadence, and file structure ~~in order  
100 to facilitate improved observation model comparisons at the supersites (Gallagher and Tjernström, 2024).~~ Uttal et al.  
101 ([20232024](#)) provides a generalized overview for the content and data structure of MODFs, i.e., a single NetCDF data file  
102 containing measurements from multiple sources, and a series of tools to facilitate their creation. [Table 1 provides information](#)

103 regarding the on-site facility location where measurements were collected and their coordinates for reference. For some sites  
104 (e.g., Sodankylä), certain geophysical variables are measured at multiple locations; these are all reported in the MODF with  
105 their corresponding measurement coordinates embedded within the file so as to distinguish each measurement. Final DOIs for  
106 the MODF<sub>yms</sub> are listed in Table 2.

107  
108 The MODF's standardized file structure directly aligns with the NWP's MMDFs. Thus, MODFs easily facilitate observation-  
109 model comparisons at any/all of the seven sites (Gallagher and Tjernström, 2024). The purpose of the present work is to  
110 describe the construction and contents of MODFs for seven of the YOPP-designated Arctic supersites during SOPs 1 and  
111 2 (hereafter, "MODF<sub>ysm</sub>"): Whitehorse, Canada (60.71 °N, 135.07 °W, 682 m a.s.l.); Iqaluit, Canada (63.74 °N, 68.51 °W, 11  
112 m a.s.l.); Sodankylä, Finland (67.367 °N, 26.629 °E, 179 m a.s.l.); Utqiagvik (Barrow), Alaska (71.325 °N, 156.625 °W, 8 m  
113 a.s.l.); Tiksi, Russia (71.596 °N, 128.889 °E, 30 m a.s.l.); Ny-Ålesund, Norway (78.923 °N, 11.926 °E, 15 m a.s.l.); and Eureka,  
114 Canada (80.083 °N, 86.417 °W, 89 m a.s.l.). Methods used to organize a site's dataset and develop MODFs are provided. Each  
115 sites' instrumentation and data processing are also described in this work to provide users with additional context and  
116 information about the source of the geophysical variables contained in the MODF. The MODFs' counterpart, MMDFs, are  
117 described in Uttal et al. (2024). ~~Table 1 provides information regarding the on-site facility location where measurements were~~  
118 ~~collected and their coordinates for reference. For some sites (e.g., Sodankylä), certain geophysical variables are measured at~~  
119 ~~multiple locations; these are all reported in the MODF with their corresponding measurement coordinates embedded within~~  
120 ~~the file so as to distinguish each measurement. These MODFs closely mirror the format used to archive the YOPPsiteMIP~~  
121 ~~NWP data, in order to enable model evaluation. Final DOIs for the MODF<sub>yms</sub> are listed in Table 2.~~

122  
123 Creating a standardized dataset such as MODF that contains observations from different meteorological and research agencies'  
124 sites is an extremely complex, non-trivial task. For the sake of brevity and to reduce redundancy, this paper references site- or  
125 instrument-specific publications in order to fully describe all of the aspects of the MODF dataset, including instrumentation,  
126 quality control, and processing techniques. In the case where non-trivial aspects about the MODF data arise, the data's origin,  
127 reference publications (e.g., dataset dois), and site contacts have been provided. Section 2 describes the data processing chain  
128 conducted at each supersite, including information about the site's local topography, climate, and instrumentation in order  
129 to provide site-specific context to aid the interpretation of model-observation comparisons. Section 3 describes the  
130 instrumentation and calculated variables. Section 4 describes the standardized MODF dataset file format, quality control, and  
131 post processing, which in some cases differed slightly from site-to-site. Section 5 describes the MODF data structure, attributes,  
132 and example Figures that illustrate the available dataset. Data and code availability is provided in Section 6, and concluding  
133 remarks are provided in Section 7.

134 **2 Site Descriptions**

135 ~~It is important to~~To properly contextualize and interpret the observations contained within the MODF since they come from  
136 vastly different sites. A map of the distribution of the ~~supersites is shown in Figure 1 and local maps showing the vicinity~~  
137 ~~around each supersite are found in Figure 2. For context, also shown in Figure 2, are native spatial grids of the forecast models~~  
138 ~~that participated in YOPPsiteMIP. While all supersites sites is shown in Figure 1. While all sites~~ are also designated surface  
139 synoptic observation (SYNOP) stations, the meteorological data provided in the MODFs is significantly more detailed and  
140 includes additional geophysical variables and thus is not the same as the SYNOP data. Table 3 lists the geophysical variables  
141 observed at each site that are stored in the standardized MODF format, their measurement location(s), and other attributes; the  
142 MODF featureType corresponds to the type of geophysical variable being observed at each site (they are split up into broad  
143 categories).

144 **2.1 Whitehorse, Canada**

145 The Whitehorse ~~supersitesite~~ (Figure 2) was commissioned as part of the Canadian Arctic Weather Science (CAWS) project  
146 (Mariani et al., 2018; Joe et al., 2020). ~~CAWS was initiated to evaluate upper air observing technologies that can complement~~  
147 ~~and improve Polar forecasts, perform satellite calibration / validation over Arctic terrain, and to provide recommendations to~~  
148 ~~optimize the Canadian Arctic observing network. The supersite'ssite's~~ instruments (Figure 2 and Table 4) are installed on an  
149 elevated platform, all within a few meters of each other. ~~Whitehorse has a population greater than 26,000 inhabitants. It is the~~  
150 ~~primary gateway for air traffic for all of the Yukon Territories, parts of Alaska, and the Western Canadian Arctic. The~~  
151 ~~supersiteThe site~~ is located at the Erik Nielsen Whitehorse International Airport, which is situated on a plateau ~50 m above  
152 the rest of the city. The city is located in a valley between the Yukon Ranges to its West (~1.6 km a.s.l.) and East (~1.4 km  
153 a.s.l.); this complex mountainous terrain strongly influences the weather systems that reach Whitehorse, which mostly originate  
154 from the Eastern Pacific or over Alaska.

155  
156 ~~Whitehorse experiences cold to temperate average monthly temperatures ranging from -15 to 14 °C (annual mean of -2 °C)~~  
157 ~~and average monthly precipitation ranging from 7 to 38 mm (annual total of ~500 mm). Since the city is in the rain shadow of~~  
158 ~~the Coast Mountains, precipitation totals are relatively low year-round. The primary surface wind direction follows the valley~~  
159 ~~(NNW) and the average roughness length is estimated to be 1.0 m (Pinard et al., 2005). The soil type at and around the site is~~  
160 a mixture of grained alluvial and colluvial slopes and, as part of the Boreal Cordillera ecozone, the surface type is primarily  
161 Boreal Forest, including complex plateaus, mountains, valleys and Cordilleran vegetation. ~~Whitehorse experiences cold to~~  
162 ~~temperate average monthly temperatures ranging from -15 to 14 °C and average monthly precipitation ranging from 7 to 38~~  
163 ~~mm. Since the town is in the rain shadow of the Coast Mountains, precipitation totals are relatively low year-round. With a~~

164 population greater than 26,000 inhabitants. Whitehorse is the primary gateway for air traffic for all of the Yukon Territories,  
165 parts of Alaska, and the Western Canadian Arctic. During the YOPP SOPs, radiosondes were launched four times daily.

## 166 2.2 Iqaluit, Canada

167 Like Whitehorse, the Iqaluit ~~supersitesite~~ (Figure 3) was commissioned as part of the CAWS project (Mariani et al., 2022).  
168 ~~It~~The site is located ~200 m from the airport runway and all instruments (Figure 3 and Table 5) are co-located to within no  
169 more than 140 m of each other on flat terrain. ~~Co-located instrument evaluation studies were conducted for several remote~~  
170 ~~sensing and upper air observations (Mariani et al., 2020, 2021), including preliminary model verification studies during the~~  
171 ~~YOPP SOPs and beyond. Iqaluit has over 8,000 inhabitants and is the primary gateway for air and sea traffic for the central~~  
172 ~~and Eastern Canadian Arctic. The city itself is located along the coast in a valley that runs in the NW to SE direction; thus, the~~  
173 primary direction of surface winds, which are frequently severe ( $> 15 \text{ m/sms}^{-1}$ ), follows this direction. The surrounding region  
174 is relatively flat Arctic tundra except for nearby hills (~300 m a.s.l.) approximately two kilometers to the NE of the ~~supersite~~.  
175 ~~The average roughness length determined from the variance of wind speed is 0.14 m (Gordon et al., 2010)-site.~~

176  
177 Iqaluit experiences an extreme range of average monthly temperatures ranging from -28 to 8 °C (annual mean of -9 °C) and  
178 average monthly precipitation ranging from 18 to 70 mm (annual total of ~460 mm). The soil type at and around the site is  
179 cryosolic and the surface type is ~70% tundra and ~30% ocean within a 10 km radius of the ~~supersitesite~~. Most storm tracks  
180 that reach Iqaluit originate over the Western Canadian Arctic or the Prairies; these storms can produce strong Easterly winds  
181 which frequently cause blowing snow that severely reduces visibility during non-summer months. Given the site's proximity  
182 to Frobisher Bay (< 600 m), the site is influenced by sea surface conditions during onshore flow (NW). ~~Iqaluit experiences an~~  
183 ~~extreme range of average monthly temperatures ranging from -28 to 8 °C and average monthly precipitation ranging from 18~~  
184 ~~to 70 mm.~~

185 Co-located instrument evaluation studies were conducted for several remote sensing and upper air observations (Mariani et  
186 al., 2020, 2021), including preliminary model verification studies during the YOPP SOPs and beyond. Iqaluit has over 8,000  
187 inhabitants and is the primary gateway for air and sea traffic for the central and Eastern Canadian Arctic. During the YOPP  
188 SOPs, radiosondes were launched four times daily.

## 189 2.3 Sodankylä, Finland

190 The Sodankylä ~~supersitesite~~ (Figure 4) is managed by the Arctic Space Centre of the Finnish Meteorological Institute (FMI-  
191 ARC) ~~and~~. It is located in the Scandinavian taiga, which consists of a mix of spruces, pines and birches. The  
192 ~~measurementsinstruments~~ (Figure 4 and Table 6) at the Sodankylä ~~supersitesite~~ are distributed over seven main observational

193 sites, each of them including several installations (48m, 24m, 20m or 16m towers, automatic weather stations (AWS),  
194 structures supporting snow and soil measurements) that cover an area of approximately 1.5 km<sup>2</sup>. The environment of the  
195 observational sites varies between dense forest, sparse forest, forest openings, and wetland, each of these environments having  
196 its own particular surface characteristics. ~~The supersite~~

197  
198 Sodankylä experiences monthly temperatures ranging from -11 to 15 °C (annual mean of 1 °C) and average monthly  
199 precipitation ranging from 35 to 85 mm (annual total of ~660 mm). The site is a calibration/validation site for numerous  
200 satellite products (such as snow water equivalent and snow extent (Luoju et al., 2021), and soil freeze-thaw (Cohen et al.,  
201 2021 and Rautiainen et al., 2016), ~~hence the~~). ~~The~~ spatial distribution of the observational sites reflects the need of measuring  
202 the spatial variability of observed parameters over different spatial scales and satellite footprints (Hannula et al., ~~2016~~-2016).  
203 During the YOPP SOPs, radiosondes were launched four times daily.

#### 204 2.4 Utqiagvik (formerly Barrow), USA

205 The Utqiagvik ~~supersite~~ (Figure 5) consists of observatories located ~3 km southeast from the coastline where the Beaufort  
206 and Chukchi Seas meet. The ~~supersite~~ is situated over tundra interspersed with thermokarst lakes having a coverage of up  
207 to 40% area (Sellmann et al., 1975). There are two primary observatories located outside of Utqiagvik (formerly Barrow),  
208 Alaska: The Atmospheric Radiation Measurement (ARM) North Slope of Alaska (NSA) observatory operated by the  
209 Department of Energy (DOE), and the Barrow Atmospheric Baseline Observatory facility operated by the National Oceanic  
210 and Atmospheric Administration (NOAA) Global Monitoring Laboratory (GML). These observatories are equipped with a  
211 suite of meteorological instruments (Figure 5 and Table 7) located 8 km east of the town of Utqiagvik. This is likely beyond  
212 the influence of a local heat island in town (Hinkel et al., 2007) and disturbance to snow cover by human activity (Stone et al.,  
213 2002). The site includes several towers and space for guest instruments.

214  
215 Utqiagvik experiences monthly temperatures ranging from -26 to 9 °C (annual mean of -10 °C) and average monthly  
216 precipitation ranging from 35 to 85 mm (annual total of ~770 mm). The climate in Utqiagvik, and much of the Alaskan North  
217 Slope, is regulated by seasonal sea ice cover and the dominance of easterlies that circulate around the Beaufort High. This  
218 atmospheric pattern is punctuated by episodes of southerly advection of air masses from the north Pacific, which frequently  
219 arrive from the direction of the Bering Strait and are influential the timing of seasonal transitions of terrestrial snow cover and  
220 sea ice coverage in both autumn and spring (Cox et al., 2017).

221  
222 ~~There are two primary observatories located outside of Utqiagvik (formerly Barrow), Alaska: The Atmospheric Radiation~~  
223 ~~Measurement (ARM) North Slope of Alaska (NSA) observatory operated by the Department of Energy, and the Barrow~~

224 Atmospheric Baseline Observatory facility operated by the NOAA Global Monitoring Laboratory (GML). These observatories  
225 are located 8 km east of the town of Utqiagvik, and likely beyond the influence of a local heat island in town (Hinkel et al.,  
226 2007) and disturbance to snow cover by human activity (Stone et al., 2002). The site includes several towers and space for  
227 guest instruments. The GML Barrow Atmospheric Baseline Observatory recently built a newly furnished on-site laboratory  
228 that was completed in 2020. The site's previous facility was constructed in 1972  
229 (<https://gml.noaa.gov/obop/brw/history/index.html>), and was deconstructed in 2021. The ARM NSA observatory was  
230 established in 1997 (Verlinde et al., 2016). Together, the GML and ARM observatories provide an extensive set of long-term  
231 measurements at this coastal location. Measurements include properties of aerosols, clouds, precipitation, trace gases, the  
232 atmospheric state and the surface energy balance. Radiosondes Unlike the other YOPP sites, radiosondes were launched three  
233 times daily during the SOPs specifically in response to a WMO YOPP organizational request.

## 234 2.5 Tiksi, Russia

235 The Tiksi observatory (Figure 6) The original Tiksi science station was established in 1932 and at its height had 60-80 staff  
236 and families that lived onsite with a school and grocery store comprising an independent community. The current Tiksi  
237 observatory, in the same location, is 7 km away from the town of Tiksi, Russia, in the Sakha Republic of northern Siberia and  
238 is staffed by personnel that commute from the town. Tiksi hosts a 20-m flux tower, a clean air facility, a weather station, a  
239 Climate Reference Network (CRN) platform, and a Baseline Surface Radiation Network (BSRN) platform, among other  
240 instruments (Figure 6 and Table 8) (Ohmura et al., 1998; Driemel et al., 2018). In collaboration with the Russian Federal  
241 Service for Hydrometeorological and Environmental Monitoring (Roshydromet), a partnership was established with the  
242 National Oceanic and Atmospheric Administration (NOAA) and the Finnish Meteorological Institute (FMI) in 2005 to collect  
243 climate grade meteorological, surface energy budget, greenhouse gases and aerosol data (Uttal et al., 2013). The Tiksi station  
244 is a coastal site, with facilities built in a high latitude tundra regime, comprising several different types of tundra land  
245 classifications including shrub (most predominant), lichen, wet/dry fen, grassy, bog, water, bare and meadow (Mikola et al.,  
246 2018).

247  
248 On site, Tiksi hosts a 20-m flux tower, a clean air facility, a weather station, a Climate Reference Network (CRN) platform,  
249 and a Baseline Surface Radiation Network (BSRN) platform (Ohmura et al., 1998; Driemel et al., 2018). Radiosonde data  
250 were incorporated into the Integrated Global Radiosonde Archive (IGRA) and are available through NOAA's National Centers  
251 for Environmental Information (NCEI) portal (Durre et al., 2018). Radiosondes had twice daily launches during the SOPs  
252 specifically in response to a WMO YOPP organizational request. Meteorologically, Tiksi is located in a boundary region  
253 between Atlantic and Pacific air masses. The resulting variability in atmospheric conditions with air masses originating from  
254 various source regions in Russia, Northern America, Europe and Central Asia require careful attention and interpretation of



255 in-situ measurements. Tiksi is also influenced by its location at the mouth of the Lena River, the second largest river draining  
256 into the Arctic Ocean and the only major Russian river underlain by permafrost which has impacts on the processes and  
257 evolution of surface fluxes. Tiksi is also situated on the coast of the Laptev Sea, which is historically a region of large sea-ice  
258 production.

259  
260 Tiksi experiences monthly temperatures ranging from -29 to 11 °C (annual mean of -10 °C) and average monthly precipitation  
261 ranging from 15 to 65 mm (annual total of ~510 mm). The original Tiksi science station was established in 1932 and at its  
262 height had 60-80 staff and families that lived onsite with a school and grocery store comprising an independent community.  
263 In collaboration with the Russian Federal Service for Hydrometeorological and Environmental Monitoring (Roshydromet), a  
264 partnership was established with NOAA and the FMI in 2005 to collect climate grade meteorological, surface energy budget,  
265 greenhouse gases and aerosol data (Uttal et al., 2013). Radiosonde data were incorporated into the Integrated Global  
266 Radiosonde Archive (IGRA) and are available through NOAA's National Centers for Environmental Information (NCEI)  
267 portal (Durre et al., 2018). Unlike the other YOPP sites, radiosondes had twice daily launches during the SOPs.

## 268 2.6 Ny-Ålesund, Norway

269 At Ny-Ålesund Research Station (Figure 7) in Svalbard, Norway, multi-disciplinary observations are operated by several  
270 institutions of different nationalities. The Norwegian Meteorological Institute (aka MET Norway; www.met.no) is operating  
271 the standard meteorological surface and synoptic observations (Figure 7 and Table 9) reported to the WMO (Maturilli et al.,  
272 2013). The settlement at 78.9°N, 11.9°E, is situated on the south coast of the Kongsfjord, which opens at the west coast of  
273 Svalbard towards the Fram Strait. The fjord stretches in southeast-northwest direction from the large glacier plateau to the  
274 open ocean, and is surrounded by glaciated mountains with altitudes up to 1 km. This geographical setting impacts the local  
275 wind field in the lowermost kilometer, resulting in a mainly southeastern wind direction at Ny-Ålesund, which is temporarily  
276 replaced by a north-westerly wind direction when large-scale synoptic wind is also coming from the according direction. Only  
277 in calm conditions with wind speed  $< 2 \text{ m/sms}^{-1}$  do katabatic winds from the glaciers south of Ny-Ålesund prevail.

278  
279 Ny-Ålesund experiences monthly temperatures ranging from -8 to 9 °C (annual mean of -6 °C) and average monthly  
280 precipitation ranging from 17 to 46 mm (annual total of ~590 mm). Ny-Ålesund may be located in the high Arctic, but due to  
281 its location in a coastal environment affected by the West Spitsbergen Current, the local climate is quite maritime and relatively  
282 warm. During the summer months, air temperatures above freezing and the otherwise snow-covered landscape exhibits tundra  
283 ground and the active layer soil surface of permafrost. An overview of the climate conditions and changes in Svalbard is given  
284 by the Norwegian Centre for Climate Services (NCCS, 2018), while the specific atmospheric and radiation conditions in Ny-  
285 Ålesund are described by Maturilli et al. (2019).

286  
287 ~~The Norwegian Meteorological Institute (aka MET Norway; www.met.no) is operating the standard meteorological surface~~  
288 ~~and synoptic observations reported to the WMO.~~ For the YOPP SOPs, the radiosonde launch frequency was increased from  
289 daily to 6-hourly. Radiosonde launches, four times daily, are contributed by the Alfred Wegener Institute (AWI), and carried  
290 out by the German-French AWIPEV research base that AWI jointly operates with the French Polar Institute Paul-Émile Victor  
291 (IPEV). The radiosondes and weekly ozone sondes are launched from a balloon platform about 200m west of the MET Norway  
292 weather mast. Atmospheric trace gases and cloud condensation nuclei are observed at the Zeppelin Observatory at about 474  
293 m a.s.l. on Zeppelin Mountain south of Ny-Ålesund, operated by the Norwegian Polar Institute (NPI), the Norwegian Institute  
294 for Air Research (NILU), Stockholm University, the Japanese National Institute of Polar Research (NIPR), and others. The  
295 full complement of atmospheric measurements at Ny-Ålesund highlights the interwoven research community that contributes  
296 to making Ny-Ålesund an observational supersite. More information on the Ny-Ålesund Research Station is available at  
297 <https://nyalesundresearch.no>.

## 298 2.7 Eureka, Canada

299 The ~~CA~~nadianCanadian Network for the Detection of Atmospheric Change (CANDAC) runs the Polar Environment  
300 Atmospheric Research Laboratory (PEARL) (Figure 8) near the Environment and Climate Change Canada (ECCC) Eureka  
301 Weather Station (EWS) in Nunavut, Canada. PEARL has three facilities: the Ridge Laboratory (RL), the Zero Altitude PEARL  
302 Auxiliary Laboratory (OPAL), and the Surface and Atmospheric Flux Irradiance Extension (SAFIRE). PEARL collects a wide  
303 variety of measurements across all three facilities (Figure 8 and Table 10). The observations used from the Eureka station for  
304 the MODF<sub>ysm</sub> (Akish and Morris, 2023a) were primarily measured at the OPAL and SAFIRE on-site facilities. The OPAL lab  
305 is situated at approximately 10 m a.s.l. elevation to capture measurements in the lowermost atmosphere. The SAFIRE facility  
306 is located about 5 km from the EWS, and it is located away from any structures. At SAFIRE, there is a former BSRN station,  
307 a flux tower, and additional remote sensing instrumentation. ~~and in depth~~Additional details about the site including its  
308 instrumentation, dataset validation and uncertainties, etc., can be found in Fogal et al. (2013) and at [https://www.pearl-](https://www.pearl-candac.ca/website/index.php/facilities)  
309 [candac.ca/website/index.php/facilities](https://www.pearl-candac.ca/website/index.php/facilities). Only a subset of the available measurements collected have been included in the  
310 MODF<sub>ysm</sub> (Akish ~~&~~and Morris, 2023a) due to time constraints and processing resources.

311  
312 ~~Details of Eureka's climatology are described in Lesins et al. (2010) and water vapor climatology in Weaver et al. (2017). For~~  
313 ~~the period from 1954–2007, the monthly average dry-bulb air temperature minimum occurs in February at approximately –37~~  
314 ~~°C, with the maximum in July at approximately 5 °C. ECCC also publishes climate normals for Eureka at~~  
315 ~~[https://climate.weather.gc.ca/climate\\_normals/results\\_1981\\_2010\\_e.html?stnID=1750&autofwd=1](https://climate.weather.gc.ca/climate_normals/results_1981_2010_e.html?stnID=1750&autofwd=1), which for a time period~~  
316 ~~of 1981–2010, report a minimum monthly average temperature of –37.4 °C in February and a maximum of 6.1 °C in July.~~

317 ~~Average yearly precipitation is reported as 79.1 mm, with a yearly average snowfall of 60.3 cm and yearly average rainfall of~~  
318 ~~32.5 mm. The soils are mostly marine deposits, and the topography, apart from the stony ridges, is driven mostly by ground~~  
319 ~~ice (Pollard & Bell, 1998; Pollard et al., 2015). Eureka is generally colder and drier than Utqiagvik (Cox et al., 2012). Cloud~~  
320 ~~cover over Eureka is anomalous relative to other Arctic observatories, with generally higher cloud bases, a smaller proportion~~  
321 ~~of supercooled liquid, and a seasonal cycle offset from the typical pattern observed elsewhere (Shupe, 2011; Shupe et al.,~~  
322 ~~2011). Ellesmere Island, where Eureka is situated, is characterized by complex topography that generates mesoscale~~  
323 ~~atmospheric circulations, such as downsloping winds (e.g., Persson and Stone, 2007). The local summertime atmosphere is~~  
324 ~~likely regulated also by nearby ice conditions (Persson and Stone, 2007; Tremblay et al., 2019), which vary between the~~  
325 ~~northern side of the island where multiyear pack ice persists (e.g., Alert) and other coastal areas, which are generally adjacent~~  
326 ~~to seasonal ice cover (e.g., Eureka). However, the general dryness of the atmosphere over Ellesmere is likely a regional~~  
327 ~~anomaly related to location relative to dominant pressure patterns over the Beaufort Sea and near the pole rather than being~~  
328 ~~local (Cox et al., 2012).~~

330  
331 Eureka has a minimum monthly average temperature of -37.4 °C in February, a maximum of 6.1 °C in July, and a yearly  
332 average of -19 °C. Average monthly precipitation ranges from 9 to 53 mm (annual total of ~285 mm). Details of Eureka's  
333 climatology are described in Lesins et al. (2010) and water vapor climatology in Weaver et al. (2017). For the period from  
334 1954–2007, the monthly average dry bulb air temperature minimum occurs in February at approximately -37 °C, with the  
335 maximum in July at approximately 5 °C. ECCC also publishes climate normals for Eureka at  
336 [https://climate.weather.gc.ca/climate\\_normals/results\\_1981\\_2010\\_e.html?stnID=1750&autofwd=1](https://climate.weather.gc.ca/climate_normals/results_1981_2010_e.html?stnID=1750&autofwd=1). Eureka is generally  
337 colder and drier than Utqiagvik (Cox et al., 2012). The soils are mostly marine deposits, and the topography, apart from the  
338 stony ridges, is driven mostly by ground ice (Pollard and Bell, 1998; Pollard et al., 2015). Cloud cover over Eureka is  
339 anomalous relative to other Arctic observatories, with generally higher cloud bases, a smaller proportion of supercooled liquid,  
340 and a seasonal cycle offset from the typical pattern observed elsewhere (Shupe, 2011; Shupe et al., 2011). The observations  
341 used from the Eureka station for the MODF<sub>ysm</sub> (Akish & Eureka increased their twice daily radiosonde launches to four daily  
342 launches during the SOPs, Morris, 2023a) were primarily measured at the OPAL and SAFIRE on-site facilities. The OPAL lab  
343 is situated at approximately 10 m a.s.l. elevation to capture measurements in the lowermost atmosphere. The SAFIRE facility  
344 is located about 5 km from the EWS, and it is located away from any structures. At SAFIRE, there is a former BSRN station,  
345 a flux tower, and additional remote sensing instrumentation. Eureka increased their twice daily radiosonde launches to four  
346 daily launches during the SOPs, specifically in response to a WMO YOPP organizational request.

348 **3 Instrumentation and Derived Variable Calculation**

349 Standard surface meteorological observations (winds, temperature, pressure, humidity, precipitation) were conducted by  
350 instruments of similar design, operation, and accuracy at the different sites. The MODF files have an attribute "Instrument,"  
351 which specifies the exact instrument model used for each variable at each site. ~~OTT Pluvio2 precipitation weighing gauges,~~  
352 ~~which have a quoted precision of  $\pm 0.001$  mm and uncertainty  $< 5\%$ , were deployed at all sites to measure precipitation with~~  
353 ~~a single Alter shield configuration (no under catchment corrections were performed; see Section 4). The reported accuracy of~~  
354 ~~the Campbell Scientific probes used at some of the sites to measure soil temperature and moisture is 0.3 K and 1.5%,~~  
355 ~~respectively. For each site, the full list of measured variables, instrument model and manufacturer, temporal resolution,~~  
356 ~~measurement uncertainty, and operating configuration is provided in Tables 4-10 (note that the information in these tables is~~  
357 ~~also documented in the attributes of the MODFs themselves). The uncertainties provided in these tables originate from the~~  
358 ~~manufacturer and often depend on the meteorological conditions (e.g., relative humidity observations are less accurate during~~  
359 ~~very low temperatures); as such, the largest reported uncertainty was provided for each geophysical variable to provide a~~  
360 ~~conservative error estimate.~~

361  
362 ~~For Whitehorse and Iqaluit, a Vaisala WXT520 was used to measure wind, air temperature, pressure, and relative humidity~~  
363 ~~with an accuracy of  $\pm 0.3$  m/s,  $\pm 0.3$  °C,  $\pm 0.5$  hPa, and  $\pm 3\%$ , respectively. The other sites employed slightly different~~  
364 ~~instruments to measure these variables; in general, their reported accuracy is similar or slightly better than the WXT520. Wind~~  
365 ~~observations were collected by an RM Young Model 43408/43482/3001 at Utqiaġvik, Tiksi, and Ny Ålesund, a Vaisala~~  
366 ~~WAA25 or METEK USA 1 sonic anemometer at Sodankylä, and a Lufft Anemometer at Eureka. Temperature and relative~~  
367 ~~humidity observations were collected by Vaisala HMP35D/HMP45D/HMP155/HMT337 sensors in aspirators at Utqiaġvik,~~  
368 ~~Tiksi, Sodankylä, Ny Ålesund, and Eureka; they were shielded/housed in the same way. Pressure was obtained from a Vaisala~~  
369 ~~PT100/PTB110/PTB220/PTB201 at Utqiaġvik, Tiksi, Ny Ålesund, Sodankylä, and Eureka.~~

370  
371 For all sites, Vaisala RS92 or RS41 radiosondes were used to collect vertical profile observations from the surface up to the  
372 stratosphere. For Iqaluit and Whitehorse, however, the radiosonde manufacturer changed during SOP2 from Vaisala (RS92)  
373 to GRAW on September 12, 2018 (no impact on the data quality is anticipated). ~~These radiosondes have a quoted uncertainty~~  
374 ~~of  $< \pm 0.5$ °C, 1.0 hPa, 0.15 m/s, and 5% for temperature, pressure, wind, and relative humidity, respectively, in the lower~~  
375 ~~atmosphere.~~

376  
377 The radiation flux, cloud base height, and snowfall flux observations are the only derived variables that were explicitly  
378 calculated in the MODF (as opposed to the direct observations described in the paragraphs above). The ~~radiation~~heat flux  
379 observations were processed using the eddy correlation and bulk method (see for instance Baldocchi, 2014). ~~Kipp and Zonen~~  
380 ~~pyranometers and pyrgeometers (e.g., CMP22/CNR4/CM11/CMA11/CGR4 models) were used at Iqaluit, Utqiaġvik, and~~

381 ~~Sodankylä, whereas an Eppley PSP pyranometer and PIR pyrgeometer was used at Tiksi, Ny-Ålesund, and Eureka. In general,~~  
382 ~~these pyranometers and pyrgeometers have spectral ranges of 200 to 3600 nm (e.g., CMP22) and 4500 to 42000 nm (e.g.,~~  
383 ~~CGR4), respectively, a directional error  $< \pm 5 \text{ W/m}^2$ , sensitivity of  $5\text{--}15 \text{ }\mu\text{V/W/m}^2$  and an offset of  $< 7 \text{ W/m}^2$  (night time for~~  
384 ~~the pyranometer). All upwelling and downwelling, longwave and shortwave radiation measurements were collected at 1-~~  
385 ~~minute intervals with instruments in aspirated housing units and no heating elements applied to the instruments.~~ Additional  
386 processing and quality control methods for these observations are discussed in Section 4. Cloud-base height observations were  
387 output by the Vaisala CL51 ceilometer at most sites (where available) using a proprietary algorithm to determine the lowest  
388 cloud base height; the uncertainty of this algorithm isn't reported but the ceilometer has a reported distance accuracy of  $\pm 5 \text{ m}$   
389 from the manufacturer. ~~The snowfall flux data was derived from a Ka-band ARM Zenith Radar (KAZR) used at the ARM~~  
390 ~~facility, following ARM quality control measures (Widener et al., 2012).~~ ARM technical reports, instrument validation /  
391 evaluation, and quality control measures are linked and available within the Utqiagvik/Barrow MODF<sub>ysm</sub> (Akish ~~&~~and Morris,  
392 2023c).

393  
394 For all observations, instantaneous time is reported at the instruments' raw sampling cadence in UTC. The typical temporal  
395 cadence for most observations are around 1 minute or less. No temporal interpolation or averaging was performed on the data.  
396 The only exception to this is for turbulent fluxes (the only calculated variable), where some averaging (1 to 30 minutes,  
397 depending on the variable) is implicit in the calculation of fluxes. Heights are reported as above ground level (AGL), with the  
398 exception of the soil thermistor string, which reports depths below the surface in units of cm. ~~Note that the uncertainties~~  
399 ~~provided in this Section originate from the manufacturer and often depend on the meteorological conditions (e.g., relative~~  
400 ~~humidity observations are less accurate during very low temperatures); as such, the largest reported uncertainty was provided~~  
401 ~~for each geophysical variable in order to provide a conservative error estimate.~~ For more information on the instrumentation  
402 used or further details on the instrument accuracy, precision, and co-located validation studies for certain instruments, refer to  
403 the site-specific references listed in Section 2 and/or the WMO Guide to Instruments and Methods of Observation (WMO,  
404 2021).

#### 406 **4 Dataset Preparation, quality control, and post-processing**

407 Guidelines for creating MODFs were published as a table in both human-readable (PDF file) and machine-readable (JSON  
408 files) formats by Hartten and Khalsa (2022). This "H-K Table" adopts the standards and conventions commonly used in the  
409 earth sciences, including NetCDF encoding with Climate and Forecast (CF) Conventions and following ~~CMIP6~~CMIP6  
410 naming, as agreed upon by the YOPP community (Uttal et al., 20232024). This H-K standard facilitates the creation of MODFs  
411 using current requirements and the creator's software of choice, with the MODF toolkits providing tools to assist the user in

412 creating MODFs (Section 6). For the present work, we used H-K Table version 1.3 to guide the criteria for the generation and  
413 standardization of naming conventions, units, and global/variable attribute metadata. Observational datasets were collated and  
414 formatted for each of the seven [supersites/sites](#) into a set of NetCDF files in accordance with the table’s criteria. The native  
415 variable name is saved as an attribute in the MODFs and as previously discussed, no resampling was performed to harmonize  
416 different time stepping (the instrument’s instantaneous raw sampling frequency is reported, usually about minutely).  
417 Acceptance of data into the MODF<sub>ysm</sub> was generally determined by the variable list described in the table. The processing  
418 script is openly available and described in Section 6.

419  
420 Radiosonde (timeSeriesProfileSonde variables) data in the MODF were binned into 5-meter intervals (10 m for Iqaluit and  
421 Whitehorse) of geopotential height and all measurements within each bin were averaged. In the case of 5-meter intervals, this  
422 most often results in 0, 1, or 2 measurements in each bin: 8%, 82%, 9%, respectively, in SOP1 and 6%, 80%, 13% in SOP2.  
423 In both SOP1 and SOP2 at least 99.9% of the measurements have 2 or fewer measurements, but a given bin can have up  
424 to 14 measurements. The number of measurements per bin has been included in the dataset to filter for these situations, as have  
425 the actual time and height of each measurement (though also averaged within each bin). For surface precipitation observations,  
426 no corrections for solid precipitation under-catchment were performed (the dataset is raw in the MODF); where appropriate,  
427 users are recommended to process under-catchment corrections via Kochendorfer et al. (2020).

428  
429 The ~~principal goal of the~~ present phase of the MODF concept is to [standardize/use standardized](#) data organization, metadata,  
430 and interoperability. While data quality assurance and measurement operation procedures remain in the purview of the  
431 contributing stations, considerable effort was undertaken to ensure MODF production followed a transparent, consistent, and  
432 standardized data processing chain. This includes efforts to standardize post-processing and filtering techniques (e.g., quality  
433 control methods) as much as possible for the same geophysical variable across the different sites. This consistent processing  
434 chain is another unique feature of the MODF dataset as it enforces a level of consistency across vastly different observation  
435 sites that normally follow their agencies’ own data production procedures and methods. ~~As identified~~[A summary of the](#)  
436 [processing and quality control applied for each site’s observations is provided in Tables 4-10. As discussed in more detail](#)  
437 in the below subsections, there are some cases where site-specific data processing could not be avoided; data should be used  
438 cautiously and with due consideration to each [supersite’s/site’s](#) processing techniques and quality control (QC) methods for the  
439 MODF<sub>ysm</sub>.

#### 440 4. 1 Whitehorse and Iqaluit, Canada

441 All geophysical variables observed at the Iqaluit and Whitehorse sites were processed in the same manner and included in the  
442 MODF<sub>ysm</sub> (Huang et al., [2023a](#); [2023b](#); [2023a](#)). For most geophysical variables, limited QC was performed on the raw dataset

Formatted: Not Highlight

443 with the intention to remove obvious outliers only. ~~Surface variables were checked against climatology ranges and the rate of~~  
444 ~~change thresholds, which were based on hourly criteria. Details regarding the QC performed are provided in Tables 4-5.~~ A very  
445 small number (<5%) of observations were flagged by the QC algorithm. The radiation flux observations should be treated with  
446 caution since they typically require additional QC processing prior to analysis; no additional QC was performed on these  
447 observations to account for potential frost or snow deposition on the sensors, for instance. No additional QC was performed  
448 on the cloud base height data, which was processed by the Vaisala software. Vaisala also processed the raw data feed from the  
449 radiosonde observations, which was obtained at 2 s resolution; no additional QC was performed. When no data was available  
450 (due to the instrument being down, loss of power at the site, or because it was flagged by the QC algorithm), a missing value  
451 (-9999.0) was reported in the MODF<sub>ysm</sub> (Huang et al., 2023a; 2023b) and is notated via the “missing\_value” attribute associated  
452 with each variable. Mariani et al. (2020, 2021) provides instrument validation studies and more detailed information on the  
453 quality control processing routines for the remote sensing and upper air observations.

#### 454 **4. 2 Sodankylä, Finland**

455 The Sodankylä observations included in the MODF<sub>ysm</sub> (O'Connor, 2023) are automatically uploaded every day to the FMI  
456 open access web site <https://litdb.fmi.fi/> where the data are organized on the basis of platforms and stations. Before being  
457 uploaded to the web page, the data undergo an automatic quality check to remove outliers, ~~as described in Table 6.~~ In the  
458 current MODF<sub>ysm</sub> version (O'Connor, 2023), no further quality check was applied to the data, implying that errors from several  
459 sources ~~(such as are occasionally included. These sources of error may include snow/frost deposition on radiation and~~  
460 ~~temperature sensors or absorption of solar radiation by unsheltered temperature sensors) are occasionally included.~~ In a future  
461 version of the MODF<sub>ysm</sub>, a deeper quality check will be applied to some of the variables included in the current MODF<sub>ysm</sub>  
462 (O'Connor, 2023). This quality check is based on the comparison among the same variables measured at different sites, on  
463 visual inspection and, in the case of global radiation, on the comparison with radiative transfer model calculations. This  
464 processing will enable the identification of the shortwave data affected by the shadows casted by the vegetation, of errors  
465 caused by frost formation on the domes of pyranometers, and of the error in unshaded thermometers caused by the absorption  
466 of solar radiation. As in the case of the Eureka observatory, the radiosonde data in the MODF was ingested and processed by  
467 IGRA and is available through NOAA's NCEI portal (Durre et al., 2018).

#### 468 **4. 3 Utqiaġvik (formerly barrow), USA, Tiksi, Russia and Eureka, Canada**

469 The Utqiaġvik/Barrow data within the MODF<sub>ysm</sub> (Akish ~~&and~~ Morris, 2023c) originated from both ~~Atmospheric Radiation~~  
470 ~~Measurement (DOE/ARM) and the Global Monitoring Laboratory ( and NOAA GML) datasets, with GML proving datasets~~  
471 for ozone, snow thickness, skin temperature, soil temperature profile. Value added products were generated and disseminated

472 to the users using the ARM Data Discovery interface. Both the ARM and GML datasets were ingested into a single MODF<sub>ysm</sub>  
473 with variable attribution detailing how each variable and data set was quality controlled, processed and accessed, as described  
474 in Tables 7-8, 10. The surface ozone data was collected in 1-minute intervals and was manually quality controlled and  
475 submitted to NCEI.

477 The measurements collected by the ARM facility were processed, QC analyzed, and archived at the ARM Data Center archive.  
478 The long-term Eureka and Tiksi datasets (flux tower and radiation) are hosted by the NOAA Physical Sciences Laboratory  
479 (PSL), in collaboration with ECCC (Eureka site only), and Roshydromet (Tiksi site only).

480  
481 ~~For the three sites, the~~ radiation measurements were QC'd and processed following Long ~~& Shi (2008). Heat and~~  
482 ~~improved correction of the infrared loss in diffuse shortwave measurements was included (Younkin and Long, 2003).~~  
483 ~~Turbulent heat~~ fluxes were processed and QC'd via Eddy correlation corrections including stability correction, Webb-Pearman  
484 correction, frequency correction, sensor separation correction, filtering correction, line-averaging correction, and volume-  
485 averaging correction (Cook et al. 2008, Fuehrer and Friehe 2002). Bulk corrections were also employed and utilized ARM  
486 data from the radiation, ground, met, and tower. Radiosonde data were ingested and processed by NOAA's NCEI and was  
487 processed through IGRA, following their standards (Durre et al., 2018) and is available through NOAA's NCEI portal. The  
488 IGRA 2 QA system processed the sonde data, which is based largely on the QA procedures in the IGRA 1 system (Durre et  
489 al. 2006; Durre et al. 2008). Like the IGRA 1 system, it consists of a deliberate sequence of specialized algorithms, each of  
490 which makes a binary decision on the quality of a value, level, or sounding; either the data item passes the check and remains  
491 available, or it is identified as erroneous and thus set to missing. For all ~~other observations' QC~~ observations, a ~~first-level~~  
492 ~~automated QC was established by climatology ranges in the same way as for Whitehorse and Iqaluit. A~~ second level of ~~manual~~  
493 QC was performed whereby data was reviewed by instrument mentors and ~~visually~~ assessed by the site scientist/data quality  
494 office.

#### 495 **4.4 Tiksi, Russia and Eureka, Canada**

496 ~~Data collection and processing techniques for Eureka are the same as for the Tiksi site. The long-term Eureka and Tiksi datasets~~  
497 ~~(flux tower and radiation) are hosted by the NOAA Physical Sciences Laboratory (PSL), in collaboration with ECCC (Eureka~~  
498 ~~site only), and Roshydromet (Tiksi site only). All meteorological measurements within the MODF<sub>ysm</sub> (Akish & Morris, 2023b),~~  
499 ~~i.e., air temperature, skin temperature, soil temperature, snow thickness, pressure, relative humidity, wind speed and direction,~~  
500 ~~were manually quality controlled first via an automated QC established by climatological ranges in the same way as for~~  
501 ~~Whitehorse et al. Following this, a manual/visual inspection was performed.~~ This included removing non-physical values and  
502 outliers, after confirming that they were either biased, incorrect, or collected during site maintenance periods. ~~The radiation~~



503 ~~measurements were validated and processed using the Long QCrad method (Long & Shi, 2008) and improved correction of~~  
504 ~~the infrared loss in diffuse shortwave measurements (Younkin & Long, 2004), and again, were visually inspected. The~~  
505 ~~radiosonde dataset was processed through IGRA's processing techniques and is based on the QC procedures in the IGRA-1~~  
506 ~~system (Durre et al., 2006; Durre et al., 2008). If data was not available for any of the collected measurements across any of~~  
507 ~~the variables, due to the instrument being down, loss of power at the site, or because it was flagged by the QC algorithm, a~~  
508 ~~missing value (-9999) was reported in the MODF<sub>ysm</sub> (Akish & Morris, 2023b).~~

Formatted: Font color: Auto

#### 509 4.5 Ny-Ålesund, Norway

510 The meteorological measurements used for the MODF<sub>ysm</sub> (Holt, 2023) are taken from the AWIPEV weather mast (Driemel et  
511 al., 2018; Maturilli, 2020b). Except for precipitation, all other data used in the MODF<sub>ysm</sub> for Ny-Ålesund originated from the  
512 following data sets: Maturilli, (2020a, 2020b, 2020c, 2022). The precipitation data reported in the MODF<sub>ysm</sub> are the direct  
513 instrument output and no quality checks were applied; as such this data should be treated with caution (Holt, 2023). The Ny-  
514 Ålesund observations included in the MODF<sub>ysm</sub> are a subset of those regularly uploaded in the PANGAEA data repository  
515 ([www.pangaea.de](http://www.pangaea.de)). Before being uploaded, all data undergo an automatic quality check ~~established by climatological~~  
516 ~~ranges (described in the same way as for Whitehorse et al. Table 9).~~ Following this, additional manual/visual inspection was  
517 performed ~~accounting for e.g., physical plausibility as for Utqiagvik, Tiksi, and Eureka.~~ Surface radiation data were validated  
518 and have undergone all quality checks of BSRN before archiving (Maturilli, 2020a). ~~Automated QC was performed on the~~  
519 ~~radiosonde data, established by climatological norms; a second level of data was reviewed by the instrument mentor before~~  
520 ~~storing the data at the PANGAEA repository.~~

#### 521 5 MODF Data Structure

522 The data inside a MODF comprises of all the observations listed in Table 3 for a given observation site. The data itself follows  
523 the same standardized format and structure for all observations and sites and is stored into a single NetCDF file using CF  
524 conventions. NetCDF file formatting was chosen to best accommodate the high-level of metadata detail required for merging  
525 such large quantities of individual measurements together, particularly given the need to be as transparent as possible when  
526 reporting instrument-specific details for each observation. ~~NWP model output was stored in MMDFs, matching the MODF~~  
527 ~~format to facilitate model-observation comparisons. Local maps showing the synoptic region around each site are provided in~~  
528 ~~Figure 9, with native spatial grids of the forecast models that participated in YOPPsiteMIP overlaid. This provides visual~~  
529 ~~context of where the site and the nearest NWP grid points exist in and around each site.~~

531 All  $\text{MODF}_{\text{ysm}}$  measurements provided in the data files maintained their native time cadence (typically on the order of minutely)  
532 with no averaging undertaken, and details of the collection and processing techniques can be found in the variable attributes  
533 within the files. Each DOI in Table 2 contains four (e.g., Whitehorse) or six (e.g., Utqiagvik) files, depending on whether the  
534 site had timeSeriesProfile observations on a tower/mast. The filename convention for each MODF is as follows: site name +  
535 “obs” + MODF\_featureType + start\_date + end\_date.nc.

536  
537 Guidelines for creating inventories of variable and attribute information (metadata) necessary for the MODF file attributes  
538 were published in spreadsheet format by Morris and Akish (2022). This “A-M Template” uses variable content criteria from  
539 the H-K Table to generate a metadata matrix of attribute and variable information for each of the measurements contained  
540 within the MODFs. The template has individual tabs for each of the corresponding CF metadata featureTypes (i.e., timeSeries  
541 and timeSeriesProfile) of the MODF NetCDF files, as well as one tab for the Global Attributes of the MODFs. The CF  
542 Conventions can be found here: <https://cfconventions.org/cf-conventions/cf-conventions.html>. The attributes within the  
543 template are mandatory when applicable, and serve as a guideline for MODF creators. The A-M Template is machine-readable  
544 and can be ingested into MODF software to create the final output.

545  
546 The file content is well-illustrated in Table 3; other details of the  $\text{MODF}_{\text{ysm}}$  format and structure are outlined in Uttal et al.  
547 (2023, 2024). MODFs can contain featureTypes such as timeSeries and timeSeriesProfile, which refer to time series having one  
548 and two data dimensions, respectively. In cases where data subcategories exist, featureType modifications can be depicted in  
549 the file name, for example timeSeriesProfileSonde exist for the  $\text{MODF}_{\text{ysm}}$ . Currently, more than one featureType can be used  
550 within an individual MODF file, but all subscribe to the same formatting structure and nomenclature. To generate an MODF,  
551 creators would first visit the H-K Table to determine the variables that will be included in their MODF, and then they should  
552 utilize the A-M Template to fill in the needed attribute and variables information requested by existing MODF software. Once  
553 the A-M Template has been completed, then users can ingest the template into their MODF software to create the final MODF  
554 outputs. For the  $\text{MODF}_{\text{ysm}}$ , individual toolkits were developed by MODF makers for each YOPP [supersitesite](#). Python code  
555 was developed for Whitehorse, Iqaluit and Ny-Alesund, and MATLAB code for Utqiagvik, Tiksi, Eureka and Soldankyla (see  
556 Section 6). After the generation of the  $\text{MODF}_{\text{ysm}}$  outputs, the files were run through an MODF checker that identifies the  
557 various inconsistencies or issues with the files before their upload to the MET Norway data portal. The  $\text{MODF}_{\text{ysm}}$  checker  
558 developed for the YOPPsiteMIP files is part of a larger toolkit being designed to continue the creation of MODFs.

559  
560 As an example of the uniformity of the observations (in terms of data format, post-processing, temporal cadence, etc.)  
561 contained within each [supersite'ssite's](#)  $\text{MODF}_{\text{ysm}}$  and their ~~excellent~~ data coverage during the two YOPP SOPs, Figures 310  
562 and 411 provide the surface downwelling longwave radiation and near-surface temperature observations from each  
563 [supersite'ssite's](#)  $\text{MODF}_{\text{ysm}}$  during SOP1, respectively and Figures 512 and 613 show the same except for SOP2. The MET

564 Norway data portal and MODF maker toolkit (Sect. 6) also provides plotting tools that work with any MODF or MMDF and  
565 can produce similar figures automatically. Periods of interest can be quickly identified by users and analyzed for further  
566 investigation and/or comparison with their corresponding MMDFs. MODFs significantly simplify the process of analyzing  
567 observations from multiple sites and multiple instruments, as analyses and Figures can be produced for each site using a single  
568 code that works for any observed geophysical variable and (if desired) their corresponding NWP model output in the MMDF.  
569 In contrast, without MODFs a user would have to contact each meteorological agency individually, find each sites' data  
570 repository, obtain data access privileges, find the files they need from multiple instruments, reprocess and reformat multiple  
571 uniquely-formatted datasets and file types, then develop several different codes (e.g., readers) specific to each instruments'  
572 dataset to ingest the multi-variate datasets and plot them.

573

574 The MODF<sub>ysm</sub> at Sodankylä are unique in that their measurements are collected across a series of sub-sites in the area;  
575 therefore, it is important to describe here the possible methods for extracting the data for specific locations, or for co-located  
576 measurements. The Sodankylä station comprises at least 25 distinct locations, the precise number of which is given by the  
577 dimension 'site\_id' inside the MODF data file. Each distinct location is given a unique index key in the variable 'subsite\_name',  
578 with these indices also identifying the 'lat', 'lon' and 'soil\_type' for each location. The corresponding FMI names for each  
579 location are identified in the attribute 'flag\_meanings' for the variable 'subsite\_name' via their indices; for example, the index  
580 value of 16 pointing to IOA003\_spot\_8, which is one of the automatic weather stations located in the Intensive Observations  
581 Area (IOA). There may be multiple locations providing the same measurement. However, not all locations provide the same  
582 set of measurements, and to keep the MODF compact, each measurement variable has the location dimension truncated to  
583 include only locations which measure that variable; i.e., the location dimension for the measurement variables is 'nsites\_X',  
584 where X is the number of locations making the particular measurement. This set of locations is accessed through the indices  
585 given in the attribute 'subsite\_name' for the measurement variable, which corresponds to the key given in the 'subsite\_name'  
586 variable; i.e., a subsite\_name attribute of "1, 3, 10" means that these measurements were made at the locations identified by  
587 their indices, from which their locations (latitudes and longitudes) and soil\_type can also be determined.

588

589 This method permits diverse options of collecting measurements for particular uses. All measurements, for example, at one  
590 location can be obtained by identifying the appropriate 'subsite\_name' index inside the MODF data file, iterating through the  
591 'subsite\_name' attribute of each variable to see if it contains the selected index, and, if so, selecting the column or slice of data  
592 for the data that matches the location of the index (i.e. if subsite\_name = 10 and the subsite\_name attribute for a timeSeries  
593 variable is "1, 3, 10", the measurement timeSeries for the requested location is in the third column, the next variable may have  
594 a subsite\_name attribute of "1, 3, 5, 6, 10" and the measurement timeSeries for the requested location is in the fifth column).  
595 The user could also select a specific area of interest and identify all measurements made within this region as follows: select

596 the indices for the locations within a specified latitude and longitude range, then iterate through the 'subsite\_name' attribute of  
597 each variable to see if it contains the selected indices and return the columns or slices that match them.

598

599 Note that each [supersitesite](#) conducts additional observations not listed in table 3 that will be included in upcoming updates to  
600 the  $MODF_{ysm}$  with the intent to eventually incorporate all observations into the  $MODF_{ysm}$  for each [supersitesite](#). This process  
601 of developing and appending to MODFs can be extended to other sites and/or research programs that wish to create MODFs  
602 of their observations. Given the standardized nature of the MODFs, reading and analyzing datasets from any of the YOPP  
603 [supersitesites](#) is simplified. Quick-look plotting tools have been developed via the MET Norway YOPP data portal and the  
604 MODF maker toolkit (Sect. 6), which enable near-instantaneous plotting of the observations contained within the  $MODF_{ysm}$ .

605

## 606 **6 Data and Code Availability**

607 The  $MODF_{ysm}$  for each [supersitesite](#) are available via the MET Norway YOPP Data Portal (<https://yopp.met.no/>) where they  
608 are indexed through FAIR compliant discovery metadata and can be directly accessed at:

609 [https://thredds.met.no/thredds/catalog/alertness/YOPP\\_supersite/obs/catalog.html](https://thredds.met.no/thredds/catalog/alertness/YOPP_supersite/obs/catalog.html) (Whitehorse:

610 <https://doi.org/10.21343/a33e-j150>, Iqaluit: <https://doi.org/10.21343/yrnf-ck57>, Sodankylä: <https://doi.org/10.21343/m16p->

611 [pq17](https://doi.org/10.21343/a2dx-nq55), Utqiagvik: <https://doi.org/10.21343/a2dx-nq55>, Tiksi: <https://doi.org/10.21343/5bwn-w881>, Ny-Ålesund:

612 <https://doi.org/10.21343/y89m-6393>, Eureka: <https://doi.org/10.21343/r85j-tc61>).

613

614 Proper data citation ensures appropriate credits to authors of both input data sources and merged  $MODF_{ysm}$  datasets. Data from  
615 each station has been assigned a DOI. The variable attributes of the merged data products contain information about the source  
616 datastreams and their DOIs, to more clearly establish data provenance in a traceable manner. When using data from the  
617  $MODF_{ysm}$ , it is expected that the user references the  $MODF_{ysm}$  DOI, and any subsidiary variable DOIs when available.  
618 Assigning citations for merged data streams such as the  $MODF_{ysm}$  is a challenging and still evolving concept. For example,  
619 the US ~~Department of Energy (DOE) Atmospheric Radiation Measurement (ARM)~~ Program uses a combination of DOI and  
620 citation structure for continuous data streams, as outlined in Prakash et al. (2016). They recommend when registering DOIs  
621 for derived and higher-order data, source DOIs in the metadata of the newly created DOI should be added and linked when  
622 possible.

623

624 The source code used to produce the  $MODF_{ysm}$  for each [supersitesite](#) (and MODFs in general) are available via gitlab:  
625 <https://gitlab.com/mdf-makers/mdf-toolkit>. This MODF toolkit is openly available for anyone interested in developing their  
626 own MODF file or generating quick-look plots of the data contents inside the MODFs. The toolkit is regularly updated as the

627 MODF community grows and new geophysical variables and/or functions are added. Additional site-specific python and  
628 MATLAB codes that were used to prepare the observation data files for MODF ingestion are available upon request (e.g.,  
629 contact the site principle investigator).  
630

## 631 7 Concluding Remarks

632 The enhanced ground-based observations conducted at both Poles during the YOPP fill significant and identified gaps in our  
633 current meteorological observation capabilities for the Polar Regions. YOPPsiteMIP MODFs ( $\text{MODF}_{\text{ysm}}$ ) have been published  
634 for seven of the YOPP Arctic [supersites](#), whereby all geophysical variables are stored in an identical, standardized format  
635 in a single NetCDF file following CF conventions, ~~fulfilling~~. This fulfills a key objective of the program to perform single- or  
636 multi-variate model-observation comparisons. These MODFs archive data in a manner as similar as possible to corresponding  
637 MMDF (see Uttal et al., [20232024](#)) that contain high-resolution forecast variables from a single NWP model at and around a  
638 [supersite](#) (Figure 29). Thus, combined, MODFs and MMDFs greatly simplify integration of these complex datasets,  
639 enabling further scientific study as demonstrated in the recent publications using the latest  $\text{MODF}_{\text{ysm}}$  and  $\text{MMDF}_{\text{ysm}}$  (Day et  
640 al., [20232024](#)).  
641

642 Standardized geophysical variable nomenclature, cadences, metadata, basic QC, and file structure were employed to create  
643 these files. MODFs provide the first standardized files for archiving all the different ground-based observation [supersites](#)  
644 observations, containing a multitude of geophysical variables observed by (at times) different instruments. This amalgamation  
645 of different sites' observations into a standardized, user-friendly MODF format enables easier analysis of the MODF dataset,  
646 inter-site comparisons, and detailed NWP model validation, evaluation, intercomparisons, and process-based diagnostic  
647 studies that are currently underway (see.g., Figures 310 to 6 as an example13). The further adoption, creation, and use of  
648 MODFs outside of YOPP is encouraged; a suite of tools and documentation is openly available via Gitlab (see-Sect. 6) for  
649 other site managers, researchers, and users to develop and create their own site-specific MODFs outside of YOPP or to analyze  
650 an observation sites' dataset.  
651

652 The YOPP  $\text{MODF}_{\text{ysm}}$  discussed here provide novel access to datasets of enhanced meteorological observations collected at  
653 several [supersites](#) across the Arctic. The MODF concept is not limited for use in polar regions and could be exported  
654 elsewhere. Seven YOPP-designated [supersites](#) in the Arctic developed and published  $\text{MODF}_{\text{ysm}}$  covering both SOP periods  
655 (February – March 2018 and July – September 2018), including Iqaluit, Whitehorse, and Eureka in Canada, Utqiagvik in the  
656 United States, Tiksi in Russia, Sodankylä in Finland, and Ny-Ålesund in Norway. Additional geophysical variables observed  
657 at each of these seven [supersites](#) will be included in a future update of their  $\text{MODF}_{\text{ysm}}$ , with the goal of having ~~100%~~almost

658 [all](#) of a site's observations available. Observations at most of these sites continue today beyond YOPP and are available for  
659 subsequent analyses, in some cases using updated MODFs generated in near-real time. MODF<sub>ysm</sub> for the other YOPP sites,  
660 including ship-based platforms and [supersites](#) in the Antarctic, will be made available in the future to complete the YOPP  
661 dataset. The MODF<sub>ysm</sub> described here directly ties to process-oriented verification studies aiming to improve NWP predictions  
662 at the Poles by contributing and enabling NWP inter-comparisons.

663

#### 664 **Author contributions**

665 SM, ZM, and TU wrote the first draft of the manuscript. SM and ZM conducted scientific analyses and created tables and  
666 figures with JD and JT. All authors managed data archiving, creation of the MODF<sub>ysm</sub>, and publication to the MET Norway  
667 YOPP Data Portal. All authors contributed to the writing and the editing of the manuscript.

668

#### 669 **Competing interests**

670 The authors declare that they have no conflict of interest.

671

#### 672 **Disclaimer**

673 Use of specific instrument manufacturers/models and suppliers mentioned in the manuscript and/or used at the  
674 [supersites](#) is not a commercial endorsement of their products.

675

#### 676 **Acknowledgements**

677 This is a contribution to the Year of Polar Prediction (YOPP), a flagship activity of the Polar Prediction Project (PPP), initiated  
678 by the World Weather Research Programme (WWRP) of the World Meteorological Organisation (WMO). We acknowledge  
679 the WMO WWRP for its role in coordinating this international research activity. This study was supported by NOAA's Global  
680 Ocean Monitoring and Observing Program through the Arctic Research Program (FundRef:  
681 <https://doi.org/10.13039/100018302>)-<https://doi.org/10.13039/100018302>). Special thanks to the station technicians and  
682 operators at the [supersites](#) for deploying instruments, maintenance, and technical services. In particular, thank you to the  
683 radiosonde operators for providing extra daily sonde launches during the two SOP periods. Thank you to Jenn Glaser for her  
684 contract work in creating the station graphic in Figure 1, and to Kyrie Newby and Calvin Jesse for [updating](#) [creating](#) the Google

685 Earth images in Figure 29. JD was supported by the European Union funded INTERACTIII project (Grant Agreement:  
686 871120). AK and LMH were supported in part by NOAA cooperative agreements NA17OAR4320101 and  
687 NA22OAR4320151. Portions of the  $MODF_{\text{ysm}}$  data were obtained from the Atmospheric Radiation Measurement (ARM) user  
688 facility, a U.S. Department of Energy (DOE) office of science user facility managed by the biological and environmental  
689 research program. Thank you to MET Norway for hosting the YOPP data portal. All data products are produced by their  
690 respective institutions and are available via the YOPP data portal (<https://yopp.met.no>) and directly at:  
691 [https://thredds.met.no/thredds/catalog/alertness/YOPP\\_supersite/obs/catalog.html](https://thredds.met.no/thredds/catalog/alertness/YOPP_supersite/obs/catalog.html).  
692  
693

694 **References**

- 695 Akish, E., & Morris, S.: MODF for Eureka, Canada, during YOPP SOP1 and SOP2, Norwegian Meteorological Institute,  
696 [dataset, https://doi.org/10.21343/R85J-TC61](https://doi.org/10.21343/R85J-TC61), 2023a.
- 697
- 698 Akish, E., & Morris, S.: MODF for Tiksi, Russia, during YOPP SOP1 and SOP2, Norwegian Meteorological Institute,  
699 [dataset, https://doi.org/10.21343/SBWN-W881](https://doi.org/10.21343/SBWN-W881), 2023b.
- 700
- 701 Akish, E., & Morris, S.: MODF for Utqiagvik, Alaska, during YOPP SOP1 and SOP2, Norwegian Meteorological  
702 Institute, [dataset, https://doi.org/10.21343/A2DX-NQ55](https://doi.org/10.21343/A2DX-NQ55), 2023c.
- 703
- 704 Baldocchi, D.: Measuring fluxes of trace gases and energy between ecosystems and the atmosphere – the state and future of  
705 the eddy covariance method. *Global Change Biology* (2014)20, 3600–3609, <https://doi.org/10.1111/gcb.12649>, 2014.
- 706
- 707 [Becherini, F., Vitale, V., Lupi, A. et al. Surface albedo and spring snow melt variations at Ny-Ålesund, Svalbard. \*Bull. of\*  
708 \*Atmos. Sci. & Technol.\* 2, 14 \(2021\). <https://doi.org/10.1007/s42865-021-00043-8>.](https://doi.org/10.1007/s42865-021-00043-8)
- 709
- 710 Cassano, J. J., Higgins, M. E., and Seefeldt, M. W.: Performance of the Weather Research and Forecasting Model for  
711 Month-Long Pan-Arctic Simulations, *Monthly Weather Review*, 139, 3469–3488, [doi: 10.1175/mwr-d-10-05065.1](https://doi.org/10.1175/mwr-d-10-05065.1), 2011.
- 712
- 713 Cohen, J., Rautiainen, K., Lemmetyinen, J., Smolander, T., Vehvilainen, J., and Pulliainen, J.: Sentinel-1 based soil  
714 freeze/thaw estimation in boreal forest environments, *Remote Sens Environ*, 254, [ARTN  
112267https://doi.org/10.1016/j.rse.2020.112267](https://doi.org/10.1016/j.rse.2020.112267), 2021.
- 715
- 716 [Cook, B.I., Bonan, G.B., Levis, S. et al. \*10.1016/j.rse.2020.112267\*, 2021-](https://doi.org/10.1016/j.rse.2020.112267)
- 717 [The thermoinsulation effect of snow cover within a climate model. \*Clim Dyn\* 31, 107–124. \[https://doi.org/10.1007/s00382-\]\(https://doi.org/10.1007/s00382-007-0341-y\)](https://doi.org/10.1007/s00382-007-0341-y)
- 718 [007-0341-y](https://doi.org/10.1007/s00382-007-0341-y), 2008.
- 719
- 720
- 721 Cox, C.J., Stone, R.S., Douglas, D.C., Stanitski, D.M., Divoky, G.J., Dutton, E.S., Sweeney, C., George, J.C., and  
722 Longenecker, D.U.: Drivers and Environmental Responses to the Changing Annual Snow Cycle of Northern Alaska, *B Am*  
723 *Meteorol Soc*, 98, 2559–2577, <https://doi.org/10.1175/BAMS-D-16-0201.1>, 2017.
- 724
- 725 Cox, C.J., Walden, V.P., and Rowe, P.M.: A Comparison of the atmospheric conditions at Eureka, Canada, and Barrow,  
726 Alaska (2006–2008), *J Geophys Res*, 117, <https://doi.org/10.1029/2011JD017164>, 2012.
- 727
- 728 Day, J.J., Sandu, I., Magnusson, L., Rodwell, M.J., Lawrence, H., Bormann, N., and Jung, T.: Increased Arctic influence on  
729 the midlatitude flow during Scandinavian Blocking episodes, *Q.J.R. Meteorol. Soc.*, 725, 3846–3862,  
730 <https://doi.org/10.1002/qj.3673>, 2019.
- 731
- 732 Day, J., Svensson, G., Casati, B., Uttal, T., Khalsa, S.J., Bazile, E., Akish, E., Azouz, N., Ferrighi, L., Frank, H., Gallagher,  
733 M., Godoy, Ø., Hartten, L., Huang, L., Holt, J., Di Stefano, M., Mariani, Z., Morris, S., O’Connor, E., Pirazzini, R., Remes,  
734 T., Fadeev, R., Solomon, A., Tjerström, J., and Tolstykh, M.: The YOPP site Model Intercomparison Project (YOPPsiteMIP)  
735 phase I: project overview and Arctic winter forecast evaluation, [20232024](https://doi.org/10.5194/gmd-2023-2024), submitted to *Geoscientific Model Development*  
736 *(GMD) August 25, 2023* –submitted - under review 2024.

Formatted: Font color: Blue

Formatted: Font color: Blue

Formatted: Font color: Blue

Formatted: Font color: Blue



737  
738 Driemel A, Augustine JA, Behrens K, Colle S, Cox C, Cuevas-Agulló E, Denn FM, Duprat T, Fukuda M, Grobe H,  
739 Haeffelin M, Hyett N, Ijima O, Kallis A, Knap W, Kustov V, Long CN, Longenecker D, Lupi A, Maturilli M, Mimouni M,  
740 Ntsangwane L, Ogihara H, Olano X, Olefs M, Omori M, Passamani L, Pereira EB, Schmithüsen H, Schumacher S, Sieger R,  
741 Tamlyn J, Vogt R, Vuilleumier L, Xia X, O A, König-Langlo G. Baseline Surface Radiation Network (BSRN): structure and  
742 data description (1992–2017) *Earth Syst Sci Data*, 10, 1491–1501, 2018.

743  
744 Durre, I., Menne, M. J., and Vose, R. S.: Strategies for evaluating quality assurance procedures, *J Appl Meteorol Clim*, 47,  
745 1785-1791, [doi:10.1175/2007jamc1706.1](https://doi.org/10.1175/2007jamc1706.1), 2008.

746  
747 Durre, I., Vose, R. S., and Wuertz, D. B.: Overview of the Integrated Global Radiosonde Archive, *J Climate*, 19, 53-68,  
748 [doi:10.1175/Jcli3594.1](https://doi.org/10.1175/Jcli3594.1), 2006.

749  
750 Durre, I., Yin, X., Vose, R. S., Applequist, S., and Arnfield, J.: Enhancing the Data Coverage in the Integrated Global  
751 Radiosonde Archive. *J. Atmos. Oceanic Technol.*, 35, 1753–1770, <https://doi.org/10.1175/JTECH-D-17-0223.1>, 2018.

752  
753 Fogal, P. F., LeBlanc, L. M., and Drummond, J. R.: The Polar Environment Atmospheric Research Laboratory (PEARL):  
754 Sounding the Atmosphere at 80 degrees North, Arctic, 66, 377-386, 2013.

755  
756 [Fuehrer, P.L., Friehe, C.A. Flux Corrections Revisited. \*Boundary-Layer Meteorology\* 102, 415–458.](https://doi.org/10.1023/A:1013826900579)  
757 <https://doi.org/10.1023/A:1013826900579>, 2002.

758  
759 Gallagher & Tjernström: Accelerating research in weather prediction and model improvement with new free community  
760 open source software tools. To be submitted, 2024.

761  
762 Goessling, H. F., Jung, T., Klebe, S., Baeseman, J., Bauer, P., Chen, P., Chevallier, M., Dole, R., Gordon, N., Ruti, P.,  
763 Bradley, A., Bromwich, D. H., Casati, B., Chechin, D., Day, J. J., Massonnet, F., Mills, B., Renfrew, I., Smith, G., and  
764 Tatusko, R.: Paving the Way for the Year of Polar Prediction, *B Am Meteorol Soc*, 97, Es85-Es88, [doi:10.1175/Bams-D-](https://doi.org/10.1175/Bams-D-15-00270.1)  
765 [15-00270.1](https://doi.org/10.1175/Bams-D-15-00270.1), 2016.

766  
767 [Gordon, M., Biswas, S., Taylor, P. A., Hanesiak, J., Albarran-Melzer, M., and Fargey, S.: Measurements of Drifting and](https://doi.org/10.3137/Ao1105.2010)  
768 [Blowing Snow at Iqaluit, Nunavut, Canada during the STAR Project, \*Atmos Ocean\*, 48, 81–100, 10.3137/Ao1105.2010,](https://doi.org/10.3137/Ao1105.2010)  
769 [2010.](https://doi.org/10.3137/Ao1105.2010)

770  
771 Hannula, H. R., Lemmetyinen, J., Kontu, A., Derksen, C., and Pulliainen, J.: Spatial and temporal variation of bulk snow  
772 properties in northern boreal and tundra environments based on extensive field measurements, *Geosci Instrum Meth*, 5, 347-  
773 363, [doi:10.5194/gi-5-347-2016](https://doi.org/10.5194/gi-5-347-2016), 2016.

774  
775 Hartten, L. M. and Khalsa, S. J. S.: The H-K Variable SchemaTable developed for the YOPPsiteMIP (1.2), Zenodo,  
776 <https://doi.org/10.5281/zenodo.6463464>, 2022.

777  
778 Hinkel, K.M. and Nelson, F.E.: Anthropogenic heat island at Barrow, Alaska, during winter: 2001-2005, *J Geophys*  
779 *Research*, 112, <https://doi.org/10.1029/2006JD007837>, 2007.

780  
781 Holt, J.: Merged Observatory Data File (MODF) for Ny Alesund, Norwegian Meteorological Institute, [dataset](https://doi.org/10.21343/Y89M-6393),  
782 <https://doi.org/10.21343/Y89M-6393>, 2023.  
783  
784 Huang, L., Mariani, Z., & Crawford, R.: MODF for Erik Nielsen Airport, Whitehorse, Canada during YOPP SOP1 and  
785 SOP2, Norwegian Meteorological Institute, [dataset](https://doi.org/10.21343/A33E-J150), <https://doi.org/10.21343/A33E-J150>, 2023a.  
786  
787 Huang, L., Mariani, Z., & Crawford, R.: MODF for Iqaluit Airport, Iqaluit, Nunavut, Canada during YOPP SOP1 and  
788 SOP2, Norwegian Meteorological Institute, [dataset](https://doi.org/10.21343/YRNF-CK57), <https://doi.org/10.21343/YRNF-CK57>, 2023b.  
789  
790 Illingworth, A. J., Cimini, D., Gaffard, C., Haeffelin, M., Lehmann, V., Lohnert, U., O'Connor, E. J., and Ruffieux, D.:  
791 Exploiting Existing Ground-Based Remote Sensing Networks to Improve High-Resolution Weather Forecasts, *B Am*  
792 *Meteorol Soc*, 96, 2107-2125, [doi: 10.1175/Bams-D-13-00283.1](https://doi.org/10.1175/Bams-D-13-00283.1), 2015.  
793  
794 Joe, P., Melo, S., Burrows, W. R., Casati, B., Crawford, R. W., Deghan, A., Gascon, G., Mariani, Z., Milbrandt, J., and  
795 Strawbridge, K.: The Canadian Arctic Weather Science Project Introduction to the Iqaluit Site, *B Am Meteorol Soc*, 101,  
796 E109-E128, [doi: 10.1175/Bams-D-18-0291.1](https://doi.org/10.1175/Bams-D-18-0291.1), 2020.  
797  
798 Jung, T., Gordon, N. D., Bauer, P., Bromwich, D. H., Chevallier, M., Day, J. J., Dawson, J., Doblus-Reyes, F., Fairall, C.,  
799 Goessling, H. F., Holland, M., Inoue, J., Iversen, T., Klebe, S., Lemke, P., Losch, M., Makshtas, A., Mills, B., Nurmi, P.,  
800 Perovich, D., Reid, P., Renfrew, I. A., Smith, G., Svensson, G., Tolstykh, M., and Yang, Q. H.: Advancing Polar Prediction  
801 Capabilities on Daily to Seasonal Time Scales, *B Am Meteorol Soc*, 97, 1631-+, [doi: 10.1175/Bams-D-14-00246.1](https://doi.org/10.1175/Bams-D-14-00246.1), 2016.  
802  
803 Kochendorfer, J., M. Earle, D. Hodyss, A. Reverdin, Y-A. Roulet, R. Nitu, R. Rasmussen, S. Landolt, S. Buisan, and T.  
804 Laine: Undercatch Adjustments for Tipping-Bucket Gauge Measurements of Solid Precipitation. *J. Hydrometeor.*, 21, 1193-  
805 1205, <https://doi.org/10.1175/JHM-D-19-0256.1>, 2020.  
806  
807 Koltzow, M., Casati, B., Bazile, E., Haiden, T., and Valkonen, T.: An NWP Model Intercomparison of Surface Weather  
808 Parameters in the European Arctic during the Year of Polar Prediction Special Observing Period Northern Hemisphere 1,  
809 *Weather Forecast*, 34, 959-983, [doi: 10.1175/Waf-D-19-0003.1](https://doi.org/10.1175/Waf-D-19-0003.1), 2019.  
810  
811 Lawrence, H., Bormann, N., Sandu, I., Day, J., Farnan, J., and Bauer, P.: Use and impact of Arctic observations in the  
812 ECMWF Numerical Weather Prediction system, *Q J Roy Meteor Soc*, 145, 3432-3454, [doi: 10.1002/qj.3628](https://doi.org/10.1002/qj.3628), 2019.  
813  
814 Lesins, G., Duck, T. J., and Drummond, J. R.: Climate trends at Eureka in the Canadian high arctic, *Atmos Ocean*, 48, 59-80,  
815 [doi: 10.3137/AO1103.2010](https://doi.org/10.3137/AO1103.2010), 2010.  
816  
817 Long, C. N. and Shi, Y.: An Automated Quality Assessment and Control Algorithm for Surface Radiation Measurements,  
818 *Open Atmospheric Science Journal*, 23-37, [doi: 10.2174/1874282300802010023](https://doi.org/10.2174/1874282300802010023), 2008.  
819  
820 Luojus, K., Pulliainen, J., Takala, M., Lemmetyinen, J., Mortimer, C., Derksen, C., Mudryk, L., Moisaner, M., Hiltunen,  
821 M., Smolander, T., Ikonen, J., Cohen, J., Salminen, M., Norberg, J., Veijola, K., and Venalainen, P.: GlobSnow v3.0

Formatted: Font color: Blue

Formatted: Font color: Blue

Formatted: Font color: Blue

Formatted: Font color: Blue

822 Northern Hemisphere snow water equivalent dataset, *Sci Data*, 8, ARTN 463, <https://doi.org/10.1038/s41597-021-00939-2>,  
823 2021.  
824  
825 Mariani, Z., Crawford, R., Casati, B., and Lemay, F.: A Multi-Year Evaluation of Doppler Lidar Wind-Profile Observations  
826 in the Arctic, *Remote Sens-Basel*, 12, ARTN 323, [10.3390/rs12020323](https://doi.org/10.3390/rs12020323), <https://doi.org/10.3390/rs12020323>, 2020.  
827  
828 Mariani, Z.; Hicks-Jalali, S.; Strawbridge, K.; Gwozdecky, J.; Crawford, R.W.; Casati, B.; Lemay, F.; Lehtinen, R.;  
829 Tuominen, P.: Evaluation of Arctic Water Vapor Profile Observations from a Differential Absorption Lidar. *Remote*  
830 *Sens.* 2021, 13, 551. <https://doi.org/10.3390/rs13040551>, 2021.  
831  
832 Mariani, Z., Dehghan, A., Gascon, G., Joe, P., Hudak, D., Strawbridge, K., and Corriveau, J.: Multi-Instrument Observations  
833 of Prolonged Stratified Wind Layers at Iqaluit, Nunavut, *Geophys Res Lett*, 45, 1654-1660, doi: 10.1002/2017gl076907,  
834 2018.  
835  
836 Mariani, Z., Hicks-Jalali, S., Strawbridge, K., Gwozdecky, J., Crawford, R. W., Casati, B., Lemay, F., Lehtinen, R., and  
837 Tuominen, P.: Evaluation of Arctic Water Vapor Profile Observations from a Differential Absorption Lidar, *Remote Sens-*  
838 *Basel*, 13, ARTN 551, [10.3390/rs13040551](https://doi.org/10.3390/rs13040551), 13(4), 551, <https://doi.org/10.3390/rs13040551>, 2021.  
839  
840 Mariani, Z., Huang, G., Crawford, R., Blanchet, J. P., Hicks-Jalali, S., Mekis, E., Pelletier, P., Rodriguez, P., and  
841 Strawbridge, K.: Enhanced automated meteorological observations at the Canadian Arctic weather science (CAWS)  
842 supersites, *Earth System Science Data*, 2022-14, 4995-5017, <https://doi.org/10.5194/essd-14-4995-2022>, 2022.  
843  
844 Maturilli, M., Herber, A., and König-Langlo, G.: Climatology and time series of surface meteorology in Ny-Ålesund, Svalbard,  
845 *Earth Syst. Sci. Data*, 5, 155-163, <https://doi.org/10.5194/essd-5-155-2013>, 2013.  
846  
847 Maturilli, M.: Basic and other measurements of radiation at station Ny-Ålesund (2006-05 et seq). Alfred Wegener Institute -  
848 Research Unit Potsdam, PANGAEA, <https://doi.org/10.1594/PANGAEA.914927>, 2020a.  
849  
850 Maturilli, M.: Continuous meteorological observations at station Ny-Ålesund (2011-08 et seq). Alfred Wegener Institute -  
851 Research Unit Potsdam, PANGAEA, <https://doi.org/10.1594/PANGAEA.914979>, 2020b.  
852  
853 Maturilli, M.: High resolution radiosonde measurements from station Ny-Ålesund (2017-04 et seq). Alfred Wegener Institute  
854 - Research Unit Potsdam, PANGAEA, <https://doi.org/10.1594/PANGAEA.914973>, 2020c.  
855  
856 Maturilli, M.: Ceilometer cloud base height from station Ny-Ålesund (2017-08 et seq). Alfred Wegener Institute - Research  
857 Unit Potsdam, PANGAEA, <https://doi.org/10.1594/PANGAEA.942331>, 2022.  
858  
859 Maturilli, M., Hanssen-Bauer, I., Neuber, R., Rex, M., and Edvardsen, K.: The Atmosphere above Ny-Ålesund – Climate  
860 and global warming, ozone and surface UV radiation / Hop, H. and Wiencke, C. (editors), *Advances in Polar Ecology, The*  
861 *Ecosystem of Kongsfjorden, Svalbard*, Springer, ISBN: 978-3-319-46423-7, doi:10.1007/978-3-319-46425-1\_2, 2019.  
862  
863 Mikola, J., Virtanen, T., Linkosalmi, M., Vaha, E., Nyman, J., Postanogova, O., Rasanen, A., Kotze, D. J., Laurila, T.,  
864 Juutinen, S., Kondratyev, V., and Aurela, M.: Spatial variation and linkages of soil and vegetation in the Siberian Arctic

Formatted: c-bibliographic-information\_\_value

865 tundra - coupling field observations with remote sensing data, Biogeosciences, 15, 2781-2801, [doi: 10.5194/bg-15-2781-](https://doi.org/10.5194/bg-15-2781-2018)  
866 2018, 2018.

867

868 Morris, S. M. and Akish, E.: A-M Variable ~~&~~ Attribute Template Table developed for the YOPPSiteMIP (1.2), Zenodo,  
869 <https://doi.org/10.5281/zenodo.6974550>, 2022.

870

871 NCCS: Climate in Svalbard 2100 – a knowledge base for climate adaptation, [2018-ISSN 2387-3027,](https://doi.org/10.25607/OBP-888)  
872 <http://dx.doi.org/10.25607/OBP-888>, 2018.

873

874 O'Connor, E.: Merged observation data file for Sodankyla, Norwegian Meteorological Institute, [dataset,](https://doi.org/10.21343/M16P-PQ17)  
875 <https://doi.org/10.21343/M16P-PQ17>, 2023.

876

877 Ohmura, A., Dutton, E.G., Forgan, B., Frohlich, C., Gilgen, H., Hegner, H., Heimo, A., Konig-Langlo, G., McArther, B.,  
878 Muller, G., Philipona, R., Pinker, R., Whitlock, C.H., Dehne, K., and Wild, M.: Baseline Surface Radiation Network  
879 (BSRN/WCRP): New Precision Radiometry for Climate Research, B Am Meteorol Soc, 79, 2115-2136,  
880 [https://doi.org/10.1175/1520-0477\(1998\)079<2115:BSRNBW>2.0.CO;2](https://doi.org/10.1175/1520-0477(1998)079<2115:BSRNBW>2.0.CO;2), 1998.

881

882 Persson, O. and Stone, R.: Evidence of forcing of Arctic regional climates by mesoscale processes, AMS Symposium on  
883 Connection Between Mesoscale Processes and Climate Variability, San Antonio, Texas, 15-16 January 2007, 2.6,  
884 [https://ams.confex.com/ams/87ANNUAL/techprogram/paper\\_119015.htm](https://ams.confex.com/ams/87ANNUAL/techprogram/paper_119015.htm), 2007.

885

886 ~~Pinard, J. D. J. P., Benoit, R., and Yu, W.: A WEST wind climate simulation of the mountainous Yukon, Atmos Ocean, 43,~~  
887 ~~259-282, DOI 10.3137/ao.430306, 2005.~~

888

889 Pollard, W. H. and Bell, T.: Massive Ice Formation in the Eureka Sound Lowlands: A Landscape Model, PERMAFROST -  
890 Seventh International Conference, Yellowknife, Canada, Collection Nordicana, 1998.

891

892 Pollard, W. H., Ward, M. A., and Becker, M. S.: The Eureka Sound lowlands: an ice-rich permafrost landscape in transition,  
893 Dept. of Geography, McGill University, <https://members.cgs.ca/documents/conference2015/GeoQuebec/papers/402.pdf>,  
894 2015.

895

896 Prakash, G., Shrestha, B., Younkin, K., Jundt, R., Martin, M., and Elliott, J.: Data Always Getting Bigger—A Scalable DOI  
897 Architecture for Big and Expanding Scientific Data, 1, 11, 2016.

898

899 Rantanen, M., Karpechko, A. Y., Lipponen, A., Nordling, K., Hyvarinen, O., Ruosteenoja, K., Vihma, T., and Laaksonen,  
900 A.: The Arctic has warmed nearly four times faster than the globe since 1979, Commun Earth Environ, [3, ARTN 168](https://doi.org/10.1038/s43247-022-00498-3)  
901 <https://doi.org/10.1038/s43247-022-00498-3>, 2022.

902

903 Rautiainen, K., Parkkinen, T., Lemmetyinen, J., Schwank, M., Wiesmann, A., Ikonen, J., Derksen, C., Davydov, S.,  
904 Davydova, A., Boike, J., Langer, M., Drusch, M., and Pulliainen, J.: SMOS prototype algorithm for detecting autumn soil  
905 freezing, Remote Sens Environ, 180, 346-360, [doi: 10.1016/j.rse.2016.01.012](https://doi.org/10.1016/j.rse.2016.01.012), 2016.

906

Formatted: Font color: Blue

Formatted: Font color: Blue

907 Sellmann, P.V., Brown, J., Lewellen, R., McKim, H.L., Merry, C.J.: The classification and geomorphic implications of thaw  
908 lakes on the Arctic coastal plain, Alaska. Cold Regions Research and Engineering Laboratory (CRREL); CRREL-No. 344,  
909 <https://hdl.handle.net/11681/5852>, 1975.

910

911 Shupe, M.D.: Clouds at Arctic Atmospheric Observatories. Part II: Thermodynamic Phase Characteristics, *J Appl Meteorol*  
912 *Clim*, 50, 645-661, <https://doi.org/10.1175/2010JAMC2468.1>, 2011.

913

914 Shupe, M.D., Walden, V.P., Eloranta, E., Uttal, T., Campbell, J.R., Starkweather, S.M., and Shiobara, M.: Clouds at Arctic  
915 Atmospheric Observatories. Part I: Occurrence and Macrophysical Properties, *J Appl Meteorol Clim*, 50, 626-644,  
916 <https://doi.org/10.1175/2010JAMC2467.1>, 2011.

917

918 Stone, R.S., Dutton, E.G., Harris, J.M., and Longenecker, D.: Earlier spring snowmelt in northern Alaska as an indicator of  
919 climate change, *J Geophys Research*, 107, <https://doi.org/10.1029/2000JD000286>, 2002.

920

921 Tremblay, S., Picard, J.-C., Bachelder, J. O., Lutsch, E., Strong, K., Fogal, P., Leaitch, W. R., Sharma, S., Kolonjari, F., Cox,  
922 C. J., Chang, R. Y.-W. and Hayes, P. L.: Characterization of aerosol growth events over Ellesmere Island during the  
923 summers of 2015 and 2016, *Atmos. Chem. Phys.*, 19, 5589-5604, [doi: 10.5194/acp-19-5589-2019](https://doi.org/10.5194/acp-19-5589-2019).

924

925 Uttal, T., Makshtas, A. and Laurila, T.: The Tiksi International Hydrometeorological Observatory - An Arctic Members  
926 Partnership, *WMO Bulletin Vol 62 (1) – 2013*, 2013.

927

928 Uttal, T., Hartten, L.M., Khalsa, S.J., Casati, B., Svensson, G., Day, J., Gallagher, M., Holt, J., Akish, E., Morris, S.,  
929 O'Connor, E., Pirazzini, R., Huang, L., Crawford, R., Mariani, Z., Godoy, Ø., Tjernström, J.A.K., Prakesh, G., Hickmon, N.,  
930 Maturilli, M., and Cox, C.: Merged Observatory Data Files (MODFs): An Integrated Research Data Product Supporting  
931 Process Oriented Investigations and Diagnostics, *2023/2024, submitted to Model Intercomparison and Improvement Projects*  
932 *(MIIPs) for the polar regions and beyond (GMD/ESSD inter-journal SI) submitted October 17, 2023 – under review 2024*.

933

934 Verlinde, J., Zak, B. D., Shupe, M. D., Ivey, M. D., and Stamnes, K.: The ARM North Slope of Alaska (NSA) Sites, *Meteor*  
935 *Mon*, 57, [doi: 10.1175/Amsmonographs-D-15-0023.1](https://doi.org/10.1175/Amsmonographs-D-15-0023.1), 2016.

936

937 Weaver, D., Strong, K., Schneider, M., Rowe, P. M., Sioris, C., Walker, K. A., Mariani, Z., Uttal, T., McElroy, C. T.,  
938 Vömel, H., Spassiani, A., and Drummond, J. R.: Intercomparison of atmospheric water vapour measurements at a  
939 Canadian High Arctic site, *Atmos. Meas. Tech.*, 10, 2851–2880, <https://doi.org/10.5194/amt-10-2851-2017>, 2017.

940

941 Widener, K., Bharadwaj, N., and Johnson, K.: Ka-Band ARM Zenith Radar (KAZR) Instrument Handbook, United States  
942 Department of Energy (USDOE), <https://doi.org/10.2172/1035855>, 2012.

943

944 WMO: Guide to Meteorological Instruments and Methods of Observation. WMO-No.8, Geneva, Switzerland, ISBN: 978-  
945 92-63-10008-5, <https://library.wmo.int/idurl/4/68662>, 2021.

946

947 Wohner, C., Peterseil, J., and Klug, H.: Designing and implementing a data model for describing environmental monitoring  
948 and research sites, *Ecol Inform*, 70, [ARTN 101708https://doi.org/10.1016/j.ecoinf.2022.101708, 2022](https://doi.org/10.1016/j.ecoinf.2022.101708),  
949 [10.1016/j.ecoinf.2022.101708, 2022](https://doi.org/10.1016/j.ecoinf.2022.101708).

950  
951 Younkin, K. and Long, C.: Improved Correction of IR Loss in Diffuse Shortwave Measurements: An ARM Value-Added  
952 Product, PNNL; Richland, WA, United States, Medium: ED, [doi: 10.2172/1020732](https://doi.org/10.2172/1020732), 2003.  
953

954  
955  
956

957

958

959 **Table 1.** List of facility coordinates for locations where  $MODF_{vsm}$  measurements were collected at each site. The measured variables that  
960 are observed at each site are listed (refer to Table 3). In some cases, the same variable is measured at multiple locations for a single site;  
961 these observations and their corresponding coordinates are embedded within the MODF.

|  | <b>Facility Name</b>   | <b>Coordinates</b>  | <b>Measured Variables</b>   |
|--|--|---|---|
| <i>"All" refers to the entire list of the measured variables in Table 3, whereas "All radiation" refers to all radiation-related measured variables.</i> |  |   |   |
|  | <b>Facility Name</b>   | <b>Coordinates</b>  | <b>Measured Variables (from Table 3)</b>  |
| <b>Whitehorse</b>  | Whitehorse   | N60.71,<br>W135.07  | All   |
| <b>Iqaluit</b>   | Iqaluit  | N63.74,<br>W68.51   | All   |
| <b>Sodankylä</b>   | Operative Sounding Station Area; Automatic Weather Station (LUOxxxx) | N67.366618 -<br>N67.367220,<br>E26.628253 -<br>E26.63144  | Pressure, Visibility  |
|  | CO2 Flux Mast Area (VUOxxxx)   | N67.361883,<br>E26.643003 -<br>E26.64323                  | Total precipitation of water, all wind, vertical velocity, temperature, dew-point temperature, relative humidity, snow thickness, all radiation, cloud base height                        |
|  | Intensive Observation Area (IOAxxxx)                                 | N67.361654 -<br>N67.361950,<br>E26.633190 -<br>E26.634191 | Temperature, relative humidity, snow thickness, snowfall flux, snow water equivalent, all short-wave radiation, soil temperature profile, soil moisture, snow temperature                 |
|  | Lichen Fence (JAKxxxx)   | N67.36710 -<br>N67.36716,<br>E26.634740 -<br>E26.63513    | All radiation   |
|  | Micrometeorological Mast Area (METxxxx)                              | N67.361711 -<br>N67.36216,<br>E26.63726 -<br>E26.65117    | All wind, temperature, vertical velocity, relative humidity, snow thickness, all radiation, all heat fluxes, friction velocity, soil temperature profile, soil moisture, snow temperature |
|  | Peatland Area (SUOxxxx)  | N67.361903 -<br>N67.36707,<br>E26.633802 -<br>E26.654067  | Temperature, dew-point temperature, relative humidity, snow thickness, all short-wave radiation, soil temperature profile, soil moisture, snow temperature                                |
| <b>Utqiagvik</b>   | ARM Facility   | N71.19228,<br>W156.3654                                   | All except ozone concentration, snow thickness, and soil temperature profile  |
|  | GML Barrow Atmospheric Baseline Observatory                          | N71.3230,<br>W156.6114                                    | Ozone concentration, snow thickness, and soil temperature profile   |
| <b>Tiksi</b>   | Baseline Surface Radiation Network (BSRN)                            | N71.5862,<br>E128.9188                                    | All radiation observations  |
|  | Fluxtower  | N71.595,<br>E128.882                                      | All except radiation observations   |
| <b>Ny-Ålesund</b>  | Baseline Surface Radiation Network (BSRN)                            | N78.92278,<br>E11.92725                                   | All radiation observations, pressure, cloud base height   |
|  | AWIPEV Met.Tower   | N78.92226,<br>E11.92667                                   | All wind, temperature, relative humidity, specific humidity   |
|  | Balloon Launch Facility  | N78.92301,<br>E11.92271                                   | All timeSeriesProfileSonde observations   |
| <b>Eureka</b>  | Baseline Surface Radiation Network (BSRN)                            | N79.989,<br>W85.9404                                      | All radiation observations  |

Formatted: Font: Not Bold

Formatted Table

Formatted: Font: Not Bold

Formatted: Font: Not Bold

Formatted: Font: Not Bold

Formatted: Font: Not Bold

Formatted: Font: Not Bold

Formatted: Font: Not Bold

|              |                       |  |
|--------------|-----------------------|--|
| Fluxtower    | N80.083,<br>W86.417   | Pressure, all wind, temperature, relative humidity,<br>snow thickness, ground heat flux, soil temperature<br>profile |
| Sonde Launch | N79.9833,<br>W85.9333 | All timeSeriesProfileSonde observations  |

**Table 1.** List of facility coordinates for locations where  $MODF_{y_{sm}}$  measurements were collected at each of the supersite locations. The variables (listed in Table 3) that are measured at each location are listed.



966 **Table 2.** List of final DOIs for each site's MODF<sub>YMB</sub>.

967 ~~In some cases, the same variable is measured at multiple locations for a single site; these observations and their corresponding coordinates~~  
968 ~~are embedded within the MODF.~~

969

970

971

| DOI   | Title  | Citation              |
|---|--|-----------------------|
| <b>Whitehorse</b> , <a href="https://doi.org/10.21343/a33e-j150">https://doi.org/10.21343/a33e-j150</a> | MODF for Erik Nielsen Airport, Whitehorse, Canada during YOPP SOP1 and SOP2  | Huang et al., 2023a   |
| <b>Iqaluit</b> , <a href="https://doi.org/10.21343/yymf-ck57">https://doi.org/10.21343/yymf-ck57</a>    | MODF for Iqaluit Airport, Iqaluit, Nunavut, Canada during YOPP SOP1 and SOP2 | Huang et al., 2023b   |
| <b>Sodankylä</b> , <a href="https://doi.org/10.21343/m16p-pq17">https://doi.org/10.21343/m16p-pq17</a>  | Merged observation data file for Sodankylä                                   | O'Connor, 2023        |
| <b>Utqiagvik</b> , <a href="https://doi.org/10.21343/a2dx-nq55">https://doi.org/10.21343/a2dx-nq55</a>  | MODF for Utqiagvik, Alaska, during YOPP SOP1 and SOP2                        | Akish & Morris, 2023c |
| <b>Tiksi</b> , <a href="https://doi.org/10.21343/5bwn-w881">https://doi.org/10.21343/5bwn-w881</a>      | MODF for Tiksi, Russia, during YOPP SOP1 and SOP2                            | Akish & Morris, 2023b |
| <b>Ny-Ålesund</b> , <a href="https://doi.org/10.21343/y89m-6393">https://doi.org/10.21343/y89m-6393</a> | Merged Observatory Data File (MODF) for Ny Ålesund                           | Holt, 2023            |
| <b>Eureka</b> , <a href="https://doi.org/10.21343/r85j-tc61">https://doi.org/10.21343/r85j-tc61</a>     | MODF for Eureka, Canada, during YOPP SOP1 and SOP2                           | Akish & Morris, 2023a |

Formatted: Font: Not Bold

Formatted: Font: Not Bold

Formatted: Font: Not Bold

Formatted Table

Formatted: Font: Not Bold

Formatted: Font: Not Bold

Formatted: Font: Not Bold

Formatted: Font: Not Bold

Formatted: Font: Not Bold

Formatted: Font: Not Bold

Formatted: Font: Not Bold

Formatted: Font: Not Bold

Formatted: Font: Not Bold

972

973

974

975 **Table 3.** List of the geophysical variables currently included in each site's MODF. Note that this table only includes variables  
976 currently in the existing MODF<sub>ysm</sub>, and does not indicate the complete list of variables that are observed at each site. **Table 2.**  
977 List of final DOIs for each of the supersite's MODF<sub>ysm</sub>.

978

979  
980  
981  
982

An asterisk (\*) denotes a variable not included in the H-K table (Hartten and Khalsa, 2022) and a double asterisk (\*\*) denotes a calculated variable. The level and type(s) of additional processing for the heat fluxes are also provided, where EC = eddy covariance and bulk = bulk method.

| MODE<br>featureType            | Measured Variables  | Whitehorse<br>lat: 60.71 N<br>lon: 135.07 W | Iqaluit<br>lat: 63.74 N<br>lon: 68.51 W | Sodankylä<br>lat: 67.367 N<br>lon: 26.629 E | Utqiagvik<br>lat: 71.325 N<br>lon: 156.625 W | Tiksi<br>lat: 71.596 N<br>lon: 128.889 E | Ny-Alesund<br>lat: 78.923 N<br>lon: 11.926 E | Eureka<br>lat: 80.083 N<br>lon: 86.417 W |
|--------------------------------|---|---|---|---|--|--|--|--|
| timeSeries<br>Variables        | Pressure (Pa)   | surface                                     | surface                                 | surface, mean<br>sea-level                  | surface                                      | surface                                  | surface                                      | surface                                  |
|                                | Total precipitation of water in<br>all phases per unit area<br>( $\text{kg m}^{-2} \text{s}^{-1}$ ) | surface                                     | surface                                 |   |  |  | surface                                      |  |
|                                | Eastward Wind ( $\text{m s}^{-1}$ )   | surface                                     | near-surface                            | near-surface                                | near-surface<br>(2m)                         | near-surface<br>(4m)                     | near-surface<br>(10m)                        | near-surface<br>(6m)                     |
|                                | Northward Wind ( $\text{m s}^{-1}$ )  | surface                                     | near-surface                            | near-surface                                | near-surface<br>(2m)                         | near-surface<br>(4m)                     | near-surface<br>(10m)                        | near-surface<br>(6m)                     |
|                                | *Wind gust ( $\text{m s}^{-1}$ )  |   |   | near-surface<br>(10m)                       |  |  |  |  |
|                                | Vertical velocity ( $\text{m s}^{-1}$ )   |   |   | near-surface (2<br>m)                       |  |  |  |  |
|                                | Temperature (K)   | near-surface<br>(2m)                        | near-surface<br>(2m)                    | skin, near-<br>surface (2m)                 | skin, near-<br>surface (2m)                  | skin, near-<br>surface (2m)              | near-surface<br>(2m)                         | skin, near-<br>surface (2m)              |
|                                | Dew-point Temperature (K)   | near-surface<br>(2m)                        | near-surface<br>(2m)                    | near-surface<br>(2m)                        | near-surface<br>(2m)                         |  |  |  |
|                                | Relative Humidity (1 or %)  | near-surface<br>(2m)                        | near-surface<br>(2m)                    | near-surface<br>(2m)                        | near-surface<br>(2m)                         | near-surface<br>(2m)                     | near-surface<br>(2m)                         | near-surface<br>(2m)                     |
|                                | Specific Humidity (1 or $\text{kg kg}^{-1}$ )   |   |   |   |  |  | near-surface<br>(2m)                         |  |
|                                | Ozone Concentration in Air<br>(mole fraction)   |   |   |   | surface                                      |  |  |  |
|                                | Snow thickness (m)  |   | surface                                 | surface                                     | surface                                      | surface                                  |  | surface                                  |
|                                | Snowfall Flux ( $\text{kg m}^{-1} \text{s}^{-1}$ )  |   |   |   | surface                                      |  |  |  |
|                                | Snow water equivalent ( $\text{kg m}^{-2}$ )  |   |   |   | surface                                      |  |  |  |
|                                | Upward Short-wave<br>Radiation ( $\text{W m}^{-2}$ )  |   | surface                                 | surface                                     | surface                                      | surface                                  | surface                                      | surface                                  |
|                                | Downward Short-wave<br>Radiation ( $\text{W m}^{-2}$ )  |   | surface                                 | surface                                     | surface                                      | surface                                  | surface                                      | surface                                  |
|                                | Upward Long-wave Radiation<br>( $\text{W m}^{-2}$ )   |   | surface                                 | surface                                     | surface                                      | surface                                  | surface                                      |  |
|                                | Downward Long-wave<br>Radiation ( $\text{W m}^{-2}$ )   |   | surface                                 | surface                                     | surface                                      | surface                                  | surface                                      | surface                                  |
|                                | Net Short-wave Radiation at<br>the Surface ( $\text{W m}^{-2}$ )                                    |   |   | surface                                     |  |  |  |  |
|                                | *Horizontal East-facing<br>Long-wave Radiation ( $\text{W m}^{-2}$ )                                |   | surface                                 |   |  |  |  |  |
|                                | *Horizontal West-facing<br>Long-wave Radiation ( $\text{W m}^{-2}$ )                                |   | surface                                 |   |  |  |  |  |
|                                | *Horizontal South-facing<br>Long-wave Radiation ( $\text{W m}^{-2}$ )                               |   | surface                                 |   |  |  |  |  |
|                                | *Horizontal North-facing<br>Long-wave Radiation ( $\text{W m}^{-2}$ )                               |   | surface                                 |   |  |  |  |  |
|                                | **Turbulent Latent Heat Flux<br>( $\text{W m}^{-2}$ )   |   |   | surface (EC)                                | surface (EC,<br>bulk)                        |  |  |  |
|                                | **Turbulent Sensible Heat<br>Flux ( $\text{W m}^{-2}$ )   |   |   | surface (EC)                                | surface (EC,<br>bulk)                        |  |  |  |
|                                | **Turbulent time-average<br>eastward stress (Pa)  |   |   | surface (EC)                                | surface                                      |  |  |  |
|                                | **Turbulent time-average<br>northward stress (Pa)   |   |   |   | surface                                      |  |  |  |
|                                | *Friction Velocity ( $\text{m s}^{-1}$ )  |   |   | surface (EC)                                |  |  |  |  |
|                                | Cloud Base Height (m)   | ground-based<br>remote<br>sensing           | ground-based<br>remote<br>sensing       | ground-based<br>remote sensing              |  |  | ground-based<br>remote<br>sensing            |  |
|                                | Ground Heat Flux ( $\text{W m}^{-2}$ )  |   |   | near-surface                                | near-surface                                 | near-surface                             |  | near-surface                             |
|                                | Visibility (m)  |   |   | near-surface                                |  |  |  |  |
| timeSeriesProfile<br>Variables | Atmospheric pressure (Pa)   |   | near-surface<br>(2m, 10m)               |   |  |  |  |  |

Formatted: Font: Not Bold

Formatted: Font: Not Bold

Formatted: Font: Not Bold

Formatted: Font: Not Bold

Formatted: Font: Not Bold

Formatted: Font: Not Bold

Formatted: Font: Not Bold

Formatted: Font: Not Bold

Formatted: Font: Not Bold

Formatted Table

Formatted: Font: Not Bold

Formatted: Superscript

Formatted: Superscript

Formatted: Superscript

Formatted: Superscript

Formatted: Superscript

Formatted: Superscript

Formatted: Superscript

Formatted: Superscript

Formatted: Superscript

Formatted: Superscript

Formatted: Superscript

Formatted: Superscript

Formatted: Superscript

Formatted: Superscript

Formatted: Superscript

Formatted: Superscript

Formatted: Superscript

Formatted: Superscript

Formatted: Superscript

Formatted: Superscript

Formatted: Superscript

Formatted: Superscript

Formatted: Superscript

|   |   |                        |   |  |  |  |
|---|---|------------------------|---|--|--|--|
| Total precipitation of water in all phases per unit area ( $\text{kg m}^{-2} \text{s}^{-1}$ ) |   | near-surface (2m, 10m) |   |  |  |  |
| Eastward Wind ( $\text{m s}^{-1}$ )   |   | near-surface (2m, 10m) | near-surface (18m, 32m, 38m, 48m)   | near-surface (2m, 10m, 20m, 40m)   | near-surface (2m, 10m)   | near-surface (6m, 11m)   |
| Northward Wind ( $\text{m s}^{-1}$ )  |   | near-surface (2m, 10m) | near-surface (18m, 32m, 38m, 48m)   | near-surface (2m, 10m, 20m, 40m)   | near-surface (2m, 10m)   | near-surface (6m, 11m)   |
| Temperature (K)   |   | near-surface (2m, 10m) | near-surface (3m, 8m, 18m, 32m, 48m)  | near-surface (2m, 10m, 20m, 40m)   | near-surface (2m, 6m, 10m)   | near-surface (2m, 10m)   |
| Dew-point Temperature (K)   |   |                        |   | near-surface (2m, 10m, 20m, 40m)   |  |  |
| Relative Humidity (1 or %)  |   | near-surface (2m, 10m) | near-surface (3m, 8m, 18m, 32m, 48m)  | near-surface (2m, 10m, 20m, 40m)   | near-surface (2m, 6m, 10m)   | near-surface (2m, 6m, 10m)   |
| Soil Temperature Profile (K)  |   |                        | sub-surface (5cm, 30cm)   | sub-surface (5cm, 10cm, 15cm, 20cm, 25cm, 30cm, 45cm, 70cm, 95cm, 120cm) | sub-surface (5cm, 10cm, 15cm, 20cm, 25cm, 30cm, 45cm, 70cm, 95cm, 120cm) | sub-surface (5cm, 10cm, 15cm, 20cm, 25cm, 30cm, 45cm, 70cm, 95cm, 120cm) |
| Soil Moisture ( $\text{kg m}^{-3}$ )  |   |                        | sub-surface (5cm, 30cm)   |  |  |  |
| Snow Temperature (K)  |   |                        | near-surface (10cm, 20cm, 30cm, 40cm, 50cm, 60cm, 70cm, 80cm, 90cm, 100cm, 110cm) |  |  |  |
| <b>timeSeriesProfilesSonde Variables</b>  | Atmospheric pressure (Pa)                     | radiosonde             | radiosonde  | radiosonde   | radiosonde   | radiosonde   |
|   | Eastward Wind ( $\text{m s}^{-1}$ )           | radiosonde             | radiosonde  | radiosonde   | radiosonde   | radiosonde   |
|   | Northward Wind ( $\text{m s}^{-1}$ )          | radiosonde             | radiosonde  | radiosonde   | radiosonde   | radiosonde   |
|   | Temperature (K)                               | radiosonde             | radiosonde  | radiosonde   | radiosonde   | radiosonde   |
|   | Dew-point Temperature (K)                     | radiosonde             | radiosonde  | radiosonde   | radiosonde   | radiosonde   |
|   | Specific Humidity (1 or $\text{kg kg}^{-1}$ ) |                        |   |  | radiosonde   |  |
|   | Relative Humidity (1 or %)                    | radiosonde             | radiosonde  | radiosonde   | radiosonde   | radiosonde   |

\* Denotes a variable NOT included in the H-K Table

\*\* Denotes a calculated variable (not a direct observation)

**Table 3.** List of the geophysical variables currently included in each supersite's MODF. Note that this table only includes variables currently in the existing MODF<sub>psm</sub> and does not indicate the complete list of variables that are observed at each site. An asterisk (\*) denotes a variable not included in the H-K table and a double asterisk (\*\*) denotes a calculated variable.

Formatted: Superscript

Formatted: Superscript

Formatted: Superscript

Formatted: Superscript

Formatted: Superscript

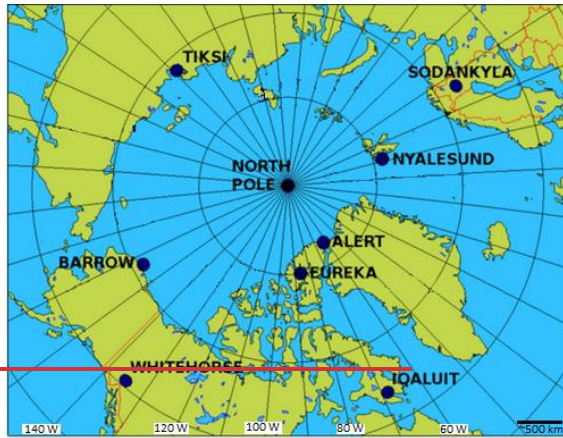
Formatted: Superscript

Formatted: Superscript

Formatted: Superscript

Formatted: Font: Not Bold

a)



b)



993  
994  
995  
996

997

998

**Table 4.** List of the instruments that contributed to the Whitehorse MODF, including details about the instrument manufacturer, measured variables, configuration, temporal resolution, measurement uncertainty, and quality control applied.

| <u>MODF feature type</u>    | <u>Instrument</u> | <u>Manufacturer</u> | <u>Measured variables</u>  | <u>Instrument Configuration</u>  | <u>Temporal Resolution</u> | <u>Uncertainty (+/-)</u>   | <u>Quality Control</u>  |
|-----------------------------|-------------------|---------------------|--|--|----------------------------|----------------------------|---|
| <u>timeSeries Variables</u> | <u>WXT520</u>     | <u>Vaisala</u>      | <u>Atmospheric pressure (Pa)</u>   | <u>Solid-state, all-in-one weather instrument in standard aspirated configuration mounted on a pole. No bird spike kit used.</u> | <u>1 min</u>               | <u>0.5 hPa</u>             | <u>Beyond the standard Vaisala processing, observations were checked against site-based climatology ranges and the rate of change thresholds, which were based on hourly criteria. Observations that fell outside of the 3-sigma normal climatological range were rejected, as were observations that had a rate of change greater than a seasonal-dependant threshold (e.g., &gt;20 hPa/hr change).</u>  |
| <u>timeSeries Variables</u> | <u>WXT520</u>     | <u>Vaisala</u>      | <u>Total precipitation of water in all phases per unit area (kg m<sup>-2</sup> s<sup>-1</sup>)</u> | <u>Solid-state, all-in-one weather instrument in standard aspirated configuration mounted on a pole. No bird spike kit used.</u> | <u>1 min</u>               | <u>5%</u>                  | <u>Beyond the standard Vaisala processing, observations were checked against site-based climatology ranges and the rate of change thresholds, which were based on hourly criteria. Observations that fell outside of the 3-sigma normal climatological range were rejected, as were observations that had a rate of change greater than a seasonal-dependant threshold (e.g., &gt; 10 mm/hr change). No corrections for solid precipitation under-catchment were performed (the dataset is raw in the MODF); where appropriate, users are recommended to process under-catchment corrections via Kochendorfer et al. (2020) (note: undercatchment is less of an issue for the WXT520 observations compared to Pluvio2).</u> |
| <u>timeSeries Variables</u> | <u>WXT520</u>     | <u>Vaisala</u>      | <u>Eastward Wind (m s<sup>-1</sup>)</u>  | <u>Solid-state, all-in-one weather instrument in standard aspirated configuration mounted on a pole. No bird spike kit used.</u> | <u>1 min</u>               | <u>0.3 ms<sup>-1</sup></u> | <u>Beyond the standard Vaisala processing, observations were checked against site-based climatology ranges and the rate of change thresholds, which were based on hourly criteria. Observations that fell outside of the 3-sigma normal climatological range were rejected, as were observations that had a rate of change greater than a seasonal-dependant threshold (e.g., &gt; 10 m/s/hr change).</u>   |
| <u>timeSeries Variables</u> | <u>WXT520</u>     | <u>Vaisala</u>      | <u>Northward Wind (m s<sup>-1</sup>)</u>   | <u>Solid-state, all-in-one weather instrument in standard aspirated configuration mounted on a pole. No bird spike kit used.</u> | <u>1 min</u>               | <u>0.3 ms<sup>-1</sup></u> | <u>Beyond the standard Vaisala processing, observations were checked against site-based climatology ranges and the rate of change thresholds, which were based on hourly criteria. Observations that fell outside of the 3-sigma normal climatological range were rejected, as were observations that had a rate of change greater than a seasonal-dependant threshold (e.g., &gt; 10 m/s/hr change).</u>   |



|  |                      |                       |   |  |              |                             |   |
|--|----------------------|-----------------------|---|--|--------------|-----------------------------|---|
| <u>timeSeries Variables</u>              | <u>WXT52</u><br>0    | <u>Vaisala</u>        | <u>Temperature (K)</u>                  | <u>Solid-state, all-in-one weather instrument in standard aspirated configuration mounted on a pole. No bird spike kit used.</u> | <u>1 min</u> | <u>0.3 K</u>                | <u>The shelter heating effect is uncorrected beyond the Vaisala standard processing. Beyond the standard Vaisala processing, observations were checked against site-based climatology ranges and the rate of change thresholds, which were based on hourly criteria. Observations that fell outside of the 3-sigma normal climatological range were rejected, as were observations that had a rate of change greater than a seasonal-dependant threshold (e.g., &gt; 5 K/hr change).</u>  |
| <u>timeSeries Variables</u>              | <u>WXT52</u><br>0    | <u>Vaisala</u>        | <u>Relative Humidity (1 or %)</u>       | <u>Solid-state, all-in-one weather instrument in standard aspirated configuration mounted on a pole. No bird spike kit used.</u> | <u>1 min</u> | <u>3%</u>                   | <u>The humidity is not corrected in a sub-freezing environment, beyond the standard Vaisala processing. Beyond the standard Vaisala processing, observations were checked against site-based climatology ranges and the rate of change thresholds, which were based on hourly criteria. Observations that fell outside of the 3-sigma normal climatological range were rejected, as were observations that had a rate of change greater than a seasonal-dependant threshold (e.g., &gt; 30 %/hr change).</u>  |
| <u>timeSeries Variables</u>              | <u>WXT52</u><br>0    | <u>Vaisala</u>        | <u>Dew-point Temperature (K)</u>        | <u>Solid-state, all-in-one weather instrument in standard aspirated configuration mounted on a pole. No bird spike kit used.</u> | <u>1 min</u> | <u>0.5 K</u>                | <u>The shelter heating effect is uncorrected and humidity is not corrected in a sub-freezing environment, beyond the standard Vaisala processing. Beyond the standard Vaisala processing, observations were checked against site-based climatology ranges and the rate of change thresholds, which were based on hourly criteria. Observations that fell outside of the 3-sigma normal climatological range were rejected, as were observations that had a rate of change greater than a seasonal-dependant threshold (e.g., &gt; 5 K/hr change).</u> |
| <u>timeSeries Profile Variables</u>      | <u>CL51</u>          | <u>Vaisala</u>        | <u>Cloud Base Height (m)</u>            | <u>Proprietary algorithm determines the lowest cloud base height</u>   | <u>1 min</u> | <u>5 m</u>                  | <u>No QC was performed, beyond the standard Vaisala proprietary algorithm that retrieves cloud base height.</u>   |
| <u>timeSeries ProfileSonde Variables</u> | <u>RS92 / DFM-09</u> | <u>Vaisala / GRAW</u> | <u>Atmospheric pressure (Pa)</u>        | <u>Standard radiosonde launch</u>  | <u>6 hr</u>  | <u>0.5 hPa</u>              | <u>Vaisala also processed the raw data feed from the radiosonde observations, which was obtained at 2 s resolution. Data were binned into 10-meter intervals of geopotential height and all measurements within each bin were averaged. No additional QC was performed beyond Vaisala's standard radiosonde processing.</u>   |
| <u>timeSeries ProfileSonde Variables</u> | <u>RS92 / DFM-09</u> | <u>Vaisala / GRAW</u> | <u>Eastward Wind (m s<sup>-1</sup>)</u> | <u>Standard radiosonde launch</u>  | <u>6 hr</u>  | <u>0.15 ms<sup>-1</sup></u> | <u>Vaisala also processed the raw data feed from the radiosonde observations, which was obtained at 2 s resolution. Data were binned into 10-meter intervals of geopotential height and all measurements within each bin were averaged. No additional QC was performed beyond Vaisala's standard radiosonde processing.</u>   |

|                            |                        |                           |   |                                     |                      |                                 |  |
|----------------------------|------------------------|---------------------------|---|-------------------------------------|----------------------|---------------------------------|--|
| <a href="#">timeSeries</a> | <a href="#">RS92 /</a> | <a href="#">Vaisala /</a> | <a href="#">Northward</a>               | <a href="#">Standard radiosonde</a> | <a href="#">6 hr</a> | <a href="#">0.15</a>            | <a href="#">Vaisala also processed the raw data feed from the radiosonde observations, which was obtained at 2 s resolution. Data were binned into 10-meter intervals of geopotential height and all measurements within each bin were averaged. No additional QC was performed beyond Vaisala's standard radiosonde processing.</a> |
| <a href="#">ProfileSo</a>  | <a href="#">DFM-</a>   | <a href="#">GRAW</a>      | <a href="#">Wind (m s<sup>-1</sup>)</a> | <a href="#">launch</a>              |                      | <a href="#">ms<sup>-1</sup></a> |  |
| <a href="#">nde</a>        | <a href="#">09</a>     |                           |   |                                     |                      |                                 |  |
| <a href="#">Variables</a>  |                        |                           |   |                                     |                      |                                 |  |
| <a href="#">timeSeries</a> | <a href="#">RS92 /</a> | <a href="#">Vaisala /</a> | <a href="#">Temperature</a>             | <a href="#">Standard radiosonde</a> | <a href="#">6 hr</a> | <a href="#">0.15 K</a>          | <a href="#">Vaisala also processed the raw data feed from the radiosonde observations, which was obtained at 2 s resolution. Data were binned into 10-meter intervals of geopotential height and all measurements within each bin were averaged. No additional QC was performed beyond Vaisala's standard radiosonde processing.</a> |
| <a href="#">ProfileSo</a>  | <a href="#">DFM-</a>   | <a href="#">GRAW</a>      | <a href="#">(K)</a>                     | <a href="#">launch</a>              |                      |                                 |  |
| <a href="#">nde</a>        | <a href="#">09</a>     |                           |   |                                     |                      |                                 |  |
| <a href="#">Variables</a>  |                        |                           |   |                                     |                      |                                 |  |
| <a href="#">timeSeries</a> | <a href="#">RS92 /</a> | <a href="#">Vaisala /</a> | <a href="#">Dew-point</a>               | <a href="#">Standard radiosonde</a> | <a href="#">6 hr</a> | <a href="#">0.5 K</a>           | <a href="#">Vaisala also processed the raw data feed from the radiosonde observations, which was obtained at 2 s resolution. Data were binned into 10-meter intervals of geopotential height and all measurements within each bin were averaged. No additional QC was performed beyond Vaisala's standard radiosonde processing.</a> |
| <a href="#">ProfileSo</a>  | <a href="#">DFM-</a>   | <a href="#">GRAW</a>      | <a href="#">Temperature</a>             | <a href="#">launch</a>              |                      |                                 |  |
| <a href="#">nde</a>        | <a href="#">09</a>     |                           | <a href="#">(K)</a>                     |                                     |                      |                                 |  |
| <a href="#">Variables</a>  |                        |                           |   |                                     |                      |                                 |  |

1001  
1002  
1003

**Table 5.** List of the instruments that contributed to the Iqaluit MODF, including details about the instrument manufacturer, measured variables, configuration, temporal resolution, measurement uncertainty, and quality control applied.

| <u>MODF feature/Variable</u> | <u>Instrument</u>        | <u>Manufacturer</u> | <u>Measured variables</u>  | <u>Instrument Configuration</u>   | <u>Temporal Resolution</u> | <u>Uncertainty (+/-)</u>   | <u>Quality Control</u>   |
|------------------------------|--------------------------|---------------------|--|---|----------------------------|----------------------------|--|
| <u>timeSeries Variables</u>  | <u>PTB110</u>            | <u>Vaisala</u>      | <u>Pressure (Pa)</u>   | <u>Installed within a naturally vented protective enclosure.</u>  | <u>1 min</u>               | <u>0.3 hPa</u>             | <u>Beyond the standard Vaisala processing, observations were checked against site-based climatology ranges and the rate of change thresholds, which were based on hourly criteria. Observations that fell outside of the 3-sigma normal climatological range were rejected, as were observations that had a rate of change greater than a seasonal-dependant threshold (e.g., &gt;20 hPa/hr change).</u>   |
| <u>timeSeries Variables</u>  | <u>Pluvio2</u>           | <u>OTT</u>          | <u>Total precipitation of water in all phases per unit area (kg m<sup>-2</sup> s<sup>-1</sup>)</u> | <u>Single Alter shield</u>  | <u>1 min</u>               | <u>5%</u>                  | <u>Beyond the standard Vaisala processing, observations were checked against site-based climatology ranges and the rate of change thresholds, which were based on hourly criteria. Observations that fell outside of the 3-sigma normal climatological range were rejected, as were observations that had a rate of change greater than a seasonal-dependant threshold (e.g., &gt; 10 mm/hr change). No corrections for solid precipitation under-catchment were performed (the dataset is raw in the MODF); where appropriate, users are recommended to process under-catchment corrections via Kochendorfer et al. (2020).</u> |
| <u>timeSeries Variables</u>  | <u>Wind monitor 5103</u> | <u>RM Young</u>     | <u>Eastward Wind (m s<sup>-1</sup>)</u>  | <u>Four-blade helicoid propeller in standard configuration with a wind vane to measure wind direction</u> | <u>1 min</u>               | <u>0.3 ms<sup>-1</sup></u> | <u>Beyond the standard Vaisala processing, observations were checked against site-based climatology ranges and the rate of change thresholds, which were based on hourly criteria. Observations that fell outside of the 3-sigma normal climatological range were rejected, as were observations that had a rate of change greater than a seasonal-dependant threshold (e.g., &gt; 10 m/s/hr change).</u>  |
| <u>timeSeries Variables</u>  | <u>Wind monitor 5103</u> | <u>RM Young</u>     | <u>Northward Wind (m s<sup>-1</sup>)</u>   | <u>Four-blade helicoid propeller in standard configuration with a wind vane to measure wind direction</u> | <u>1 min</u>               | <u>0.3 ms<sup>-1</sup></u> | <u>Beyond the standard Vaisala processing, observations were checked against site-based climatology ranges and the rate of change thresholds, which were based on hourly criteria. Observations that fell outside of the 3-sigma normal climatological range were rejected, as were observations that had a rate of change greater than a seasonal-dependant threshold (e.g., &gt; 10 m/s/hr change).</u>  |
| <u>timeSeries Variables</u>  | <u>HMP35D</u>            | <u>Vaisala</u>      | <u>Temperature (K)</u>   | <u>Sensor installed in shaded, naturally vented shelter.</u>  | <u>1 min</u>               | <u>0.1 K</u>               | <u>The shelter heating effect is uncorrected beyond the Vaisala standard processing. Beyond the standard Vaisala processing, observations were checked against site-based climatology ranges and the rate of change thresholds, which were based on hourly criteria. Observations that fell outside of the 3-sigma normal climatological range were rejected, as were observations that</u>  |

|                             |                |                            |   |   |              |                           |   |
|-----------------------------|----------------|----------------------------|---|---|--------------|---------------------------|---|
|                             |                |                            |   |   |              |                           | had a rate of change greater than a seasonal-dependant threshold (e.g., > 5 K/hr change).   |
| <u>timeSeries Variables</u> | <u>HMP35 D</u> | <u>Vaisala</u>             | <u>Dew-point Temperature (K)</u>                        | <u>Sensor installed in shaded, naturally vented shelter.</u>  | <u>1 min</u> | <u>0.2 K</u>              | <u>The shelter heating effect is uncorrected and humidity is not corrected in a sub-freezing environment, beyond the standard Vaisala processing. Beyond the standard Vaisala processing, observations were checked against site-based climatology ranges and the rate of change thresholds, which were based on hourly criteria. Observations that fell outside of the 3-sigma normal climatological range were rejected, as were observations that had a rate of change greater than a seasonal-dependant threshold (e.g., &gt; 5 K/hr change).</u> |
| <u>timeSeries Variables</u> | <u>HMP35 D</u> | <u>Vaisala</u>             | <u>Relative Humidity (1 or %)</u>                       | <u>Sensor installed in shaded, naturally vented shelter.</u>  | <u>1 min</u> | <u>0.8%</u>               | <u>The humidity is not corrected in a sub-freezing environment, beyond the standard Vaisala processing. Beyond the standard Vaisala processing, observations were checked against site-based climatology ranges and the rate of change thresholds, which were based on hourly criteria. Observations that fell outside of the 3-sigma normal climatological range were rejected, as were observations that had a rate of change greater than a seasonal-dependant threshold (e.g., &gt; 30 %/hr change).</u>  |
| <u>timeSeries Variables</u> | <u>SR50A</u>   | <u>Campbell Scientific</u> | <u>Snow thickness (m)</u>                               | <u>Sonic distance sensor at 50KHz with a perforated flat target base levelled at the surface (0 m a.g.l.)</u>   | <u>1 min</u> | <u>1 cm</u>               | <u>Observations were checked against site-based climatology ranges and the rate of change thresholds, which were based on hourly criteria. Observations that fell outside of the 3-sigma normal climatological range were rejected, as were observations that had a rate of change greater than a seasonal-dependant threshold (e.g., &gt; 20 cm/hr change).</u>  |
| <u>timeSeries Variables</u> | <u>CMP10 L</u> | <u>Kipp and Zonen</u>      | <u>Upward Short-wave Radiation (W m<sup>-2</sup>)</u>   | <u>Integrated levelling included, dome, RM Young radiation shield (6 plate), and a CVP4L Ventilation System with Integrated Heater running when temperatures where near zero to prevent frost</u> | <u>1 min</u> | <u>7 W m<sup>-2</sup></u> | <u>Data is raw and no additional QC was performed, other than the processing performed by Kipp and Zonen. No additional QC was performed on these observations to account for potential frost or snow deposition on the sensors. Data should be treated with caution since they typically require additional QC processing prior to analysis.</u>   |
| <u>timeSeries Variables</u> | <u>CMP10 L</u> | <u>Kipp and Zonen</u>      | <u>Downward Short-wave Radiation (W m<sup>-2</sup>)</u> | <u>Integrated levelling included, dome, RM Young radiation shield (6 plate), and a CVP4L Ventilation System with Integrated Heater running when temperatures where</u>                            | <u>1 min</u> | <u>7 W m<sup>-2</sup></u> | <u>Data is raw and no additional QC was performed, other than the processing performed by Kipp and Zonen. No additional QC was performed on these observations to account for potential frost or snow deposition on the sensors. Data should be treated with caution</u>  |

|                             |              |                       |   |   |              |                           |   |
|-----------------------------|--------------|-----------------------|---|---|--------------|---------------------------|---|
|                             |              |                       |   | near zero to prevent frost  |              |                           | since they typically require additional QC processing prior to analysis.  |
| <u>timeSeries Variables</u> | <u>CGR4L</u> | <u>Kipp and Zonen</u> | <u>Upward Long-wave Radiation</u><br>(W m <sup>-2</sup> )                   | <u>Integrated levelling included, dome, RM Young radiation shield (6 plate), and a CVF4L Ventilation System with Integrated Heater running when temperatures where near zero to prevent frost</u> | <u>1 min</u> | <u>7 W m<sup>-2</sup></u> | <u>Data is raw and no additional QC was performed, other than the processing performed by Kipp and Zonen. No additional QC was performed on these observations to account for potential frost or snow deposition on the sensors. Data should be treated with caution since they typically require additional QC processing prior to analysis.</u> |
| <u>timeSeries Variables</u> | <u>CGR4L</u> | <u>Kipp and Zonen</u> | <u>Downward Long-wave Radiation</u><br>(W m <sup>-2</sup> )                 | <u>Integrated levelling included, dome, RM Young radiation shield (6 plate), and a CVF4L Ventilation System with Integrated Heater running when temperatures where near zero to prevent frost</u> | <u>1 min</u> | <u>7 W m<sup>-2</sup></u> | <u>Data is raw and no additional QC was performed, other than the processing performed by Kipp and Zonen. No additional QC was performed on these observations to account for potential frost or snow deposition on the sensors. Data should be treated with caution since they typically require additional QC processing prior to analysis.</u> |
| <u>timeSeries Variables</u> | <u>CGR4L</u> | <u>Kipp and Zonen</u> | <u>*Horizontal East-facing Long-wave Radiation</u><br>(W m <sup>-2</sup> )  | <u>Integrated levelling included, dome, RM Young radiation shield (6 plate), and a CVF4L Ventilation System with Integrated Heater running when temperatures where near zero to prevent frost</u> | <u>1 min</u> | <u>7 W m<sup>-2</sup></u> | <u>Data is raw and no additional QC was performed, other than the processing performed by Kipp and Zonen. No additional QC was performed on these observations to account for potential frost or snow deposition on the sensors. Data should be treated with caution since they typically require additional QC processing prior to analysis.</u> |
| <u>timeSeries Variables</u> | <u>CGR4L</u> | <u>Kipp and Zonen</u> | <u>*Horizontal West-facing Long-wave Radiation</u><br>(W m <sup>-2</sup> )  | <u>Integrated levelling included, dome, RM Young radiation shield (6 plate), and a CVF4L Ventilation System with Integrated Heater running when temperatures where near zero to prevent frost</u> | <u>1 min</u> | <u>7 W m<sup>-2</sup></u> | <u>Data is raw and no additional QC was performed, other than the processing performed by Kipp and Zonen. No additional QC was performed on these observations to account for potential frost or snow deposition on the sensors. Data should be treated with caution since they typically require additional QC processing prior to analysis.</u> |
| <u>timeSeries Variables</u> | <u>CGR4L</u> | <u>Kipp and Zonen</u> | <u>*Horizontal South-facing Long-wave Radiation</u><br>(W m <sup>-2</sup> ) | <u>Integrated levelling included, dome, RM Young radiation shield (6 plate), and a CVF4L Ventilation System with Integrated Heater running when temperatures where near zero to prevent frost</u> | <u>1 min</u> | <u>7 W m<sup>-2</sup></u> | <u>Data is raw and no additional QC was performed, other than the processing performed by Kipp and Zonen. No additional QC was performed on these observations to account for potential frost or snow deposition on the sensors. Data should be treated with caution since they typically require additional QC processing prior to analysis.</u> |

|                              |            |                |   |  |       |               |   |
|------------------------------|------------|----------------|---|--|-------|---------------|---|
| timeSeries Variables         | CGR4L      | Kipp and Zonen | *Horizontal North-facing Long-wave Radiation ( $W m^{-2}$ )                     | Integrated levelling included, dome, RM Young radiation shield (6 plate), and a CVF4L Ventilation System with Integrated Heater running when temperatures where near zero to prevent frost | 1 min | $7 W m^{-2}$  | Data is raw and no additional QC was performed, other than the processing performed by Kipp and Zonen. No additional QC was performed on these observations to account for potential frost or snow deposition on the sensors. Data should be treated with caution since they typically require additional QC processing prior to analysis.  |
| timeSeries Profile Variables | CL51       | Vaisala        | Cloud Base Height (m)   | Proprietary algorithm determines the lowest cloud base height  | 1 min | 5 m           | No QC was performed, beyond the standard Vaisala proprietary algorithm that retrieves cloud base height.  |
| timeSeries Profile Variables | WXT52<br>0 | Vaisala        | Atmospheric pressure (Pa)   | Solid-state, all-in-one weather instrument in standard aspirated configuration mounted on a pole. No bird spike kit used.  | 1 min | 0.5 hPa       | Beyond the standard Vaisala processing, observations were checked against site-based climatology ranges and the rate of change thresholds, which were based on hourly criteria. Observations that fell outside of the 3-sigma normal climatological range were rejected, as were observations that had a rate of change greater than a seasonal-dependant threshold (e.g., >20 hPa/hr change).  |
| timeSeries Profile Variables | WXT52<br>0 | Vaisala        | Total precipitation of water in all phases per unit area ( $kg m^{-2} s^{-1}$ ) | Solid-state, all-in-one weather instrument in standard aspirated configuration mounted on a pole. No bird spike kit used.  | 1 min | 5%            | Beyond the standard Vaisala processing, observations were checked against site-based climatology ranges and the rate of change thresholds, which were based on hourly criteria. Observations that fell outside of the 3-sigma normal climatological range were rejected, as were observations that had a rate of change greater than a seasonal-dependant threshold (e.g., > 10 mm/hr change). No corrections for solid precipitation under-catchment were performed (the dataset is raw in the MODF); where appropriate, users are recommended to process under-catchment corrections via Kochendorfer et al. (2020) (note: undercatchment is less of an issue for the WXT520 observations compared to Pluvio2). |
| timeSeries Profile Variables | WXT52<br>0 | Vaisala        | Eastward Wind ( $m s^{-1}$ )  | Solid-state, all-in-one weather instrument in standard aspirated configuration mounted on a pole. No bird spike kit used.  | 1 min | 0.3 $ms^{-1}$ | Beyond the standard Vaisala processing, observations were checked against site-based climatology ranges and the rate of change thresholds, which were based on hourly criteria. Observations that fell outside of the 3-sigma normal climatological range were rejected, as were observations that had a rate of change greater than a seasonal-dependant threshold (e.g., > 10 m/s/hr change).   |
| timeSeries Profile Variables | WXT52<br>0 | Vaisala        | Northward Wind ( $m s^{-1}$ )   | Solid-state, all-in-one weather instrument in standard aspirated configuration mounted on a pole. No bird spike kit used.  | 1 min | 0.3 $ms^{-1}$ | Beyond the standard Vaisala processing, observations were checked against site-based climatology ranges and the rate of change thresholds, which were based on hourly criteria. Observations that fell outside of the 3-sigma normal climatological range were rejected, as were observations that had a rate of change   |

greater than a seasonal-dependant threshold (e.g., > 10 m/s/hr change).

|   |                               |                                |   |   |                       |                                      |   |
|---|-------------------------------|--------------------------------|---|---|-----------------------|--------------------------------------|---|
| <a href="#">timeSeries Profile Variables</a>      | <a href="#">WXT52 0</a>       | <a href="#">Vaisala</a>        | <a href="#">Temperature (K)</a>                   | <a href="#">Solid-state, all-in-one weather instrument in standard aspirated configuration mounted on a pole. No bird spike kit used.</a> | <a href="#">1 min</a> | <a href="#">0.3 K</a>                | <a href="#">The shelter heating effect is uncorrected beyond the Vaisala standard processing. Beyond the standard Vaisala processing, observations were checked against site-based climatology ranges and the rate of change thresholds, which were based on hourly criteria. Observations that fell outside of the 3-sigma normal climatological range were rejected, as were observations that had a rate of change greater than a seasonal-dependant threshold (e.g., &gt; 5 K/hr change).</a>                     |
| <a href="#">timeSeries Profile Variables</a>      | <a href="#">WXT52 0</a>       | <a href="#">Vaisala</a>        | <a href="#">Relative Humidity (1 or %)</a>        | <a href="#">Solid-state, all-in-one weather instrument in standard aspirated configuration mounted on a pole. No bird spike kit used.</a> | <a href="#">1 min</a> | <a href="#">3%</a>                   | <a href="#">The humidity is not corrected in a sub-freezing environment, beyond the standard Vaisala processing. Beyond the standard Vaisala processing, observations were checked against site-based climatology ranges and the rate of change thresholds, which were based on hourly criteria. Observations that fell outside of the 3-sigma normal climatological range were rejected, as were observations that had a rate of change greater than a seasonal-dependant threshold (e.g., &gt; 30 %/hr change).</a> |
| <a href="#">timeSeries ProfileSonde Variables</a> | <a href="#">RS92 / DFM-09</a> | <a href="#">Vaisala / GRAW</a> | <a href="#">Atmospheric pressure (Pa)</a>         | <a href="#">Standard radiosonde launch</a>  | <a href="#">6 hr</a>  | <a href="#">0.5 hPa</a>              | <a href="#">Vaisala also processed the raw data feed from the radiosonde observations, which was obtained at 2 s resolution. Data were binned into 10-meter intervals of geopotential height and all measurements within each bin were averaged. No additional QC was performed beyond Vaisala's standard radiosonde processing.</a>  |
| <a href="#">timeSeries ProfileSonde Variables</a> | <a href="#">RS92 / DFM-09</a> | <a href="#">Vaisala / GRAW</a> | <a href="#">Eastward Wind (m s<sup>-1</sup>)</a>  | <a href="#">Standard radiosonde launch</a>  | <a href="#">6 hr</a>  | <a href="#">0.15 ms<sup>-1</sup></a> | <a href="#">Vaisala also processed the raw data feed from the radiosonde observations, which was obtained at 2 s resolution. Data were binned into 10-meter intervals of geopotential height and all measurements within each bin were averaged. No additional QC was performed beyond Vaisala's standard radiosonde processing.</a>  |
| <a href="#">timeSeries ProfileSonde Variables</a> | <a href="#">RS92 / DFM-09</a> | <a href="#">Vaisala / GRAW</a> | <a href="#">Northward Wind (m s<sup>-1</sup>)</a> | <a href="#">Standard radiosonde launch</a>  | <a href="#">6 hr</a>  | <a href="#">0.15 ms<sup>-1</sup></a> | <a href="#">Vaisala also processed the raw data feed from the radiosonde observations, which was obtained at 2 s resolution. Data were binned into 10-meter intervals of geopotential height and all measurements within each bin were averaged. No additional QC was performed beyond Vaisala's standard radiosonde processing.</a>  |

|                            |                        |                           |                             |                                     |                      |                        |  |
|----------------------------|------------------------|---------------------------|-----------------------------|-------------------------------------|----------------------|------------------------|--|
| <a href="#">timeSeries</a> | <a href="#">RS92 /</a> | <a href="#">Vaisala /</a> | <a href="#">Temperature</a> | <a href="#">Standard radiosonde</a> | <a href="#">6 hr</a> | <a href="#">0.15 K</a> | <a href="#">Vaisala also processed the raw data feed from the radiosonde observations, which was obtained at 2 s resolution. Data were binned into 10-meter intervals of geopotential height and all measurements within each bin were averaged. No additional QC was performed beyond Vaisala's standard radiosonde processing.</a> |
| <a href="#">ProfileSo</a>  | <a href="#">DFM-</a>   | <a href="#">GRAW</a>      | <a href="#">(K)</a>         | <a href="#">launch</a>              |                      |                        |  |
| <a href="#">nde</a>        | <a href="#">09</a>     |                           |                             |                                     |                      |                        |  |
| <a href="#">Variables</a>  |                        |                           |                             |                                     |                      |                        |  |
| <a href="#">timeSeries</a> | <a href="#">RS92 /</a> | <a href="#">Vaisala /</a> | <a href="#">Dew-point</a>   | <a href="#">Standard radiosonde</a> | <a href="#">6 hr</a> | <a href="#">0.5 K</a>  | <a href="#">Vaisala also processed the raw data feed from the radiosonde observations, which was obtained at 2 s resolution. Data were binned into 10-meter intervals of geopotential height and all measurements within each bin were averaged. No additional QC was performed beyond Vaisala's standard radiosonde processing.</a> |
| <a href="#">ProfileSo</a>  | <a href="#">DFM-</a>   | <a href="#">GRAW</a>      | <a href="#">Temperature</a> | <a href="#">launch</a>              |                      |                        |  |
| <a href="#">nde</a>        | <a href="#">09</a>     |                           | <a href="#">(K)</a>         |                                     |                      |                        |  |
| <a href="#">Variables</a>  |                        |                           |                             |                                     |                      |                        |  |

1006

1007

1008



**Table 6.** List of the instruments that contributed to the Sodankylä MODF, including details about the instrument manufacturer, measured variables, configuration, temporal resolution, measurement uncertainty, and quality control applied.

| <u>MODF feature type</u>    | <u>Instrument</u> | <u>Manufacturer</u> | <u>Measured variables</u> | <u>Instrument Configuration</u>                       | <u>Temporal Resolution</u> | <u>Uncertainty (+/-)</u> | <u>Quality Control</u>   |
|-----------------------------|-------------------|---------------------|---------------------------|---|----------------------------|--------------------------|--|
| <u>timeSeries Variables</u> | PT100             | Vaisala             | Temperature (K)           | Sensor installed in shaded, naturally vented shelter. | 10 min                     | 0.1 K                    | The shelter heating effect is uncorrected beyond the Vaisala standard processing. Beyond the standard Vaisala processing, observations were checked against site-based climatology ranges and the rate of change thresholds, which were based on hourly criteria. Observations that fell outside of the 3-sigma normal climatological range were rejected, as were observations that had a rate of change greater than a seasonal-dependant threshold (e.g., > 5 K/hr change). |
| <u>timeSeries Variables</u> | PT100             | generic             | Temperature (K)           | Sensor installed in shaded, naturally vented shelter. | 10 min                     | 0.3 K                    | The shelter heating effect is uncorrected beyond the Vaisala standard processing. Beyond the standard Vaisala processing, observations were checked against site-based climatology ranges and the rate of change thresholds, which were based on hourly criteria. Observations that fell outside of the 3-sigma normal climatological range were rejected, as were observations that had a rate of change greater than a seasonal-dependant threshold (e.g., > 5 K/hr change). |
| <u>timeSeries Variables</u> | PT100             | Pentronic           | Temperature (K)           | Sensor installed in shaded, naturally vented shelter. | 10 min                     | 0.3 K                    | The shelter heating effect is uncorrected beyond the Vaisala standard processing. Beyond the standard Vaisala processing, observations were checked against site-based climatology ranges and the rate of change thresholds, which were based on hourly criteria. Observations that fell outside of the 3-sigma normal climatological range were rejected, as were observations that had a rate of change greater than a seasonal-dependant threshold (e.g., > 5 K/hr change). |
| <u>timeSeries Variables</u> | HMP155            | Vaisala             | Temperature (K)           | Sensor installed in shaded, naturally vented shelter. | 10 min                     | 0.1 K                    | The shelter heating effect is uncorrected beyond the Vaisala standard processing. Beyond the standard Vaisala processing, observations were checked against site-based climatology ranges and the rate of change thresholds, which were based on hourly criteria. Observations that fell outside of the 3-sigma normal climatological range were rejected, as were observations that had a rate of change greater than a seasonal-dependant threshold (e.g., > 5 K/hr change). |

|                                      |  |                                     |   |  |                        |   |   |
|--------------------------------------|--|-------------------------------------|---|--|------------------------|---|---|
| <a href="#">timeSeries Variables</a> | <a href="#">HMP155</a>                           | <a href="#">Vaisala</a>             | <a href="#">Relative Humidity (1 or %)</a>  | <a href="#">Sensor installed in shaded, naturally vented shelter.</a>  | <a href="#">10 min</a> | <a href="#">1%</a>                                | <a href="#">The humidity is not corrected in a sub-freezing environment, beyond the standard Vaisala processing. Beyond the standard Vaisala processing, observations were checked against site-based climatology ranges and the rate of change thresholds, which were based on hourly criteria. Observations that fell outside of the 3-sigma normal climatological range were rejected, as were observations that had a rate of change greater than a seasonal-dependant threshold (e.g., &gt; 30 %/hr change).</a> |
| <a href="#">timeSeries Variables</a> | <a href="#">HMP35D</a>                           | <a href="#">Vaisala</a>             | <a href="#">Relative Humidity (1 or %)</a>  | <a href="#">Sensor installed in shaded, naturally vented shelter.</a>  | <a href="#">10 min</a> | <a href="#">0.8%</a>                              | <a href="#">The humidity is not corrected in a sub-freezing environment, beyond the standard Vaisala processing. Beyond the standard Vaisala processing, observations were checked against site-based climatology ranges and the rate of change thresholds, which were based on hourly criteria. Observations that fell outside of the 3-sigma normal climatological range were rejected, as were observations that had a rate of change greater than a seasonal-dependant threshold (e.g., &gt; 30 %/hr change).</a> |
| <a href="#">timeSeries Variables</a> | <a href="#">HMP45D</a>                           | <a href="#">Vaisala</a>             | <a href="#">Relative Humidity (1 or %)</a>  | <a href="#">Sensor installed in shaded, naturally vented shelter.</a>  | <a href="#">10 min</a> | <a href="#">2% (0-90 %RH)<br/>3% (90-100 %RH)</a> | <a href="#">The humidity is not corrected in a sub-freezing environment, beyond the standard Vaisala processing. Beyond the standard Vaisala processing, observations were checked against site-based climatology ranges and the rate of change thresholds, which were based on hourly criteria. Observations that fell outside of the 3-sigma normal climatological range were rejected, as were observations that had a rate of change greater than a seasonal-dependant threshold (e.g., &gt; 30 %/hr change).</a> |
| <a href="#">timeSeries Variables</a> | <a href="#">SR50</a>                             | <a href="#">Campbell Scientific</a> | <a href="#">Snow thickness (m)</a>  | <a href="#">Sonic distance sensor at 50KHz with a perforated flat target base levelled at the surface (0 m a.g.l.)</a> | <a href="#">10 min</a> | <a href="#">1 cm</a>                              | <a href="#">Observations were checked against site-based climatology ranges, routine manual observations, and the rate of change thresholds, which were based on hourly criteria. Observations that fell outside of the 3-sigma normal climatological range were rejected, as were observations that had a rate of change greater than a seasonal-dependant threshold (e.g., &gt; 20 cm/hr change).</a>   |
| <a href="#">timeSeries Variables</a> | <a href="#">Distrometer Model: 5.4110.01.200</a> | <a href="#">Thies Climac</a>        | <a href="#">Total precipitation of water in all phases per unit area (kg m<sup>-2</sup> s<sup>-1</sup>)</a> | <a href="#">Model with extended heating</a>  | <a href="#">1 min</a>  | <a href="#">5%</a>                                | <a href="#">Beyond standard processing, observations were checked against site-based climatology ranges and the rate of change thresholds, which were based on hourly criteria. Observations that fell outside of the 3-sigma normal climatological range were rejected, as were observations that had a rate of change greater than a seasonal-dependant threshold (e.g., &gt; 10 mm/hr change).</a>   |

|                             |  |                             |   |   |               |                            |  |
|-----------------------------|--|-----------------------------|---|---|---------------|----------------------------|--|
| <u>timeSeries Variables</u> | <u>Distrometer Model:</u><br>5.4110.01.20<br>0 | <u>Thies Clima</u>          | <u>Snowfall flux unit area (kg m<sup>-2</sup> s<sup>-1</sup>)</u> | <u>Model with extended heating</u>  | <u>1 min</u>  | <u>5%</u>                  | <u>Beyond standard processing, observations were checked against site-based climatology ranges and the rate of change thresholds, which were based on hourly criteria. Observations that fell outside of the 3-sigma normal climatological range were rejected, as were observations that had a rate of change greater than a seasonal-dependant threshold (e.g., &gt; 10 mm/hr change).</u> |
| <u>timeSeries Variables</u> | <u>SSG 1000</u>                                | <u>Somme r Messtec hnik</u> | <u>Snow water equivalent (m)</u>                                  | <u>Sensor consists of seven perforated panels having a total measuring surface of 2.8 x 2.4 m with the measurement being made on the centre plate.</u>  | <u>1 min</u>  | <u>0.3%</u>                | <u>Data is raw and no additional QC was performed, other than the processing performed by the sensor.</u>  |
| <u>timeSeries Variables</u> | <u>CMA11</u>                                   | <u>Kipp and Zonen</u>       | <u>Downward Short-wave Radiation (W m<sup>-2</sup>)</u>           | <u>Integrated levelling included, dome, RM Young radiation shield (6 plate), and a CVF4L Ventilation System with Integrated Heater running when temperatures where near zero to prevent frost</u> | <u>10 min</u> | <u>7 W m<sup>-2</sup></u>  | <u>Data is raw and no additional QC was performed, other than the processing performed by Kipp and Zonen. No additional QC was performed on these observations to account for potential frost or snow deposition on the sensors. Data should be treated with caution since they typically require additional QC processing prior to analysis.</u>  |
| <u>timeSeries Variables</u> | <u>CMA11</u>                                   | <u>Kipp and Zonen</u>       | <u>Upward Short-wave Radiation (W m<sup>-2</sup>)</u>             | <u>Integrated levelling included, dome, RM Young radiation shield (6 plate), and a CVF4L Ventilation System with Integrated Heater running when temperatures where near zero to prevent frost</u> | <u>10 min</u> | <u>7 W m<sup>-2</sup></u>  | <u>Data is raw and no additional QC was performed, other than the processing performed by Kipp and Zonen. No additional QC was performed on these observations to account for potential frost or snow deposition on the sensors. Data should be treated with caution since they typically require additional QC processing prior to analysis.</u>  |
| <u>timeSeries Variables</u> | <u>CM11</u>                                    | <u>Kipp and Zonen</u>       | <u>Downward Short-wave Radiation (W m<sup>-2</sup>)</u>           | <u>Integrated levelling included, dome, RM Young radiation shield (6 plate), and a CVF4L Ventilation System with Integrated Heater running when temperatures where near zero to prevent frost</u> | <u>1 min</u>  | <u>7 W m<sup>-2</sup></u>  | <u>Data is raw and no additional QC was performed, other than the processing performed by Kipp and Zonen. No additional QC was performed on these observations to account for potential frost or snow deposition on the sensors. Data should be treated with caution since they typically require additional QC processing prior to analysis.</u>  |
| <u>timeSeries Variables</u> | <u>CMP3</u>                                    | <u>Kipp and Zonen</u>       | <u>Downward Short-wave Radiation (W m<sup>-2</sup>)</u>           | <u>Installed on a pole</u>  | <u>10 min</u> | <u>15 W m<sup>-2</sup></u> | <u>Data is raw and no additional QC was performed, other than the processing performed by Kipp and Zonen. No additional QC was performed on these observations to account for potential frost or snow deposition on the sensors. Data should be treated with</u>   |

|                                      |                       |                                |  |   |                        |                                     |  |
|--------------------------------------|-----------------------|--------------------------------|--|---|------------------------|-------------------------------------|--|
|                                      |                       |                                |  |   |                        |                                     | caution since they typically require additional QC processing prior to analysis.   |
| <a href="#">timeSeries Variables</a> | <a href="#">CMP3</a>  | <a href="#">Kipp and Zonen</a> | <a href="#">Upward Short-wave Radiation (W m<sup>-2</sup>)</a>   | <a href="#">Installed on a pole</a>                                   | <a href="#">10 min</a> | <a href="#">15 W m<sup>-2</sup></a> | <a href="#">Data is raw and no additional QC was performed, other than the processing performed by Kipp and Zonen. No additional QC was performed on these observations to account for potential frost or snow deposition on the sensors. Data should be treated with caution since they typically require additional QC processing prior to analysis.</a> |
| <a href="#">timeSeries Variables</a> | <a href="#">CMP11</a> | <a href="#">Kipp and Zonen</a> | <a href="#">Upward Short-wave Radiation (W m<sup>-2</sup>)</a>   | <a href="#">Installed on a pole</a>                                   | <a href="#">10 min</a> | <a href="#">7 W m<sup>-2</sup></a>  | <a href="#">Data is raw and no additional QC was performed, other than the processing performed by Kipp and Zonen. No additional QC was performed on these observations to account for potential frost or snow deposition on the sensors. Data should be treated with caution since they typically require additional QC processing prior to analysis.</a> |
| <a href="#">timeSeries Variables</a> | <a href="#">CNR4</a>  | <a href="#">Kipp and Zonen</a> | <a href="#">Downward Short-wave Radiation (W m<sup>-2</sup>)</a> | <a href="#">Integrated 4-component system with temperature sensor</a> | <a href="#">10 min</a> | <a href="#">7 W m<sup>-2</sup></a>  | <a href="#">Data is raw and no additional QC was performed, other than the processing performed by Kipp and Zonen. No additional QC was performed on these observations to account for potential frost or snow deposition on the sensors. Data should be treated with caution since they typically require additional QC processing prior to analysis.</a> |
| <a href="#">timeSeries Variables</a> | <a href="#">CNR4</a>  | <a href="#">Kipp and Zonen</a> | <a href="#">Upward Short-wave Radiation (W m<sup>-2</sup>)</a>   | <a href="#">Integrated 4-component system with temperature sensor</a> | <a href="#">10 min</a> | <a href="#">7 W m<sup>-2</sup></a>  | <a href="#">Data is raw and no additional QC was performed, other than the processing performed by Kipp and Zonen. No additional QC was performed on these observations to account for potential frost or snow deposition on the sensors. Data should be treated with caution since they typically require additional QC processing prior to analysis.</a> |
| <a href="#">timeSeries Variables</a> | <a href="#">CNR4</a>  | <a href="#">Kipp and Zonen</a> | <a href="#">Downward Long-wave Radiation (W m<sup>-2</sup>)</a>  | <a href="#">Integrated 4-component system with temperature sensor</a> | <a href="#">10 min</a> | <a href="#">7 W m<sup>-2</sup></a>  | <a href="#">Data is raw and no additional QC was performed, other than the processing performed by Kipp and Zonen. No additional QC was performed on these observations to account for potential frost or snow deposition on the sensors. Data should be treated with caution since they typically require additional QC processing prior to analysis.</a> |
| <a href="#">timeSeries Variables</a> | <a href="#">CNR4</a>  | <a href="#">Kipp and Zonen</a> | <a href="#">Upward Long-wave Radiation (W m<sup>-2</sup>)</a>    | <a href="#">Integrated 4-component system with temperature sensor</a> | <a href="#">10 min</a> | <a href="#">7 W m<sup>-2</sup></a>  | <a href="#">Data is raw and no additional QC was performed, other than the processing performed by Kipp and Zonen. No additional QC was performed on these observations to account for potential frost or snow deposition on the sensors. Data should be treated with caution since they typically require additional QC processing prior to analysis.</a> |

|                                      |                          |                                |  |   |                        |                                     |   |
|--------------------------------------|--------------------------|--------------------------------|--|---|------------------------|-------------------------------------|---|
| <a href="#">timeSeries Variables</a> | <a href="#">NR-Lite</a>  | <a href="#">Kipp and Zonen</a> | <a href="#">Net Short-wave Radiation (W m<sup>-2</sup>)</a>                            | <a href="#">Single-component thermopile net radiometer</a>                | <a href="#">10 min</a> | <a href="#">25 W m<sup>-2</sup></a> | <a href="#">Data is raw and no additional QC was performed, other than the processing performed by Kipp and Zonen. No additional QC was performed on these observations to account for potential frost or snow deposition on the sensors. Data should be treated with caution since they typically require additional QC processing prior to analysis.</a>  |
| <a href="#">timeSeries Variables</a> | <a href="#">NR-Lite2</a> | <a href="#">Kipp and Zonen</a> | <a href="#">Net Short-wave Radiation (W m<sup>-2</sup>)</a>                            | <a href="#">Single-component thermopile net radiometer</a>                | <a href="#">10 min</a> | <a href="#">15 W m<sup>-2</sup></a> | <a href="#">Data is raw and no additional QC was performed, other than the processing performed by Kipp and Zonen. No additional QC was performed on these observations to account for potential frost or snow deposition on the sensors. Data should be treated with caution since they typically require additional QC processing prior to analysis.</a>  |
| <a href="#">timeSeries Variables</a> | <a href="#">PAR Lite</a> | <a href="#">Kipp and Zonen</a> | <a href="#">Photosynthetic Photon Flux density (mol m<sup>-2</sup> s<sup>-1</sup>)</a> | <a href="#">Quantum sensor</a>  | <a href="#">10 min</a> | <a href="#">10%</a>                 | <a href="#">Data is raw and no additional QC was performed, other than the processing performed by Kipp and Zonen. No additional QC was performed on these observations to account for potential frost or snow deposition on the sensors. Data should be treated with caution since they typically require additional QC processing prior to analysis.</a>  |
| <a href="#">timeSeries Variables</a> | <a href="#">PQS1</a>     | <a href="#">Kipp and Zonen</a> | <a href="#">Photosynthetic Photon Flux density (mol m<sup>-2</sup> s<sup>-1</sup>)</a> | <a href="#">Quantum sensor</a>  | <a href="#">10 min</a> | <a href="#">5%</a>                  | <a href="#">Data is raw and no additional QC was performed, other than the processing performed by Kipp and Zonen. No additional QC was performed on these observations to account for potential frost or snow deposition on the sensors. Data should be treated with caution since they typically require additional QC processing prior to analysis.</a>  |
| <a href="#">timeSeries Variables</a> | <a href="#">LI190SZ</a>  | <a href="#">Licor</a>          | <a href="#">Photosynthetic Photon Flux density (mol m<sup>-2</sup> s<sup>-1</sup>)</a> | <a href="#">Quantum sensor</a>  | <a href="#">10 min</a> | <a href="#">5%</a>                  | <a href="#">Data is raw and no additional QC was performed, other than the processing performed by Licor. No additional QC was performed on these observations to account for potential frost or snow deposition on the sensors. Data should be treated with caution since they typically require additional QC processing prior to analysis.</a>   |
| <a href="#">timeSeries Variables</a> | <a href="#">PTB201A</a>  | <a href="#">Vaisala</a>        | <a href="#">Pressure (Pa)</a>  | <a href="#">Installed within a naturally vented protective enclosure.</a> | <a href="#">10 min</a> | <a href="#">0.3 hPa</a>             | <a href="#">Beyond the standard Vaisala processing, observations were checked against site-based climatology ranges and the rate of change thresholds, which were based on hourly criteria. Observations that fell outside of the 3-sigma normal climatological range were rejected, as were observations that had a rate of change greater than a seasonal-dependant threshold (e.g., &gt;20 hPa/hr change).</a> |
| <a href="#">timeSeries Variables</a> | <a href="#">FD12P</a>    | <a href="#">Vaisala</a>        | <a href="#">Surface horizontal visibility (m)</a>                                      | <a href="#">Optical forward-scatter sensor installed on a pole</a>        | <a href="#">10 min</a> | <a href="#">10%</a>                 | <a href="#">Data is raw and no additional QC was performed, other than the processing performed by the sensor.</a>  |

|                             |                               |                    |   |  |               |                             |   |
|-----------------------------|-------------------------------|--------------------|---|--|---------------|-----------------------------|---|
| <u>timeSeries Variables</u> | <u>WA25 (WAA25 and WAV25)</u> | <u>Vaisala</u>     | <u>Eastward Wind (m s<sup>-1</sup>)</u>   | <u>Cup anemometer and vane designed for Arctic conditions with integrated heaters to prevent ice buildup</u> | <u>10 min</u> | <u>0.3 m s<sup>-1</sup></u> | <u>Beyond the standard Vaisala processing, observations were checked against site-based climatology ranges and the rate of change thresholds, which were based on hourly criteria. Observations that fell outside of the 3-sigma normal climatological range were rejected, as were observations that had a rate of change greater than a seasonal-dependant threshold (e.g., &gt; 10 m/s/hr change).</u> |
| <u>timeSeries Variables</u> | <u>WA25 (WAA25 and WAV25)</u> | <u>Vaisala</u>     | <u>Northward Wind (m s<sup>-1</sup>)</u>  | <u>Cup anemometer and vane designed for Arctic conditions with integrated heaters to prevent ice buildup</u> | <u>10 min</u> | <u>0.3 m s<sup>-1</sup></u> | <u>Beyond the standard Vaisala processing, observations were checked against site-based climatology ranges and the rate of change thresholds, which were based on hourly criteria. Observations that fell outside of the 3-sigma normal climatological range were rejected, as were observations that had a rate of change greater than a seasonal-dependant threshold (e.g., &gt; 10 m/s/hr change).</u> |
| <u>timeSeries Variables</u> | <u>UA2D</u>                   | <u>Thies Clima</u> | <u>Eastward Wind (m s<sup>-1</sup>)</u>   | <u>2-D sonic anemometer</u>  | <u>10 min</u> | <u>2%</u>                   | <u>Data is raw and no additional QC was performed, other than the processing performed by the sensor.</u>   |
| <u>timeSeries Variables</u> | <u>UA2D</u>                   | <u>Thies Clima</u> | <u>Northward Wind (m s<sup>-1</sup>)</u>  | <u>2-D sonic anemometer</u>  | <u>10 min</u> | <u>2%</u>                   | <u>Data is raw and no additional QC was performed, other than the processing performed by the sensor.</u>   |
| <u>timeSeries Variables</u> | <u>USA-1</u>                  | <u>Metek</u>       | <u>Eastward Wind (m s<sup>-1</sup>)</u>   | <u>3-D sonic anemometer</u>  | <u>10 min</u> | <u>0.1 m s<sup>-1</sup></u> | <u>Data is raw and no additional QC was performed, other than the processing performed by the sensor.</u>   |
| <u>timeSeries Variables</u> | <u>USA-1</u>                  | <u>Metek</u>       | <u>Northward Wind (m s<sup>-1</sup>)</u>  | <u>3-D sonic anemometer</u>  | <u>10 min</u> | <u>0.1 m s<sup>-1</sup></u> | <u>Data is raw and no additional QC was performed, other than the processing performed by the sensor.</u>   |
| <u>timeSeries Variables</u> | <u>USA-1</u>                  | <u>Metek</u>       | <u>Vertical velocity (m s<sup>-1</sup>)</u>   | <u>3-D sonic anemometer</u>  | <u>10 min</u> | <u>0.1 m s<sup>-1</sup></u> | <u>Data is raw and no additional QC was performed, other than the processing performed by the sensor.</u>   |
| <u>timeSeries Variables</u> | <u>USA-1</u>                  | <u>Metek</u>       | <u>Surface friction velocity (eddy covariance method) (m s<sup>-1</sup>)</u>          | <u>3-D sonic anemometer</u>  | <u>10 min</u> | <u>0.1 m s<sup>-1</sup></u> | <u>Additional filtering of output from eddy covariance processing not performed</u>   |
| <u>timeSeries Variables</u> | <u>USA-1</u>                  | <u>Metek</u>       | <u>Surface turbulent latent heat flux (eddy covariance method) (W m<sup>-2</sup>)</u> | <u>3-D sonic anemometer</u>  | <u>10 min</u> | <u>20%</u>                  | <u>Additional filtering of output from eddy covariance processing not performed</u>   |
| <u>timeSeries Variables</u> | <u>USA-1</u>                  | <u>Metek</u>       | <u>Surface turbulent sensible heat flux (eddy covariance</u>                          | <u>3-D sonic anemometer</u>  | <u>10 min</u> | <u>20%</u>                  | <u>Additional filtering of output from eddy covariance processing not performed</u>   |

|   |                   |                                | method) (W<br>m <sup>-2</sup> )  |   |        |       |  |
|---|-------------------|--------------------------------|--|---|--------|-------|--|
| <a href="#">timeSeries<br/>Variables</a>              | USA-1             | Metek                          | Surface<br>momentum<br>flux (eddy<br>covariance<br>method) (W<br>m <sup>-2</sup> ) | 3-D sonic<br>anemometer   | 10 min | 25%   | Additional filtering of output from eddy<br>covariance processing not performed                          |
| <a href="#">timeSeries<br/>Variables</a>              | HFP01             | Hukseflu<br>x                  | Ground heat<br>flux (W m <sup>-2</sup> )   | Thermopile buried in<br>soil  | 10 min | 3%    | Data is raw and no additional QC was<br>performed, other than the processing<br>performed by the sensor. |
| <a href="#">timeSeries<br/>sProfile<br/>Variables</a> | QMT103            | Vaisala                        | Bulk soil<br>temperature<br>(K)  | Thin steel sheath<br>incorporating sensor,<br>buried in soil  | 10 min | 0.3 K | Data is raw and no additional QC was<br>performed, other than the processing<br>performed by the sensor. |
| <a href="#">timeSeries<br/>sProfile<br/>Variables</a> | Hydra Probe<br>II | Stevens                        | Bulk soil<br>temperature<br>(K)  | 4-needle sensor<br>buried in soil   | 10 min | 0.3 K | Data is raw and no additional QC was<br>performed, other than the processing<br>performed by the sensor. |
| <a href="#">timeSeries<br/>sProfile<br/>Variables</a> | Hydra Probe<br>II | Stevens                        | Average layer<br>soil moisture<br>(kg m <sup>-2</sup> )                            | 4-needle sensor<br>buried in soil   | 10 min | 5%    | Data is raw and no additional QC was<br>performed, other than the processing<br>performed by the sensor. |
| <a href="#">timeSeries<br/>sProfile<br/>Variables</a> | GS3               | Decago<br>n<br>Devices         | Bulk soil<br>temperature<br>(K)  | Sensor encapsulated<br>in an epoxy body with<br>stainless steel<br>needles. Buried in soil  | 10 min | 1 K   | Data is raw and no additional QC was<br>performed, other than the processing<br>performed by the sensor. |
| <a href="#">timeSeries<br/>sProfile<br/>Variables</a> | GTE               | Decago<br>n<br>Devices         | Bulk soil<br>temperature<br>(K)  | Sensor encapsulated<br>in an epoxy body with<br>stainless steel<br>needles. Buried in soil  | 10 min | 1 K   | Data is raw and no additional QC was<br>performed, other than the processing<br>performed by the sensor. |
| <a href="#">timeSeries<br/>sProfile<br/>Variables</a> | 109-L             | Campbe<br>ll<br>Scientif<br>ic | Bulk soil<br>temperature<br>(K)  | Thermistor<br>encapsulated in an<br>epoxy-filled<br>aluminum housing<br>and buried in soil  | 10 min | 0.3 K | Data is raw and no additional QC was<br>performed, other than the processing<br>performed by the sensor. |
| <a href="#">timeSeries<br/>sProfile<br/>Variables</a> | CS655             | Campbe<br>ll<br>Scientif<br>ic | Bulk soil<br>temperature<br>(K)  | Two 12-cm-long<br>stainless steel rods<br>connected to a printed<br>circuit board<br>encapsulated in epoxy<br>attached to a shielded<br>cable. Buried in soil | 10 min | 0.3 K | Data is raw and no additional QC was<br>performed, other than the processing<br>performed by the sensor. |
| <a href="#">timeSeries<br/>sProfile<br/>Variables</a> | PT100             | Pentron<br>ic                  | Bulk soil<br>temperature<br>(K)  | Thin steel sheath<br>incorporating sensor,<br>buried in soil  | 10 min | 0.3 K | Data is raw and no additional QC was<br>performed, other than the processing<br>performed by the sensor. |
| <a href="#">timeSeries<br/>sProfile<br/>Variables</a> | IKES PT100        | Nokeva<br>l                    | Bulk soil<br>temperature<br>(K)  | Thin steel sheath<br>incorporates a Pt100<br>sensor with double<br>insulation moulded in  | 10 min | 0.3 K | Data is raw and no additional QC was<br>performed, other than the processing<br>performed by the sensor. |

|                                    |                        |                            |  |   |               |                              |   |
|------------------------------------|------------------------|----------------------------|--|---|---------------|------------------------------|---|
|                                    |                        |                            |  | solid rubber with the cable. Buried in soil   |               |                              |   |
| <u>timeSeriesProfile Variables</u> | <u>ThetaProbe ML2x</u> | <u>Delta-T Devices</u>     | <u>Average layer soil moisture (kg m<sup>-2</sup>)</u> | <u>4-needle sensor buried in soil</u>   | <u>10 min</u> | <u>5.00%</u>                 | <u>Data is raw and no additional QC was performed, other than the processing performed by the sensor.</u> |
| <u>timeSeriesProfile Variables</u> | <u>107-L</u>           | <u>Campbell Scientific</u> | <u>Snow temperature (K)</u>                            | <u>Thermistor encapsulated in an epoxy-filled aluminum housing and buried in snow</u> | <u>10 min</u> | <u>0.5 K</u>                 | <u>Data is raw and no additional QC was performed, other than the processing performed by the sensor.</u> |
| <u>timeSeriesProfile Variables</u> | <u>PT100</u>           | <u>generic</u>             | <u>Air temperature (K)</u>                             | <u>Sensor installed in shaded, naturally vented shelter.</u>                          | <u>10 min</u> | <u>0.3 K</u>                 | <u>Data is raw and no additional QC was performed, other than the processing performed by the sensor.</u> |
| <u>timeSeriesProfile Variables</u> | <u>HMP</u>             | <u>Vaisala</u>             | <u>Relative Humidity (1 or %)</u>                      | <u>Sensor installed in shaded, naturally vented shelter.</u>                          | <u>10 min</u> | <u>0.80%</u>                 | <u>Data is raw and no additional QC was performed, other than the processing performed by the sensor.</u> |
| <u>timeSeriesProfile Variables</u> | <u>WAA25</u>           | <u>Vaisala</u>             | <u>Wind speed (m s<sup>-1</sup>)</u>                   | <u>Cup anemometer with integrated heater to prevent ice buildup</u>                   | <u>10 min</u> | <u>0.17 m s<sup>-1</sup></u> | <u>Data is raw and no additional QC was performed, other than the processing performed by the sensor.</u> |

1011  
1012  
1013



**Table 7.** List of the instruments that contributed to the Utqiaġvik MODF, including details about the instrument manufacturer, measured variables, configuration, temporal resolution, measurement uncertainty, and quality control applied.

| <u>MODF<br/>featureType</u>     | <u>Instrum<br/>ent</u> | <u>Manu<br/>factur<br/>er</u> | <u>Meas<br/>ured<br/>varia<br/>bles</u>   | <u>Instrument<br/>Configuration</u>   | <u>Tem<br/>pora<br/>l<br/>Reso<br/>lutio<br/>n</u> | <u>Unce<br/>rtain<br/>ty<br/>(+/-)</u> | <u>Quality Control</u>   |
|---------------------------------|------------------------|-------------------------------|---|---|--|--|--|
| <u>timeSeries<br/>Variables</u> | <u>PTB-220</u>         | <u>Vaisal<br/>a</u>           | <u>Press<br/>ure<br/>(Pa)</u>   | The Barrow meteorology station (BMET) uses mainly conventional in situ sensors mounted at four different heights (2m, 10m, 20m and 40m) on a 40 m tower to obtain profiles of wind speed, wind direction, air temperature, dew point and humidity. It also obtains barometric pressure, visibility and precipitation data from sensors at the base of the tower.<br><a href="https://www.arm.gov/capabilities/instruments/twr">https://www.arm.gov/capabilities/instruments/twr</a> | <u>1<br/>min</u>                                   | <u>0.15<br/>hPa</u>                    | Beyond the standard Vaisala processing, observations were checked against other instrumentation on the tower and compared with the surface meteorological instruments and the energy balance bowen ratio. Data was also compared with the SONDE data that was launched some distance away from the tower.<br><a href="https://www.arm.gov/publications/tech_reports/handbooks/twr_handbook.pdf">https://www.arm.gov/publications/tech_reports/handbooks/twr_handbook.pdf</a> |
| <u>timeSeries<br/>Variables</u> | <u>WS425</u>           | <u>Vaisal<br/>a</u>           | <u>Near-<br/>surfac<br/>e<br/>(2m<br/>eastw<br/>ard<br/>wind<br/>(m s<sup>-1</sup>)</u> | The Barrow meteorology station (BMET) uses mainly conventional in situ sensors mounted at four different heights (2m, 10m, 20m and 40m) on a 40 m tower to obtain profiles of wind speed, wind direction, air temperature, dew point and humidity. It also obtains barometric pressure, visibility and precipitation data from sensors at the base of the tower.<br><a href="https://www.arm.gov/capabilities/instruments/twr">https://www.arm.gov/capabilities/instruments/twr</a> | <u>1<br/>min</u>                                   | <u>0.135<br/>ms<sup>-1</sup></u>       | Beyond the standard Vaisala processing, observations were checked against other instrumentation on the tower and compared with the surface meteorological instruments and the energy balance bowen ratio. Data was also compared with the SONDE data that was launched some distance away from the tower.<br><a href="https://www.arm.gov/publications/tech_reports/handbooks/twr_handbook.pdf">https://www.arm.gov/publications/tech_reports/handbooks/twr_handbook.pdf</a> |

|                             |  |                |  |   |              |                              |  |
|-----------------------------|--|----------------|--|---|--------------|------------------------------|--|
| <u>timeSeries Variables</u> | <u>WS425</u>                           | <u>Vaisala</u> | <u>Near-surface (2m) northward wind (m s<sup>-1</sup>)</u> | <u>The Barrow meteorology station (BMET) uses mainly conventional in situ sensors mounted at four different heights (2m, 10m, 20m and 40m) on a 40 m tower to obtain profiles of wind speed, wind direction, air temperature, dew point and humidity. It also obtains barometric pressure, visibility and precipitation data from sensors at the base of the tower.</u><br><u><a href="https://www.arm.gov/capabilities/instruments/twr">https://www.arm.gov/capabilities/instruments/twr</a></u> | <u>1 min</u> | <u>0.135 ms<sup>-1</sup></u> | <u>Beyond the standard Vaisala processing, observations were checked against other instrumentation on the tower and compared with the surface meteorological instruments and the energy balance bowen ratio. Data was also compared with the SONDE data that was launched some distance away from the tower.</u><br><u><a href="https://www.arm.gov/publications/tech_reports/handbooks/twr_handbook.pdf">https://www.arm.gov/publications/tech_reports/handbooks/twr_handbook.pdf</a></u> |
| <u>timeSeries Variables</u> | <u>HMT337 (previous HMP35D/HMP45D)</u> | <u>Vaisala</u> | <u>Near-surface (2m) air temperature (K)</u>               | <u>The Barrow meteorology station (BMET) uses mainly conventional in situ sensors mounted at four different heights (2m, 10m, 20m and 40m) on a 40 m tower to obtain profiles of wind speed, wind direction, air temperature, dew point and humidity. It also obtains barometric pressure, visibility and precipitation data from sensors at the base of the tower.</u><br><u><a href="https://www.arm.gov/capabilities/instruments/twr">https://www.arm.gov/capabilities/instruments/twr</a></u> | <u>1 min</u> | <u>0.2 K</u>                 | <u>Beyond the standard Vaisala processing, observations were checked against other instrumentation on the tower and compared with the surface meteorological instruments and the energy balance bowen ratio. Data was also compared with the SONDE data that was launched some distance away from the tower.</u><br><u><a href="https://www.arm.gov/publications/tech_reports/handbooks/twr_handbook.pdf">https://www.arm.gov/publications/tech_reports/handbooks/twr_handbook.pdf</a></u> |
| <u>timeSeries Variables</u> | <u>HMT337 (previous HMP35D/HMP45D)</u> | <u>Vaisala</u> | <u>Near-surface (2m) dew point temperature (K)</u>         | <u>The Barrow meteorology station (BMET) uses mainly conventional in situ sensors mounted at four different heights (2m, 10m, 20m and 40m) on a 40 m tower to obtain profiles of wind speed, wind direction, air temperature, dew point and humidity. It also obtains barometric pressure, visibility and precipitation data from sensors at the base of the tower.</u><br><u><a href="https://www.arm.gov/capabilities/instruments/twr">https://www.arm.gov/capabilities/instruments/twr</a></u> | <u>1 min</u> | <u>0.2 K</u>                 | <u>Beyond the standard Vaisala processing, observations were checked against other instrumentation on the tower and compared with the surface meteorological instruments and the energy balance bowen ratio. Data was also compared with the SONDE data that was launched some distance away from the tower.</u><br><u><a href="https://www.arm.gov/publications/tech_reports/handbooks/twr_handbook.pdf">https://www.arm.gov/publications/tech_reports/handbooks/twr_handbook.pdf</a></u> |

| <a href="#">pabilities/instruments/twr</a> |   |                                   |  |   |                       |                       |  |
|--|---|-----------------------------------|--|---|-----------------------|-----------------------|--|
| <a href="#">timeSeries Variables</a>       | <a href="#">HMT337 (previous HMP35D/HMP45D)</a> | <a href="#">Vaisala</a>           | <a href="#">Near-surface (2m) relative humidity (%)</a>    | <a href="#">The Barrow meteorology station (BMET) uses mainly conventional in situ sensors mounted at four different heights (2m, 10m, 20m and 40m) on a 40 m tower to obtain profiles of wind speed, wind direction, air temperature, dew point and humidity. It also obtains barometric pressure, visibility and precipitation data from sensors at the base of the tower.</a><br><a href="https://www.arm.gov/capabilities/instruments/twr">https://www.arm.gov/capabilities/instruments/twr</a> | <a href="#">1 min</a> | <a href="#">1.7 %</a> | <a href="#">Beyond the standard Vaisala processing, observations were checked against other instrumentation on the tower and compared with the surface meteorological instruments and the energy balance Bowen ratio. Data was also compared with the SONDE data that was launched some distance away from the tower.</a><br><a href="https://www.arm.gov/publications/tech_reports/handbooks/twr_handbook.pdf">https://www.arm.gov/publications/tech_reports/handbooks/twr_handbook.pdf</a>   |
| <a href="#">timeSeries Variables</a>       | <a href="#">TEI49i</a>                          | <a href="#">Thermo Scientific</a> | <a href="#">Ozone concentration in air (mole fraction)</a> | <a href="#">Inlet line samples air from roof of station through filter, while instrument is housed inside station building</a>  | <a href="#">1 min</a> | <a href="#">1 ppb</a> | <a href="#">This data set contains continuous UV photometric data of surface level ozone collected at 6m above ground level. Data records consist of UTC time, date, and processed ozone mixing ratio (parts per billion). Data is collected from global locations and is provided in 1 minute and 1 hour averages. Data are archived at the NOAA National Climatic Data Center (NCDC), but are produced and available from NOAA Earth System Research Laboratory (ESRL).</a><br><a href="https://www.ncsl.noaa.gov/access/metadata/landing-page/bin/iso?id=gov.noaa.ncdc:C00894">https://www.ncsl.noaa.gov/access/metadata/landing-page/bin/iso?id=gov.noaa.ncdc:C00894</a> |
| <a href="#">timeSeries Variables</a>       | <a href="#">Toughsonic 30</a>                   | <a href="#">Senix</a>             | <a href="#">Surface snow thickness (m)</a>                 | <a href="#">Instrument is located on broadband radiation rack</a>   | <a href="#">1 min</a> | <a href="#">n/a</a>   | <a href="#">Data is compared against meteorological and global radiation data to verify accuracy; pollution/technical events are flagged and/or removed from data set; data values not physically possible are removed</a>   |
| <a href="#">timeSeries Variables</a>       | <a href="#">IRT</a>                             | <a href="#">Apogee</a>            | <a href="#">Surface (skin) temperature (K)</a>             | <a href="#">Data collected from US Climate Reference Network (CRN)</a>  | <a href="#">1 min</a> | <a href="#">0.5 K</a> | <a href="#">Inter-comparison of the 3 temperature sensors: Sensors should be within 0.3° C of one another. An hourly flag message is generated for any departure greater than 0.30° C (i.e., 0.301° C and greater). IR_max should exceed the ambient temperature, and IR_min should be less than ambient temperature.</a><br><a href="https://www1.ncdc.noaa.gov/pub/data/uscrn/documentation/program/ManualMonitoringHandbook.pdf">https://www1.ncdc.noaa.gov/pub/data/uscrn/documentation/program/ManualMonitoringHandbook.pdf</a>   |

|                             |                |            |   |   |       |                       |   |
|-----------------------------|----------------|------------|---|---|-------|-----------------------|---|
| <u>timeSeries Variables</u> | <u>GNDRA D</u> | <u>PSP</u> | Upward surface short-wave radiation (W m <sup>-2</sup> )          | <a href="https://www.arm.gov/capabilities/instruments/gndrad">https://www.arm.gov/capabilities/instruments/gndrad</a> | 1 min | 2.0 W m <sup>-2</sup> | SIRS Instrument mentors review the Data Quality Office's (DQO) weekly Data Quality Assessment Reports (DQAR). If a problem is detected, a Data Quality Problem Report (DQPR) is issued. The DQPR system is a web-based system by which the mentor, local site operations staff, and the DQO are informed and communicate to resolve a data quality problem (e.g., instrument failure, data collection issue, etc.). A DQPR is typically initiated by the DQO or instrument mentor during data review. Data Quality Reports (DQR) are prepared by instrument mentors as needed to close out corresponding DQPRs. <a href="https://www.arm.gov/capabilities/instruments/gndrad">https://www.arm.gov/capabilities/instruments/gndrad</a> |
| <u>timeSeries Variables</u> | <u>SKYRA D</u> | <u>PSP</u> | Downward short-wave radiation at the surface (W m <sup>-2</sup> ) | <a href="https://www.arm.gov/capabilities/instruments/skyrad">https://www.arm.gov/capabilities/instruments/skyrad</a> | 1 min | 4.0 W m <sup>-2</sup> | SIRS Instrument mentors review the Data Quality Office's (DQO) weekly Data Quality Assessment Reports (DQAR). If a problem is detected, a Data Quality Problem Report (DQPR) is issued. The DQPR system is a web-based system by which the mentor, local site operations staff, and the DQO are informed and communicate to resolve a data quality problem (e.g., instrument failure, data collection issue, etc.). A DQPR is typically initiated by the DQO or instrument mentor during data review. Data Quality Reports (DQR) are prepared by instrument mentors as needed to close out corresponding DQPRs. <a href="https://www.arm.gov/capabilities/instruments/skyrad">https://www.arm.gov/capabilities/instruments/skyrad</a> |
| <u>timeSeries Variables</u> | <u>GNDRA D</u> | <u>PIR</u> | Upward surface long-wave radiation (W m <sup>-2</sup> )           | <a href="https://www.arm.gov/capabilities/instruments/gndrad">https://www.arm.gov/capabilities/instruments/gndrad</a> | 1 min | 2.0 W m <sup>-2</sup> | SIRS Instrument mentors review the Data Quality Office's (DQO) weekly Data Quality Assessment Reports (DQAR). If a problem is detected, a Data Quality Problem Report (DQPR) is issued. The DQPR system is a web-based system by which the mentor, local site operations staff, and the DQO are informed and communicate to resolve a data quality problem (e.g., instrument failure, data collection issue, etc.). A DQPR is typically initiated by the DQO or instrument mentor during data review. Data Quality Reports (DQR) are prepared by instrument mentors as needed to close out corresponding DQPRs. <a href="https://www.arm.gov/capabilities/instruments/gndrad">https://www.arm.gov/capabilities/instruments/gndrad</a> |
| <u>timeSeries Variables</u> | <u>SKYRA D</u> | <u>PIR</u> | Downward surface long-wave radiation (W m <sup>-2</sup> )         | <a href="https://www.arm.gov/capabilities/instruments/skyrad">https://www.arm.gov/capabilities/instruments/skyrad</a> | 1 min | 4.0 W m <sup>-2</sup> | SIRS Instrument mentors review the Data Quality Office's (DQO) weekly Data Quality Assessment Reports (DQAR). If a problem is detected, a Data Quality Problem Report (DQPR) is issued. The DQPR system is a web-based system by which the mentor, local site operations staff, and the DQO are informed and communicate to resolve a data quality problem (e.g., instrument failure, data collection issue, etc.). A DQPR is typically initiated by the DQO or instrument mentor during data review. Data Quality Reports (DQR) are prepared by instrument mentors as needed to close out corresponding DQPRs. <a href="https://www.arm.gov/capabilities/instruments/skyrad">https://www.arm.gov/capabilities/instruments/skyrad</a> |

|                             |                                  |             |  |  |              |                  |  |
|-----------------------------|----------------------------------|-------------|--|--|--------------|------------------|--|
| <u>timeSeries Variables</u> | <u>Windmaster Pro Anemometer</u> | <u>Gill</u> | <u>Surface turbulent latent heat flux (eddy covariance method) (W m<sup>2</sup>)</u> | <u>Standard ARM site arrangement is sonic sensor "North" mark pointing along the boom to the tower; the boom is usually pointing due south; u wind component is north-south with positive toward the north; v wind component is east-west with positive toward the west. NOTE: no correction is made to convert u and v component into meteorological "north" and "east" wind components when tower boom is not aligned to south; u wind component is "along boom", v wind component is "cross boom</u><br><a href="https://www.arm.gov/publications/tech_reports/doe-sc-arm-tr-223.pdf">https://www.arm.gov/publications/tech_reports/doe-sc-arm-tr-223.pdf</a> | <u>1 min</u> | <u>&lt;1.5 %</u> | <u>The QCECOR VAP currently contains two variables: surface latent heat flux (LH) and sensible heat flux (SH), together with their QC flags. When SEBS are collocated with ECOR, the wetness measurements from SEBS are used to flag the LH that may be incorrect due to hydrometeors such as precipitation, dew, or frost. An indeterminate flag is given to those that fail the wetness test.</u><br><a href="https://www.arm.gov/publications/tech_reports/doe-sc-arm-tr-223.pdf">chrome-extension://efaidnbmnnnibpcajpcglclefindmkaj/https://www.arm.gov/publications/tech_reports/doe-sc-arm-tr-223.pdf</a> |
|-----------------------------|----------------------------------|-------------|--|--|--------------|------------------|--|

|                             |                                  |             |  |  |              |                  |  |
|-----------------------------|----------------------------------|-------------|--|--|--------------|------------------|--|
| <u>timeSeries Variables</u> | <u>Windmaster Pro Anemometer</u> | <u>Gill</u> | <u>Surface sensible heat flux (eddy covariance method) (W m<sup>2</sup>)</u> | <u>Standard ARM site arrangement is sonic sensor "North" mark pointing along the boom to the tower; the boom is usually pointing due south; u wind component is north-south with positive toward the north; v wind component is east-west with positive toward the west. NOTE: no correction is made to convert u and v component into meteorological "north" and "east" wind components when tower boom is not aligned to south; u wind component is "along boom", v wind component is "cross boom</u><br><a href="https://www.arm.gov/publications/tech_reports/doe-sc-arm-tr-223.pdf">https://www.arm.gov/publications/tech_reports/doe-sc-arm-tr-223.pdf</a> | <u>1 min</u> | <u>&lt;1.5 %</u> | <u>The QCECOR VAP currently contains two variables: surface latent heat flux (LH) and sensible heat flux (SH), together with their QC flags. When SEBS are collocated with ECOR, the wetness measurements from SEBS are used to flag the LH that may be incorrect due to hydrometeors such as precipitation, dew, or frost. An indeterminate flag is given to those that fail the wetness test.</u><br><a href="https://www.arm.gov/publications/tech_reports/doe-sc-arm-tr-223.pdf">chrome-extension://efaidnbmnnnibpcajpcglclefindmkaj/https://www.arm.gov/publications/tech_reports/doe-sc-arm-tr-223.pdf</a> |
|-----------------------------|----------------------------------|-------------|--|--|--------------|------------------|--|

|                                     |                           |  |   |   |              |                                   |  |
|-------------------------------------|---------------------------|--|---|---|--------------|-----------------------------------|--|
| <u>timeSeries Variables</u>         | <u>HFT-3, SMP1, STP-1</u> | <u>Radiation and Energy Balance System, Inc.</u> | <u>Ground heat flux (<math>W m^{-2}</math>)</u>         | <u>Soil measurements are performed by three sets of soil heat flow (5 cm depth), soil temperature (0-5 cm average), and soil moisture (centered at 2.5 cm) probes. Soil heat flow is adjusted for the effect of soil moisture above the soil heat flow plate. The storage of energy in the soil above the soil heat flow plate is determined from the change in soil temperature with time.</u>   | <u>1 min</u> | <u>10 mV</u>                      | <u>Instrument mentor routinely views graphic displays that include plots (day courses) of all calculated quantities and comparison plots (time series or scatter plots) of relevant parameters with data from collocated ECOR, SEBS, EBBR (SGP CF and EF39 only), and surface meteorological instrumentation (MET) (Cook et al. 2006). chrome-extension://efaidnbmnppacgpcglclefindmkaj/https://www.arm.gov/publications/tech_reports/handbooks/sebs_handbook.pdf</u>            |
| <u>timeSeries Profile Variables</u> | <u>WS425</u>              | <u>Vaisala</u>                                   | <u>Eastward wind component (<math>m s^{-1}</math>)</u>  | <u>The Barrow meteorology station (BMET) uses mainly conventional in situ sensors mounted at four different heights (2m, 10m, 20m and 40m) on a 40 m tower to obtain profiles of wind speed, wind direction, air temperature, dew point and humidity. It also obtains barometric pressure, visibility and precipitation data from sensors at the base of the tower. <a href="https://www.arm.gov/capabilities/instruments/twr">https://www.arm.gov/capabilities/instruments/twr</a></u> | <u>1 min</u> | <u>0.135 <math>ms^{-1}</math></u> | <u>Beyond the standard Vaisala processing, observations were checked against other instrumentation on the tower and compared with the surface meteorological instruments and the energy balance Bowen ratio. Data was also compared with the SONDE data that was launched some distance away from the tower: <a href="https://www.arm.gov/publications/tech_reports/handbooks/twr_handbook.pdf">https://www.arm.gov/publications/tech_reports/handbooks/twr_handbook.pdf</a></u> |
| <u>timeSeries Profile Variables</u> | <u>WS425</u>              | <u>Vaisala</u>                                   | <u>Northward wind component (<math>m s^{-1}</math>)</u> | <u>The Barrow meteorology station (BMET) uses mainly conventional in situ sensors mounted at four different heights (2m, 10m, 20m and 40m) on a 40 m tower to obtain profiles of wind speed, wind direction, air temperature, dew point and humidity. It also obtains barometric pressure, visibility and precipitation data from sensors at the base of the tower. <a href="https://www.arm.gov/capabilities/instruments/twr">https://www.arm.gov/capabilities/instruments/twr</a></u> | <u>1 min</u> | <u>0.135 <math>ms^{-1}</math></u> | <u>Beyond the standard Vaisala processing, observations were checked against other instrumentation on the tower and compared with the surface meteorological instruments and the energy balance Bowen ratio. Data was also compared with the SONDE data that was launched some distance away from the tower: <a href="https://www.arm.gov/publications/tech_reports/handbooks/twr_handbook.pdf">https://www.arm.gov/publications/tech_reports/handbooks/twr_handbook.pdf</a></u> |

|                                    |   |             |   |   |          |       |   |
|------------------------------------|---|-------------|---|---|----------|-------|---|
| timeSeries<br>Profile<br>Variables | HMT337<br>(previous<br>ly<br>HMP35D<br>/HMP45<br>D) | Vaisal<br>a | Air<br>tempe<br>rature<br>(K)           | The _____ Barrow<br>meteorology station<br>(BMET) uses mainly<br>conventional in situ<br>sensors mounted at four<br>different heights (2m,<br>10m, 20m and 40m) on a<br>40 m tower to obtain<br>profiles of wind speed,<br>wind direction, air<br>temperature, dew point<br>and humidity. It also<br>obtains _____ barometric<br>pressure, visibility and<br>precipitation data from<br>sensors at the base of the<br>tower.<br><a href="https://www.arm.gov/capabilities/instruments/twr">https://www.arm.gov/capabilities/instruments/twr</a> | 1<br>min | 0.2 K | Beyond the standard Vaisala processing, observations were<br>checked against other instrumentation on the tower and<br>compared with the surface meteorological instruments and<br>the energy balance bowen ratio. Data was also compared<br>with the SONDE data that was launched some distance<br>away _____ from _____ the _____ tower;<br><a href="https://www.arm.gov/publications/tech_reports/handbooks/twr_handbook.pdf">https://www.arm.gov/publications/tech_reports/handbooks/twr_handbook.pdf</a> |
| timeSeries<br>Profile<br>Variables | HMT337<br>(previous<br>ly<br>HMP35D<br>/HMP45<br>D) | Vaisal<br>a | Dew-<br>point<br>tempe<br>rature<br>(K) | The _____ Barrow<br>meteorology station<br>(BMET) uses mainly<br>conventional in situ<br>sensors mounted at four<br>different heights (2m,<br>10m, 20m and 40m) on a<br>40 m tower to obtain<br>profiles of wind speed,<br>wind direction, air<br>temperature, dew point<br>and humidity. It also<br>obtains _____ barometric<br>pressure, visibility and<br>precipitation data from<br>sensors at the base of the<br>tower.<br><a href="https://www.arm.gov/capabilities/instruments/twr">https://www.arm.gov/capabilities/instruments/twr</a> | 1<br>min | 0.2 K | Beyond the standard Vaisala processing, observations were<br>checked against other instrumentation on the tower and<br>compared with the surface meteorological instruments and<br>the energy balance bowen ratio. Data was also compared<br>with the SONDE data that was launched some distance<br>away _____ from _____ the _____ tower;<br><a href="https://www.arm.gov/publications/tech_reports/handbooks/twr_handbook.pdf">https://www.arm.gov/publications/tech_reports/handbooks/twr_handbook.pdf</a> |
| timeSeries<br>Profile<br>Variables | HMT337<br>(previous<br>ly<br>HMP35D<br>/HMP45<br>D) | Vaisal<br>a | Relati<br>ve<br>humi<br>dity<br>(%)     | The _____ Barrow<br>meteorology station<br>(BMET) uses mainly<br>conventional in situ<br>sensors mounted at four<br>different heights (2m,<br>10m, 20m and 40m) on a<br>40 m tower to obtain<br>profiles of wind speed,<br>wind direction, air<br>temperature, dew point<br>and humidity. It also<br>obtains _____ barometric<br>pressure, visibility and<br>precipitation data from<br>sensors at the base of the<br>tower.<br><a href="https://www.arm.gov/capabilities/instruments/twr">https://www.arm.gov/capabilities/instruments/twr</a> | 1<br>min | 1.7 % | Beyond the standard Vaisala processing, observations were<br>checked against other instrumentation on the tower and<br>compared with the surface meteorological instruments and<br>the energy balance bowen ratio. Data was also compared<br>with the SONDE data that was launched some distance<br>away _____ from _____ the _____ tower;<br><a href="https://www.arm.gov/publications/tech_reports/handbooks/twr_handbook.pdf">https://www.arm.gov/publications/tech_reports/handbooks/twr_handbook.pdf</a> |

|   |                       |                            |   | pabilities/instruments/tw<br>f  |                        |                       |  |
|---|-----------------------|----------------------------|---|---|------------------------|-----------------------|--|
| <a href="#">timeSeries Profile Variables</a>      | <a href="#">PT100</a> | <a href="#">in-house</a>   | <a href="#">Soil temperature profile (K)</a>                | <a href="#">Instrument is located on broadband radiation albedo rack</a>  | <a href="#">1 min</a>  | <a href="#">n/a</a>   | <a href="#">Data is compared against meteorological and global radiation data to verify accuracy; pollution/technical events are flagged and/or removed from data set; data values not physically possible are removed</a>   |
| <a href="#">timeSeries Profile Variables</a>      | <a href="#">KAZR</a>  | <a href="#">KAZR</a>       | <a href="#">Snow fall flux per unit area</a>                | <a href="#">Installed on top of the ARM facility roof</a>   | <a href="#">1 min</a>  | <a href="#">n/a</a>   | <a href="https://doi.org/10.1525/elementa.2021.00101">https://doi.org/10.1525/elementa.2021.00101</a><br><a href="chrome-extension://efaidnbmnbbpcajpcglclefindmkaj/https://www.arm.gov/publications/tech_reports/handbooks/kazr_handbook.pdf">chrome-extension://efaidnbmnbbpcajpcglclefindmkaj/https://www.arm.gov/publications/tech_reports/handbooks/kazr_handbook.pdf</a>   |
| <a href="#">timeSeries ProfileSonde Variables</a> | <a href="#">SONDE</a> | <a href="#">Radiosonde</a> | <a href="#">Atmospheric pressure (Pa)</a>                   | <a href="#">The SONDE system originally located at Barrow was an old CLASS-type that was originally operated by NOAA's Climate Measurements and Diagnostics Laboratory on TWP's Manus site.</a> | <a href="#">30 min</a> | <a href="#">1 hPa</a> | <a href="#">The manufacturer defines the cumulative sensor uncertainty at the 2-sigma (95.5%) confidence level. Repeatability is estimated from the standard deviation of differences between two successive repeated calibrations (2-sigma). Reproducibility is estimated from the standard deviation of differences in twin soundings. Citation recommendation: Atmospheric Radiation Measurement (ARM) user facility. 2002. Balloon-Borne Sounding System (SONDEWNP). 2002-04-28 to 2022-11-17, North Slope Alaska (NSA) Central Facility, Barrow AK (C1). Compiled by K. Burk. ARM Data Center. Data set accessed 2022-11-18 at <a href="http://dx.doi.org/10.5439/1595321">http://dx.doi.org/10.5439/1595321</a>.</a> |
| <a href="#">timeSeries ProfileSonde Variables</a> | <a href="#">SONDE</a> | <a href="#">Radiosonde</a> | <a href="#">Eastward wind component (m s<sup>-1</sup>)</a>  | <a href="#">The SONDE system originally located at Barrow was an old CLASS-type that was originally operated by NOAA's Climate Measurements and Diagnostics Laboratory on TWP's Manus site.</a> | <a href="#">30 min</a> | <a href="#">n/a</a>   | <a href="#">The manufacturer defines the cumulative sensor uncertainty at the 2-sigma (95.5%) confidence level. Repeatability is estimated from the standard deviation of differences between two successive repeated calibrations (2-sigma). Reproducibility is estimated from the standard deviation of differences in twin soundings. Citation recommendation: Atmospheric Radiation Measurement (ARM) user facility. 2002. Balloon-Borne Sounding System (SONDEWNP). 2002-04-28 to 2022-11-17, North Slope Alaska (NSA) Central Facility, Barrow AK (C1). Compiled by K. Burk. ARM Data Center. Data set accessed 2022-11-18 at <a href="http://dx.doi.org/10.5439/1595321">http://dx.doi.org/10.5439/1595321</a>.</a> |
| <a href="#">timeSeries ProfileSonde Variables</a> | <a href="#">SONDE</a> | <a href="#">Radiosonde</a> | <a href="#">Northward wind component (m s<sup>-1</sup>)</a> | <a href="#">The SONDE system originally located at Barrow was an old CLASS-type that was originally operated by NOAA's Climate Measurements and Diagnostics Laboratory on TWP's Manus site.</a> | <a href="#">30 min</a> | <a href="#">n/a</a>   | <a href="#">The manufacturer defines the cumulative sensor uncertainty at the 2-sigma (95.5%) confidence level. Repeatability is estimated from the standard deviation of differences between two successive repeated calibrations (2-sigma). Reproducibility is estimated from the standard deviation of differences in twin soundings. Citation recommendation: Atmospheric Radiation Measurement (ARM) user facility. 2002. Balloon-Borne Sounding System (SONDEWNP). 2002-04-28 to 2022-11-17, North Slope Alaska (NSA) Central Facility, Barrow AK (C1). Compiled by K. Burk. ARM Data Center. Data set accessed 2022-11-18 at <a href="http://dx.doi.org/10.5439/1595321">http://dx.doi.org/10.5439/1595321</a>.</a> |



|   |                       |                            |   |   |                        |                       |   |
|---|-----------------------|----------------------------|---|---|------------------------|-----------------------|---|
| <a href="#">timeSeriesProfileSondeVariables</a> | <a href="#">SONDE</a> | <a href="#">Radiosonde</a> | <a href="#">Temperature (K)</a>           | The SONDE system originally located at Barrow was an old CLASS-type that was originally operated by NOAA's Climate Measurements and Diagnostics Laboratory on TWP's Manus site. | <a href="#">30 min</a> | <a href="#">0.5 K</a> | The manufacturer defines the cumulative sensor uncertainty at the 2-sigma (95.5%) confidence level. Repeatability is estimated from the standard deviation of differences between two successive repeated calibrations (2-sigma). Reproducibility is estimated from the standard deviation of differences in twin soundings. Citation recommendation: Atmospheric Radiation Measurement (ARM) user facility. 2002. Balloon-Borne Sounding System (SONDEWNP). 2002-04-28 to 2022-11-17, North Slope Alaska (NSA) Central Facility, Barrow AK (C1). Compiled by K. Burk. ARM Data Center. Data set accessed 2022-11-18 at <a href="http://dx.doi.org/10.5439/1595321">http://dx.doi.org/10.5439/1595321</a> . |
| <a href="#">timeSeriesProfileSondeVariables</a> | <a href="#">SONDE</a> | <a href="#">Radiosonde</a> | <a href="#">Dew-point temperature (K)</a> | The SONDE system originally located at Barrow was an old CLASS-type that was originally operated by NOAA's Climate Measurements and Diagnostics Laboratory on TWP's Manus site. | <a href="#">30 min</a> | <a href="#">0.5 K</a> | The manufacturer defines the cumulative sensor uncertainty at the 2-sigma (95.5%) confidence level. Repeatability is estimated from the standard deviation of differences between two successive repeated calibrations (2-sigma). Reproducibility is estimated from the standard deviation of differences in twin soundings. Citation recommendation: Atmospheric Radiation Measurement (ARM) user facility. 2002. Balloon-Borne Sounding System (SONDEWNP). 2002-04-28 to 2022-11-17, North Slope Alaska (NSA) Central Facility, Barrow AK (C1). Compiled by K. Burk. ARM Data Center. Data set accessed 2022-11-18 at <a href="http://dx.doi.org/10.5439/1595321">http://dx.doi.org/10.5439/1595321</a> . |
| <a href="#">timeSeriesProfileSondeVariables</a> | <a href="#">SONDE</a> | <a href="#">Radiosonde</a> | <a href="#">Relative humidity (%)</a>     | The SONDE system originally located at Barrow was an old CLASS-type that was originally operated by NOAA's Climate Measurements and Diagnostics Laboratory on TWP's Manus site. | <a href="#">30 min</a> | <a href="#">5%</a>    | The manufacturer defines the cumulative sensor uncertainty at the 2-sigma (95.5%) confidence level. Repeatability is estimated from the standard deviation of differences between two successive repeated calibrations (2-sigma). Reproducibility is estimated from the standard deviation of differences in twin soundings. Citation recommendation: Atmospheric Radiation Measurement (ARM) user facility. 2002. Balloon-Borne Sounding System (SONDEWNP). 2002-04-28 to 2022-11-17, North Slope Alaska (NSA) Central Facility, Barrow AK (C1). Compiled by K. Burk. ARM Data Center. Data set accessed 2022-11-18 at <a href="http://dx.doi.org/10.5439/1595321">http://dx.doi.org/10.5439/1595321</a> . |

1016

1017

1018

**Table 8.** List of the instruments that contributed to the Tiksi MODF, including details about the instrument manufacturer, measured variables, configuration, temporal resolution, measurement uncertainty, and quality control applied.

| <u>MODE featureType</u>     | <u>Instrument</u> | <u>Manufacturer</u>        | <u>Measured variable</u>                                   | <u>Instrument Configuration</u>              | <u>Temporal Resolution</u> | <u>Uncertainty (+/-)</u>     | <u>Quality Control</u>  |
|-----------------------------|-------------------|----------------------------|--|--|----------------------------|------------------------------|---|
| <u>timeSeries Variables</u> | <u>PTB110</u>     | <u>Vaisala</u>             | <u>Surface pressure (Pa)</u>                               | <u>Located on the fluxtower at 5m height</u> | <u>1 min</u>               | <u>0.3 hPa</u>               | <u>Data are manually QC'ed to identify and eliminate instrument malfunction; outliers are filtered out if values are physically impossible; values are compared to other local variables if/when possible</u> |
| <u>timeSeries Variables</u> | <u>3001</u>       | <u>RM Young</u>            | <u>Near-surface (4m) eastward wind (m s<sup>-1</sup>)</u>  | <u>Located on the fluxtower at 4m height</u> | <u>1 min</u>               | <u>0.5 m s<sup>-1</sup></u>  | <u>Data are manually QC'ed to identify and eliminate instrument malfunction; outliers are filtered out if values are physically impossible; values are compared to other local variables if/when possible</u> |
| <u>timeSeries Variables</u> | <u>3001</u>       | <u>RM Young</u>            | <u>Near-surface (4m) northward wind (m s<sup>-1</sup>)</u> | <u>Located on the fluxtower at 4m height</u> | <u>1 min</u>               | <u>0.5 m s<sup>-1</sup></u>  | <u>Data are manually QC'ed to identify and eliminate instrument malfunction; outliers are filtered out if values are physically impossible; values are compared to other local variables if/when possible</u> |
| <u>timeSeries Variables</u> | <u>HMT330</u>     | <u>Vaisala</u>             | <u>Near-surface (2m) air temperature (K)</u>               | <u>Located on the fluxtower at 2m height</u> | <u>1 min</u>               | <u>0.2 K</u>                 | <u>Data are manually QC'ed to identify and eliminate instrument malfunction; outliers are filtered out if values are physically impossible; values are compared to other local variables if/when possible</u> |
| <u>timeSeries Variables</u> | <u>HMT330</u>     | <u>Vaisala</u>             | <u>Near-surface (2m) relative humidity (%)</u>             | <u>Located on the fluxtower at 2m height</u> | <u>1 min</u>               | <u>1.5 + 0.015 × reading</u> | <u>Data are manually QC'ed to identify and eliminate instrument malfunction; outliers are filtered out if values are physically impossible; values are compared to other local variables if/when possible</u> |
| <u>timeSeries Variables</u> | <u>SR50A</u>      | <u>Campbell Scientific</u> | <u>Surface snow thickness (m)</u>                          | <u>Located on the albedo rack</u>            | <u>1 min</u>               | <u>1 cm</u>                  | <u>Data are manually QC'ed to identify and eliminate instrument malfunction; outliers are filtered out if values are physically impossible; values are compared to other local variables if/when possible</u> |
| <u>timeSeries Variables</u> | <u>SI-111</u>     | <u>Apogee</u>              | <u>Surface (skin) temperature (K)</u>                      | <u>Located on the fluxtower at 2m height</u> | <u>1 min</u>               | <u>0.2 K</u>                 | <u>Data are manually QC'ed to identify and eliminate instrument malfunction; outliers are filtered out if values are physically impossible; values are compared to</u>  |

other local variables if/when possible

|   |                |              |  |  |       |                |  |
|---|----------------|--------------|--|--|-------|----------------|--|
| <a href="#">timeSeries Variables</a>        | PSP            | Eppley       | Upward surface short-wave radiation ( $W m^{-2}$ )   | Located on the albedo rack                         | 1 min | 2.0 $W m^{-2}$ | Data are manually QC'ed to identify and eliminate instrument malfunction; outliers are filtered out if values are physically impossible; values are compared to other local variables if/when possible |
| <a href="#">timeSeries Variables</a>        | CM22           | Kipp & Zonen | Downward surface short-wave radiation ( $W m^{-2}$ ) | Located on the tracker at the MET station building | 1 min | 5.0 $W m^{-2}$ | Data are manually QC'ed to identify and eliminate instrument malfunction; outliers are filtered out if values are physically impossible; values are compared to other local variables if/when possible |
| <a href="#">timeSeries Variables</a>        | PIR            | Eppley       | Upward surface long-wave radiation ( $W m^{-2}$ )    | Located on the albedo rack                         | 1 min | 2.0 $W m^{-2}$ | Data are manually QC'ed to identify and eliminate instrument malfunction; outliers are filtered out if values are physically impossible; values are compared to other local variables if/when possible |
| <a href="#">timeSeries Variables</a>        | PIR            | Eppley       | Downward surface long-wave radiation ( $W m^{-2}$ )  | Located on the tracker at the MET station building | 1 min | 4.0 $W m^{-2}$ | Data are manually QC'ed to identify and eliminate instrument malfunction; outliers are filtered out if values are physically impossible; values are compared to other local variables if/when possible |
| <a href="#">timeSeries Variables</a>        | HPF01          | Hukseflux    | Ground heat flux ( $W m^{-2}$ )                      | Located at the base of the fluxtower at 5cm depth  | 1 min | 3 %            | Data are manually QC'ed to identify and eliminate instrument malfunction; outliers are filtered out if values are physically impossible; values are compared to other local variables if/when possible |
| <a href="#">timeSeries Variables</a>        | HPF01          | Hukseflux    | Ground heat flux ( $W m^{-2}$ )                      | Located at the base of the fluxtower at 5cm depth  | 1 min | 3 %            | Data are manually QC'ed to identify and eliminate instrument malfunction; outliers are filtered out if values are physically impossible; values are compared to other local variables if/when possible |
| <a href="#">timeSeriesProfile Variables</a> | HMT330, HMP155 | Vaisala      | Air temperature (K)                                  | Located on the fluxtower at 2m, 6m, 10m height     | 1 min | 0.2 K          | Data are manually QC'ed to identify and eliminate instrument malfunction; outliers are filtered out if values are physically impossible; values are compared to  |

other local variables if/when possible

|   |                          |                            |   |  |                        |                                       |  |
|---|--------------------------|----------------------------|---|--|------------------------|---------------------------------------|--|
| <a href="#">timeSeriesProfileVariables</a>      | <a href="#">HMT33015</a> | <a href="#">Vaisala</a>    | <a href="#">Relative humidity (%)</a>                       | <a href="#">Located on the fluxtower at 2m, 6m, 10m height</a>   | <a href="#">1 min</a>  | <a href="#">1.5 + 0.015 × reading</a> | <a href="#">Data are manually QC'ed to identify and eliminate instrument malfunction; outliers are filtered out if values are physically impossible; values are compared to other local variables if/when possible</a> |
| <a href="#">timeSeriesProfileVariables</a>      | <a href="#">TP-101</a>   | <a href="#">MRC</a>        | <a href="#">Soil temperature profile (K)</a>                | <a href="#">Located at albedo rack at depths: 5cm, 10cm, 15cm, 20cm, 25cm, 30cm, 45cm, 70cm, 95cm, 120cm</a> | <a href="#">1 min</a>  | <a href="#">n/a</a>                   | <a href="#">Data are manually QC'ed to identify and eliminate instrument malfunction; outliers are filtered out if values are physically impossible; values are compared to other local variables if/when possible</a> |
| <a href="#">timeSeriesProfileSondeVariables</a> | <a href="#">SONDE</a>    | <a href="#">Radiosonde</a> | <a href="#">Atmospheric pressure (Pa)</a>                   | <a href="#">https://www.ncei.noaa.gov/pub/data/igra/data/data-por/</a>                                       | <a href="#">30 min</a> | <a href="#">1 hPa</a>                 | <a href="#">https://www.ncei.noaa.gov/pub/data/igra/data/data-por/</a>   |
| <a href="#">timeSeriesProfileSondeVariables</a> | <a href="#">SONDE</a>    | <a href="#">Radiosonde</a> | <a href="#">Eastward wind component (m s<sup>-1</sup>)</a>  | <a href="#">https://www.ncei.noaa.gov/pub/data/igra/data/data-por/</a>                                       | <a href="#">30 min</a> | <a href="#">n/a</a>                   | <a href="#">https://www.ncei.noaa.gov/pub/data/igra/data/data-por/</a>   |
| <a href="#">timeSeriesProfileSondeVariables</a> | <a href="#">SONDE</a>    | <a href="#">Radiosonde</a> | <a href="#">Northward wind component (m s<sup>-1</sup>)</a> | <a href="#">https://www.ncei.noaa.gov/pub/data/igra/data/data-por/</a>                                       | <a href="#">30 min</a> | <a href="#">n/a</a>                   | <a href="#">https://www.ncei.noaa.gov/pub/data/igra/data/data-por/</a>   |
| <a href="#">timeSeriesProfileSondeVariables</a> | <a href="#">SONDE</a>    | <a href="#">Radiosonde</a> | <a href="#">Temperature (K)</a>                             | <a href="#">https://www.ncei.noaa.gov/pub/data/igra/data/data-por/</a>                                       | <a href="#">30 min</a> | <a href="#">0.5 K</a>                 | <a href="#">https://www.ncei.noaa.gov/pub/data/igra/data/data-por/</a>   |
| <a href="#">timeSeriesProfileSondeVariables</a> | <a href="#">SONDE</a>    | <a href="#">Radiosonde</a> | <a href="#">Dew-point temperature (K)</a>                   | <a href="#">https://www.ncei.noaa.gov/pub/data/igra/data/data-por/</a>                                       | <a href="#">30 min</a> | <a href="#">0.5 K</a>                 | <a href="#">https://www.ncei.noaa.gov/pub/data/igra/data/data-por/</a>   |
| <a href="#">timeSeriesProfileSondeVariables</a> | <a href="#">SONDE</a>    | <a href="#">Radiosonde</a> | <a href="#">Relative humidity (%)</a>                       | <a href="#">https://www.ncei.noaa.gov/pub/data/igra/data/data-por/</a>                                       | <a href="#">30 min</a> | <a href="#">5%</a>                    | <a href="#">https://www.ncei.noaa.gov/pub/data/igra/data/data-por/</a>   |

1021  
1022  
1023

**Table 9.** List of the instruments that contributed to the Ny-Ålesund MODF, including details about the instrument manufacturer, measured variables, configuration, temporal resolution, measurement uncertainty, and quality control applied.

| <u>MODF feature type</u>   | <u>Instrument</u>                                    | <u>Manufacturer</u>  | <u>Measured variables</u>  | <u>Instrument Configuration</u>  | <u>Temporal Resolution</u> | <u>Uncertainty (+/-)</u> | <u>Quality Control</u>   |
|----------------------------|--|----------------------|--|--|----------------------------|--------------------------|--|
| <u>timeSeries Variable</u> | Digiquarz 6000-16B                                   | Paroscientific, Inc. | Pressure (Pa)  | Installed within a naturally vented protective enclosure.  | 1 min                      | 0.08 hPa                 | Observations were checked against site-based climatology ranges and the rate of change thresholds.   |
| <u>timeSeries Variable</u> | Pluvio2  | OTT                  | Total precipitation of water in all phases per unit area (kg m <sup>-2</sup> s <sup>-1</sup> ) | Single Alter shield  | 1 min                      | 5%                       | Operated and analysed by the University of Cologne. No additional QC was applied; data is raw and should be treated with caution.  |
| <u>timeSeries Variable</u> | Combined Wind Transmitter 4.3324.32.073              | Thies Clima          | Eastward Wind (m s <sup>-1</sup> )   | Opto-electronically scanned three-cup anemometer with low starting speed. The position of the wind vane is detected opto-electronically. | 1 min                      | 0.4 ms <sup>-1</sup>     | Instrument is checked on a daily basis. Observations were checked against site-based climatology ranges, the rate of change thresholds, and redundant measurements in close proximity. |
| <u>timeSeries Variable</u> | Combined Wind Transmitter 4.3324.32.073              | Thies Clima          | Northward Wind (m s <sup>-1</sup> )  | Opto-electronically scanned three-cup anemometer with low starting speed. The position of the wind vane is detected opto-electronically. | 1 min                      | 0.4 ms <sup>-1</sup>     | Instrument is checked on a daily basis. Observations were checked against site-based climatology ranges, the rate of change thresholds, and redundant measurements in close proximity. |
| <u>timeSeries Variable</u> | Ventilated air temperature transmitter 2.1265.20.000 | Thies Clima          | Temperature (K)  | The sensor is protected by a double thermal radiation shield. A built-in ventilator provides for the necessary air flow.                 | 1 min                      | 0.1 K                    | Instrument is checked on a daily basis. Observations were checked against site-based climatology ranges, the rate of change thresholds, and redundant measurements in close proximity. |
| <u>timeSeries Variable</u> | HMP155   | Vaisala              | Relative Humidity (1 or %)   | The sensor with additional temperature sensor is installed in a vented radiation shelter.  | 1 min                      | 0.80%                    | Instrument is checked on a daily basis. Observations were checked against site-based climatology ranges, the rate of change thresholds, and redundant measurements in close proximity. |
| <u>timeSeries Variable</u> | CMP22  | Kipp and Zonen       | Upward Short-wave Radiation (W m <sup>-2</sup> )   | Sensor installed in an Eigenbrodt ventilation system to prevent from icing.  | 1 min                      | 5 Wm <sup>-2</sup>       | Instrument is checked on a daily basis. Data quality check is performed according to BSRN requirements.  |

|   |                               |                |  |   |       |                |  |
|---|-------------------------------|----------------|--|---|-------|----------------|--|
| <u>timeSeries Variables</u>                   | CMP22                         | Kipp and Zonen | Downward Short-wave Radiation ( $W m^{-2}$ ) | Sensor installed in an Eigenbrodt ventilation system to prevent from icing.               | 1 min | 5 $Wm^{-2}$    | Instrument is checked on a daily basis. Data quality check is performed according to BSRN requirements.                              |
| <u>timeSeries Variables</u>                   | Precision Infrared Radiometer | Eppley         | Upward Long-wave Radiation ( $W m^{-2}$ )    | Sensor installed in an Eigenbrodt ventilation system to prevent from icing.               | 1 min | 5 $Wm^{-2}$    | Instrument is checked on a daily basis. Data quality check is performed according to BSRN requirements.                              |
| <u>timeSeries Variables</u>                   | Precision Infrared Radiometer | Eppley         | Downward Long-wave Radiation ( $W m^{-2}$ )  | Sensor is shaded and installed in an Eigenbrodt ventilation system to prevent from icing. | 1 min | 5 $W/m^2$      | Instrument is checked on a daily basis. Data quality check is performed according to BSRN requirements.                              |
| <u>timeSeries Profiles Variables</u>          | CL51                          | Vaisala        | Cloud Base Height (m)                        | Proprietary algorithm determines the lowest cloud base height                             | 1 min | ~10 m          | Operated with the standard Vaisala proprietary algorithm that retrieves cloud base height. Additional check for unphysical outliers. |
| <u>timeSeries Profiles Sounding Variables</u> | RS41                          | Vaisala        | Atmospheric pressure (Pa)                    | Standard radiosonde launch  | 6 hr  | 0.5 hPa        | No additional QC beyond the standard Vaisala proprietary algorithm.  |
| <u>timeSeries Profiles Sounding Variables</u> | RS41                          | Vaisala        | Eastward Wind ( $m s^{-1}$ )                 | Standard radiosonde launch  | 6 hr  | 0.15 $ms^{-1}$ | No additional QC beyond the standard Vaisala proprietary algorithm.  |
| <u>timeSeries Profiles Sounding Variables</u> | RS41                          | Vaisala        | Northward Wind ( $m s^{-1}$ )                | Standard radiosonde launch  | 6 hr  | 0.15 $ms^{-1}$ | No additional QC beyond the standard Vaisala proprietary algorithm.  |
| <u>timeSeries Profiles Sounding Variables</u> | RS41                          | Vaisala        | Temperature (K)                              | Standard radiosonde launch  | 6 hr  | 0.3 K          | No additional QC beyond the standard Vaisala proprietary algorithm.  |
| <u>timeSeries Profiles Sounding Variables</u> | RS41                          | Vaisala        | Relative Humidity (1 or %)                   | Standard radiosonde launch  | 6 hr  | 4%             | No additional QC beyond the standard Vaisala proprietary algorithm.  |

1026  
1027  
1028

**Table 10.** List of the instruments that contributed to the Eureka MODF, including details about the instrument manufacturer, measured variables, configuration, temporal resolution, measurement uncertainty, and quality control applied.

| <u>MODF feature Type</u>    | <u>Instrument</u>            | <u>Manufacturer</u>        | <u>Measured variables</u>                                     | <u>Instrument Configuration</u>             | <u>Temporal Resolution</u> | <u>Uncertainty (+/-)</u>     | <u>Quality Control</u>  |
|-----------------------------|------------------------------|----------------------------|---|---|----------------------------|------------------------------|---|
| <u>timeSeries Variables</u> | <u>PTB220</u>                | <u>Vaisala</u>             | <u>Surface pressure (Pa)</u>                                  | <u>Located on Flux Tower at 2 m height</u>  | <u>1 min</u>               | <u>0.3 hPa</u>               | <u>Data are manually QC'ed to identify and eliminate instrument malfunction; outliers are filtered out if values are physically impossible; values are compared to other local variables if/when possible</u>         |
| <u>timeSeries Variables</u> | <u>VENTUS-UMB Ultrasonic</u> | <u>Lufft</u>               | <u>Near-surface (6m) eastward wind (m s<sup>-1</sup>)</u>     | <u>Located on Flux Tower at 6 m</u>         | <u>1-10 s</u>              | <u>0.1 ms<sup>-1</sup></u>   | <u>Data are manually QC'ed to identify and eliminate instrument malfunction; outliers are filtered out if values are physically impossible; values are compared to other local variables if/when possible</u>         |
| <u>timeSeries Variables</u> | <u>VENTUS-UMB Ultrasonic</u> | <u>Lufft</u>               | <u>Near-surface (6m) northward wind (m s<sup>-1</sup>)</u>    | <u>Located on Flux Tower at 6 m</u>         | <u>1-10 s</u>              | <u>0.1 ms<sup>-1</sup></u>   | <u>Data are manually QC'ed to identify and eliminate instrument malfunction; outliers are filtered out if values are physically impossible; values are compared to other local variables if/when possible</u>         |
| <u>timeSeries Variables</u> | <u>HMT-337</u>               | <u>Vaisala</u>             | <u>Near-surface (2m) air temperature (K)</u>                  | <u>Located on Flux Tower at 2 m height</u>  | <u>1 min</u>               | <u>0.2 K</u>                 | <u>Data are manually QC'ed to identify and eliminate instrument malfunction; outliers are filtered out if values are physically impossible; values are compared to other local variables if/when possible</u>         |
| <u>timeSeries Variables</u> | <u>HMT-337</u>               | <u>Vaisala</u>             | <u>Near-surface (2m) relative humidity (%)</u>                | <u>Located on Flux Tower at 2 m height</u>  | <u>1 min</u>               | <u>1.5 + 0.015 × reading</u> | <u>Data are manually QC'ed to identify and eliminate instrument malfunction; outliers are filtered out if values are physically impossible; values are compared to other local variables if/when possible</u>         |
| <u>timeSeries Variables</u> | <u>SR50A</u>                 | <u>Campbell Scientific</u> | <u>Surface Snow Thickness</u>                                 | <u>Located on Flux Tower at 2 m height</u>  | <u>1 min</u>               | <u>1 cm</u>                  | <u>Manually QC'ed to identify and eliminate instrument malfunction and remove non-physical values.</u>  |
| <u>timeSeries Variables</u> | <u>IRTS-P</u>                | <u>Apogee</u>              | <u>Surface (skin) temperature (K)</u>                         | <u>Located on Flux Tower at 2 m height</u>  | <u>1 min</u>               | <u>0.2 K</u>                 | <u>Data are manually QC'ed to identify and eliminate instrument malfunction; outliers are filtered out if values are physically impossible; values are compared to other local variables if/when possible</u>         |
| <u>timeSeries Variables</u> | <u>PSP</u>                   | <u>Eppley</u>              | <u>Upward surface short-wave radiation (W m<sup>-2</sup>)</u> | <u>Located on Flux Tower at 11 m height</u> | <u>1 min</u>               | <u>2.0 W m<sup>-2</sup></u>  | <u>Processed through Long QCRad; Historical Quality Control Techniques; Long, C. N., &amp; Shi, Y. (2008). An Automated Quality Assessment and Control Algorithm for Surface Radiation Measurements. OASJ, 2, 23-</u> |

|  |                         |                                    |  |  |                       |   |   |
|--|-------------------------|------------------------------------|--|--|-----------------------|---|---|
|  |                         |                                    |  |  |                       |   | 37. doi:<br>10.2174/1874282300802010023<br>Younkin, K., & Long, C. N. (2004).<br>Improved Correction of IR Loss in<br>Diffuse Shortwave Measurements: An<br>ARM Value Added Product.  |
| <a href="#">timeSeries<br/>Variables</a>             | <a href="#">CM22</a>    | <a href="#">Kipp and<br/>Zonen</a> | <a href="#">Downward<br/>surface<br/>short-wave<br/>radiation (W<br/>m<sup>-2</sup>)</a> | <a href="#">Located on Flux<br/>Tower at 11 m<br/>height</a> | <a href="#">1 min</a> | <a href="#">5.0 W m<sup>-2</sup></a>          | Processed through Long OCRad;<br>Historical Quality Control Techniques;<br>Long, C. N., & Shi, Y. (2008). An<br>Automated Quality Assessment and<br>Control Algorithm for Surface<br>Radiation Measurements. OASJ, 2, 23-<br>37. doi:<br>10.2174/1874282300802010023<br>Younkin, K., & Long, C. N. (2004).<br>Improved Correction of IR Loss in<br>Diffuse Shortwave Measurements: An<br>ARM Value Added Product. |
| <a href="#">timeSeries<br/>Variables</a>             | <a href="#">CM22</a>    | <a href="#">Kipp and<br/>Zonen</a> | <a href="#">Upward<br/>surface<br/>long-wave<br/>radiation (W<br/>m<sup>-2</sup>)</a>    | <a href="#">Located on Flux<br/>Tower at 11 m<br/>height</a> | <a href="#">1 min</a> | <a href="#">5.0 W m<sup>-2</sup></a>          | Processed through Long QCRad;<br>Historical Quality Control Techniques;<br>Long, C. N., & Shi, Y. (2008). An<br>Automated Quality Assessment and<br>Control Algorithm for Surface<br>Radiation Measurements. OASJ, 2, 23-<br>37. doi:<br>10.2174/1874282300802010023<br>Younkin, K., & Long, C. N. (2004).<br>Improved Correction of IR Loss in<br>Diffuse Shortwave Measurements: An<br>ARM Value Added Product. |
| <a href="#">timeSeries<br/>Variables</a>             | <a href="#">PIR</a>     | <a href="#">Eppley</a>             | <a href="#">Downward<br/>surface<br/>long-wave<br/>radiation (W<br/>m<sup>-2</sup>)</a>  | <a href="#">Located on Flux<br/>Tower at 11 m<br/>height</a> | <a href="#">1 min</a> | <a href="#">4.0 W m<sup>-2</sup></a>          | Processed through Long QCRad;<br>Historical Quality Control Techniques;<br>Long, C. N., & Shi, Y. (2008). An<br>Automated Quality Assessment and<br>Control Algorithm for Surface<br>Radiation Measurements. OASJ, 2, 23-<br>37. doi:<br>10.2174/1874282300802010023<br>Younkin, K., & Long, C. N. (2004).<br>Improved Correction of IR Loss in<br>Diffuse Shortwave Measurements: An<br>ARM Value Added Product. |
| <a href="#">timeSeries<br/>Variables</a>             | <a href="#">HPFO1</a>   | <a href="#">Hukseflux</a>          | <a href="#">Ground heat<br/>flux (W m<sup>-2</sup>)</a>                                  | <a href="#">Depth 3 cm</a>                                   | <a href="#">1 min</a> | <a href="#">3 %</a>                           | Manually QC'ed to identify and<br>eliminate instrument malfunction  |
| <a href="#">timeSeriesPro<br/>file<br/>Variables</a> | <a href="#">HMT-337</a> | <a href="#">Vaisala</a>            | <a href="#">Air<br/>temperature<br/>(K)</a>  | <a href="#">Located on Flux<br/>Tower at 2, 6, 10 m</a>      | <a href="#">1 min</a> | <a href="#">0.2 K</a>                         | Manually QC'ed to identify and<br>eliminate instrument malfunction. The<br>lowest level of temperature profile is<br>also saved in the timeSeries file as<br>surface temperature tas  |
| <a href="#">timeSeriesPro<br/>file<br/>Variables</a> | <a href="#">HMT-337</a> | <a href="#">Vaisala</a>            | <a href="#">Relative<br/>humidity<br/>(%)</a>  | <a href="#">Located on Flux<br/>Tower at 2, 6, 10 m</a>      | <a href="#">1 min</a> | <a href="#">1.5 +<br/>0.015 ×<br/>reading</a> | Manually QC'ed to identify and<br>eliminate instrument malfunction. The<br>lowest level of humidity profile is also<br>saved in the timeSeries file as surface<br>humidity hurs   |



|   |                                  |       |  |   |        |                      |  |
|---|----------------------------------|-------|--|---|--------|----------------------|--|
| <u>timeSeriesPro<br/>file<br/>Variables</u> | TP-101                           | MRC   | Soil<br>temperature<br>profile (K)                     | Depth: 5cm [mV],<br>10cm [mV], 15cm<br>[mV], 20cm [mV],<br>25cm [mV], 30cm<br>[mV], 45cm [mV],<br>70cm [mV], 95cm<br>[mV], 120cm [mV] | 1 min  | n/a                  | <u>Manually QC'ed to identify and<br/>eliminate instrument malfunction.</u>  |
| <u>timeSeriesPro<br/>file<br/>Variables</u> | VENTUS<br>-UMB<br>Ultrasoni<br>c | Lufft | Eastward<br>wind<br>component<br>(m s <sup>-1</sup> )  | Located on Flux<br>Tower at 6 m and<br>11 m   | 1-10 s | 0.1 ms <sup>-1</sup> | <u>Manually QC'ed to identify and<br/>eliminate instrument malfunction. The<br/>lowest level of wind speed profile is also<br/>saved in the timeSeries file as surface<br/>wind vspeed uas</u> |
| <u>timeSeriesPro<br/>file<br/>Variables</u> | VENTUS<br>-UMB<br>Ultrasoni<br>c | Lufft | Northward<br>wind<br>component<br>(m s <sup>-1</sup> ) | Located on Flux<br>Tower at 6 m and<br>11 m   | 1-10 s | 0.1 ms <sup>-1</sup> | <u>Manually QC'ed to identify and<br/>eliminate instrument malfunction. The<br/>lowest level of wind speed profile is also<br/>saved in the timeSeries file as surface<br/>wind speed vas</u>  |

1031  
1032  
1033  
1034  
1035

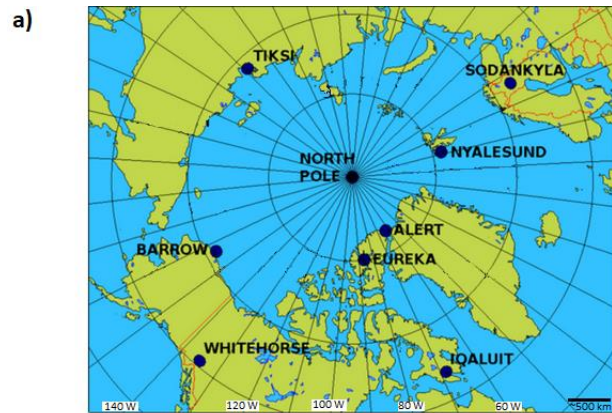
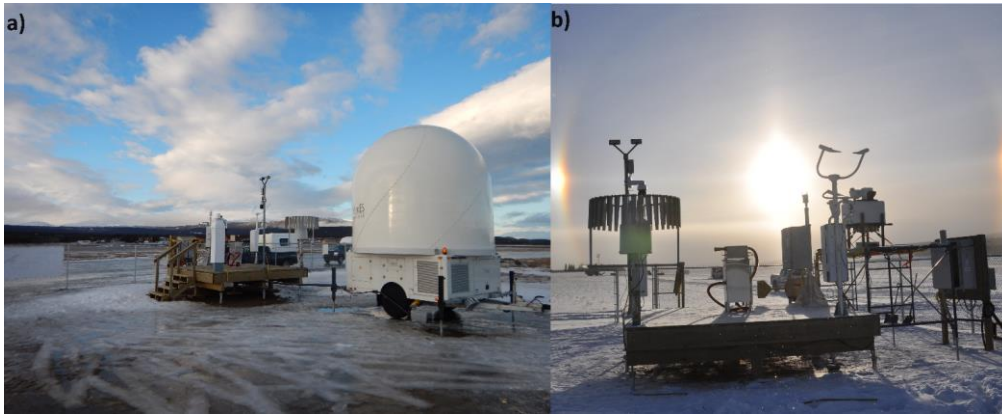


**Figure 1.** a) Locations of the MODF<sub>ysm</sub> YOPP supersites (Antarctic supersites not shown). (b) Infographic depicting iconic building(s) at each supersite. The infographic is roughly centred around the North Pole (centre). All locations shown have generated a MODF<sub>ysm</sub>, with the exception of Alert (in progress).

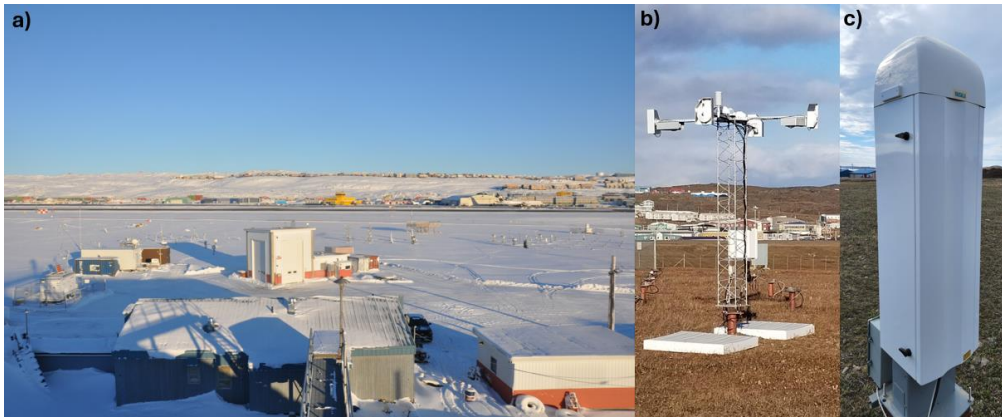
Formatted: Font color: Auto

Formatted: Font: 9 pt

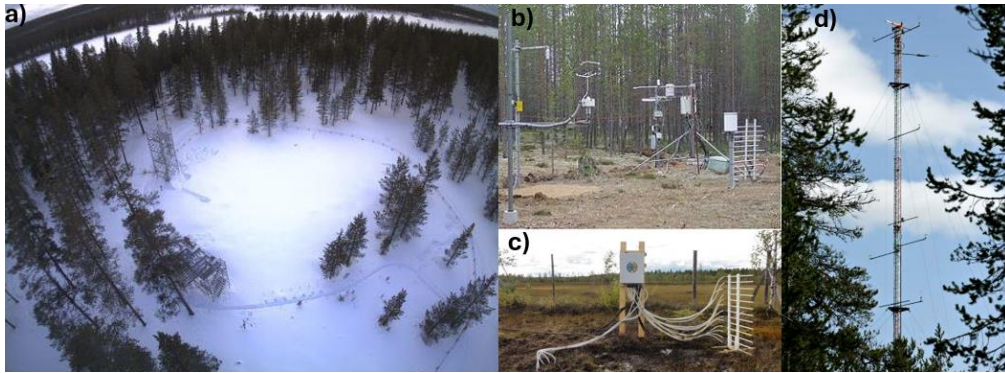
Formatted: Space After: 10 pt, Line spacing: single, Bottom: (No border), Top: (No border), Left: (No border), Right: (No border), Between : (No border)



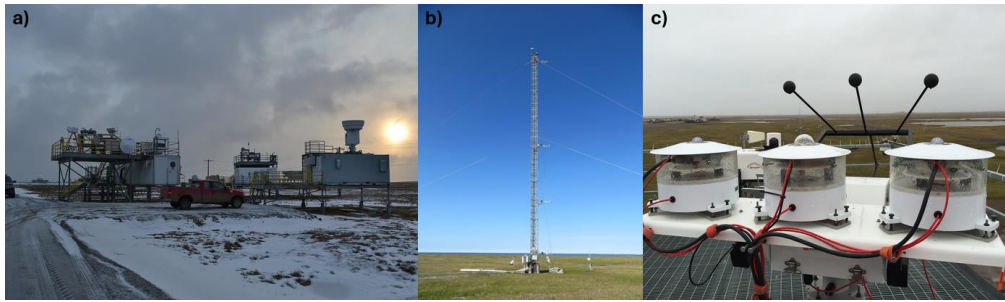
1042  
1043 **Figure 2.** The Whitehorse site and the surrounding airfield in early spring 2018 with an X-band radar (white dome) in the foreground (a),  
1044 and the main instrument platform, including a Pluvio2, Parsivel, FS11P, WXT520, and CL51 ceilometer (from left to right) with a sundog  
1045 in the background (b). Photos adapted from Figure 5 in Mariani et al. (2022).



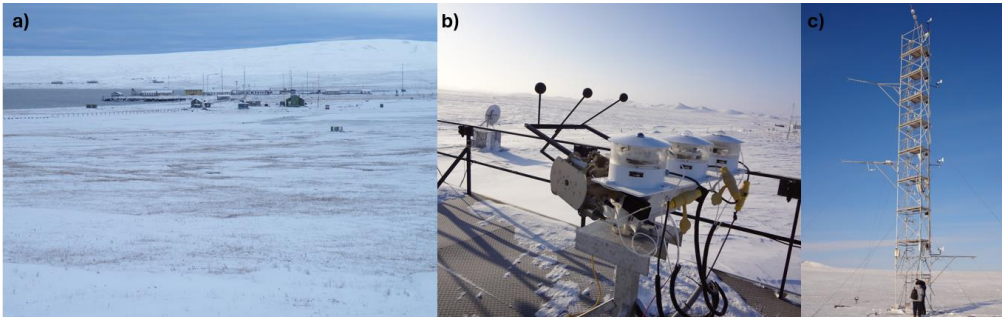
1047  
1048 **Figure 3.** The Iqaluit site surroundings taken in winter 2018 with the Iqaluit airport in the background (a), the radiation flux sensor suite  
1049 during the summer, consisting of several CMP10Ls, CGR4Ls, and SR50As (b), and the CL51 ceilometer during the summer (c). Photos  
1050 adapted from Figure 2 (Mariani et al., 2022).



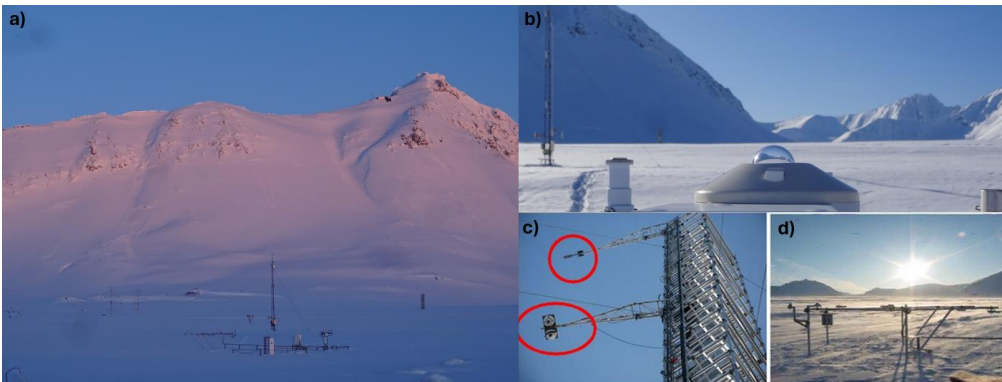
1052  
1053 **Figure 4.** The Sodankylä site surroundings during the winter at the Intensive Observation Area, IOA, in the boreal forest (a), snow, soil and  
1054 meteorological measurements in the MET measurement field (b), multi-level snow and soil measurements at the Peatland site, SUO, (c) and  
1055 the meteorological tower with meteorological and radiation sensors (d). Photos: FMI ([litdb.fmi.fi](http://litdb.fmi.fi)).  
1056



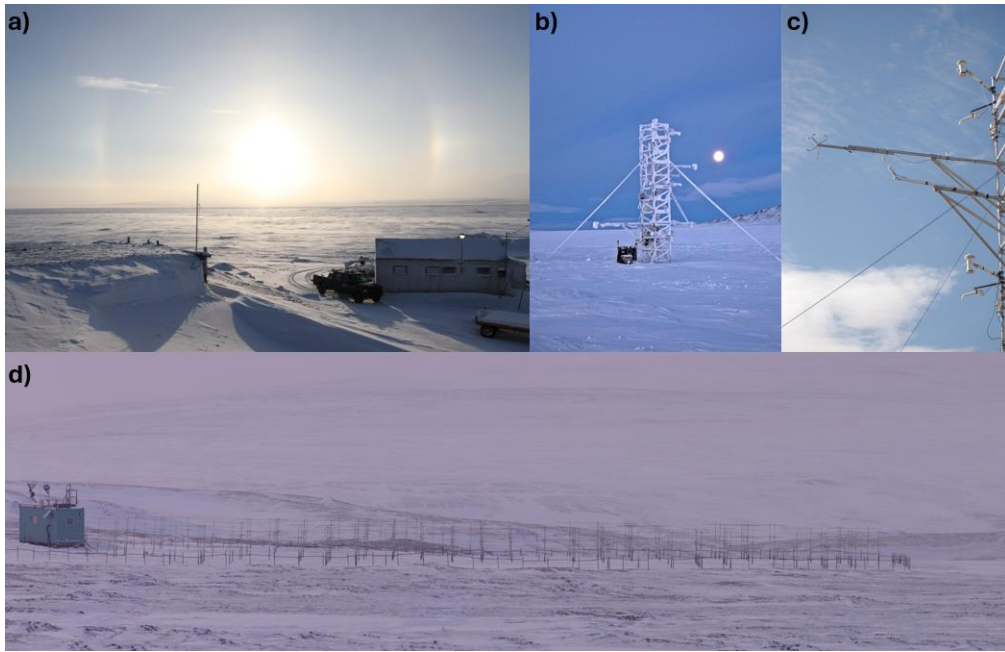
1058  
1059 **Figure 5.** The Utqiaġvik site surroundings during the winter, including the main observation stations and their rooftop instrument suites (a),  
1060 the meteorological tower with radiation flux sensors deployed in the summer (b), and the SKYRAD downward longwave radiation sensor  
1061 deployed on the roof in the spring (c). Photos: [www.arm.gov](http://www.arm.gov).  
1062



1063  
1064 **Figure 6.** The Tiksi site surroundings, taken from afar in the winter (a), the SKYRAD downward longwave radiation sensor deployed on  
1065 the roof of the Tiksi observation building (b), and the meteorological tower equipped with radiation flux sensors (c). Photos: Taneil Uttal  
1066 (NOAA).



1068  
1069 **Figure 7.** The Ny-Ålesund site surroundings taken in the winter with the meteorological sensors and radiation tower in the foreground (a),  
1070 the CMP22 downward shortwave radiation sensor at the site (b), the meteorological tower with the radiation flux sensors circled (c), and  
1071 several surface meteorological and albedo-measuring sensors at the BSRN station (d). Photos (c-d) are adapted from Figure 1 in Becherini  
1072 et al., 2021.



1074  
1075 **Figure 8.** The Eureka site surroundings in the winter, facing south from the Eureka Weather Station (EWS) looking over the frozen fjord  
1076 with a sundog in the background (a), the meteorological tower at the Surface and Atmospheric Flux Irradiance Extension (SAFIRE)  
1077 (b) with radiation flux (e.g., PSP) and meteorological sensors deployed (c), and the SAFIRE site surroundings taken from afar (d).

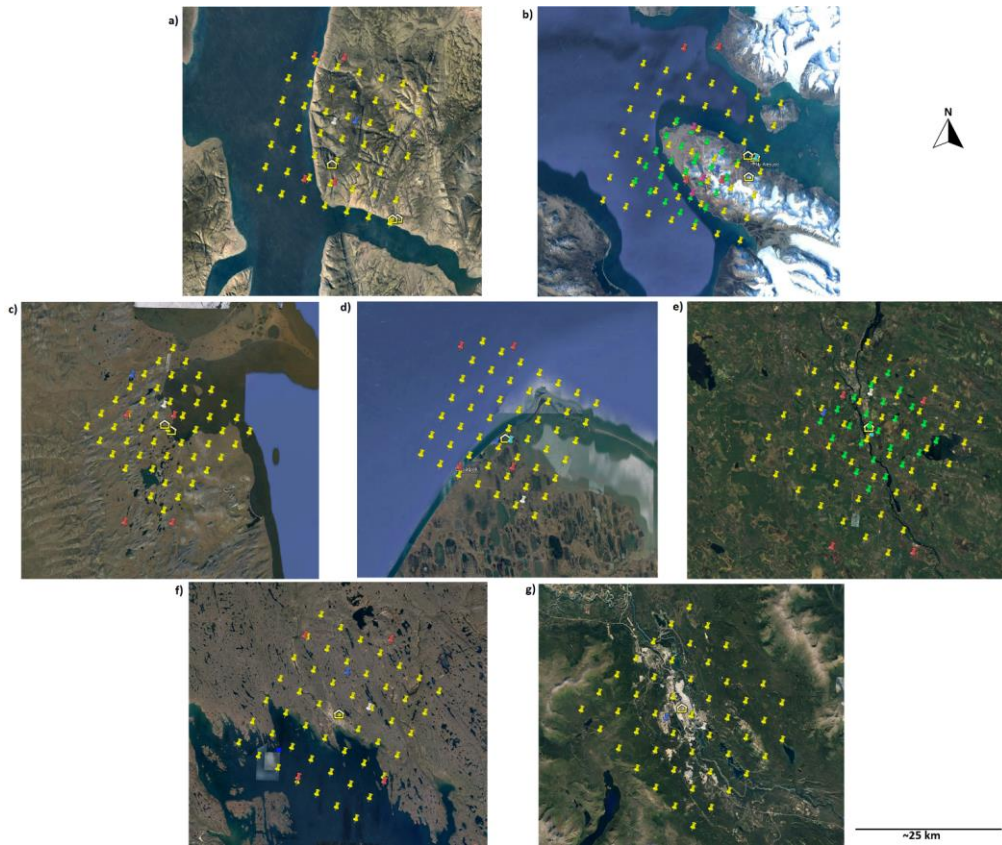


**Figure 29.** Model grid points at and around each [supersite](#) (a) Eureka, (b) Ny-Ålesund, (c) Tiksi, (d) Utqiagvik, (e) Sodankylä, (f) Iqaluit, and (g) Whitehorse, displayed through the Google Earth web-platform: *Image Landsat / Copernicus, Image ©2023 Maxar Technologies*. Sites are organized from highest latitude (Eureka) to lowest (Whitehorse). Yellow building icons represent the location of the facility on-site which contains all co-located instruments. Similarly, icons for the AROME-Arctic model grid are indicated by a green pin, ARPEGE pins are in white, DWD-ICON pins are light blue, ECCC-CAPS pins are yellow, ECMWF-IFS pins are dark blue, and SL-AV pins are in red. All images are north-aligned, nadir view.

1080

1081

1082

1083

1084

1085

1086

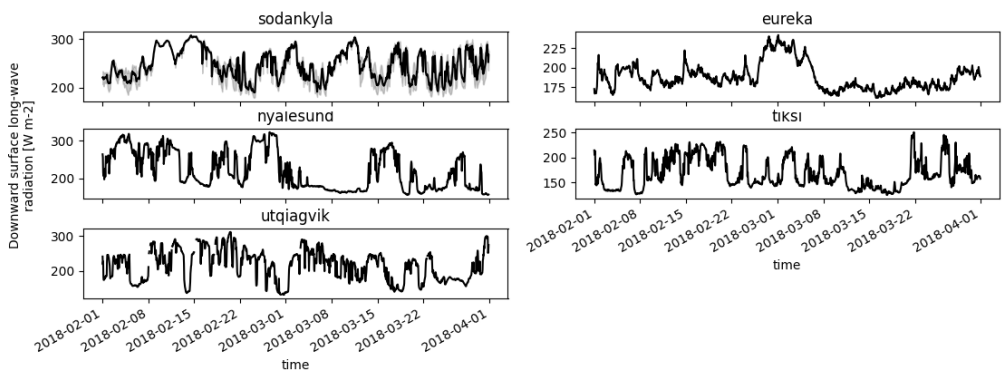
1087

1088

1089

1090

1091



1092

1093

1094

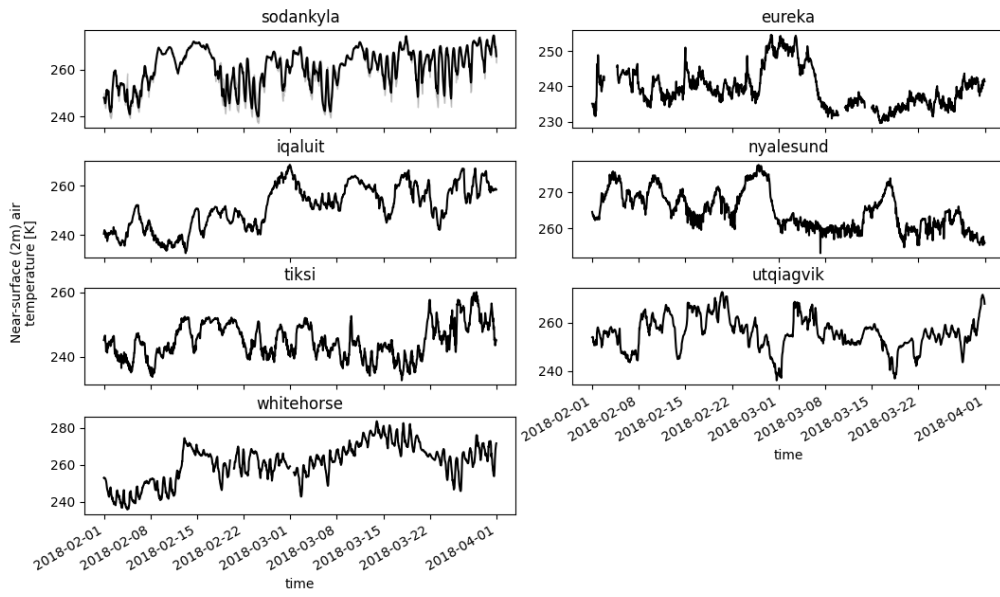
1095

**Figure 310.** Observations (30-min) of downward surface long-wave radiation (“rlds”) conducted during SOP1 at each supersitesite. Observations from Whitehorse and Iqaluit were not available during SOP1. Sodankylä conducts multiple observations of rlds; the mean (black line) and min/max spread in observed rlds (grey shaded area) are shown.

1096

1097

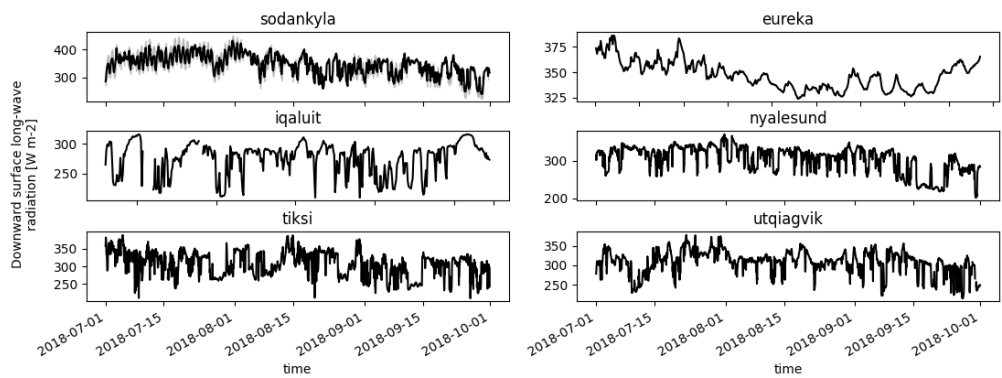




1098 **Figure 411.** Similar to Figure 3, except for observations of near-surface (2 m) air temperature (“tas”) conducted at each [supersite](#) during  
 1099 SOP1.  
 1100

1098  
 1099  
 1100  
 1101

1102



1103

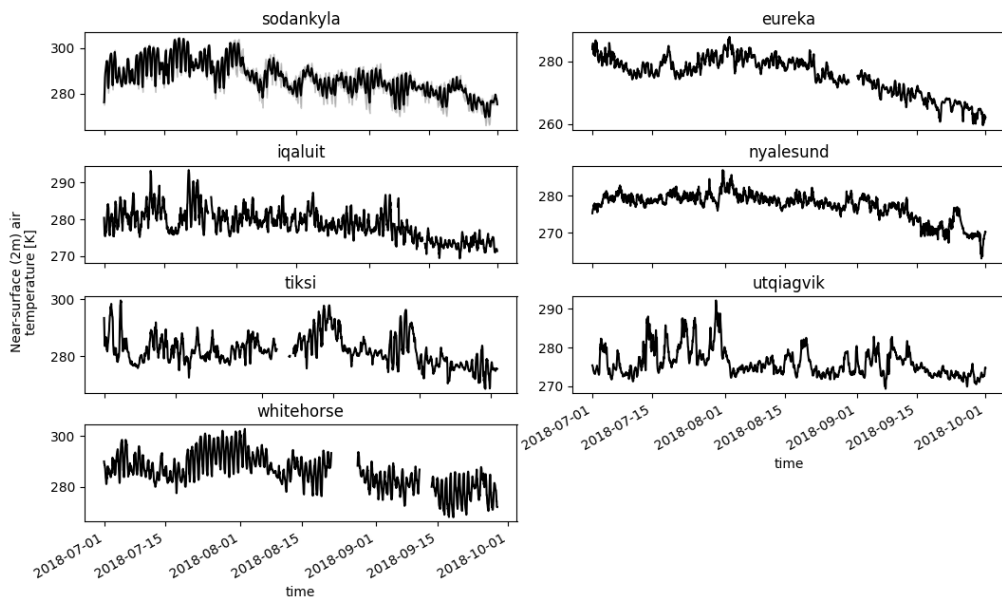
1104

1105

1106

1107

**Figure 512.** Similar to Figure 3, except for observations of downward surface long-wave radiation (“rlds”) conducted during SOP2 at each [supersite](#). Observations from Whitehorse were not available during SOP2.



1108

1109

1110

**Figure 6.13.** Similar to Figure 3, except for observations of near-surface (2 m) air temperature (“tas”) conducted at each [supersite](#) during SOP2.